UNIVERSITÀ
DEGLI STUDI
FIRENZE

Dipartimento di Neuroscienze, Psicologia, Area del Farmaco
e Salute del Bambino

DOTTORATO TOSCANO DI NEUROSCIENZE

CICLO XXIX

Coordinatore Prof. Renato Corradetti

Developmental ischemic stroke in rat induces maladaptive plasticity in corticospinal system

Settore Scientifico Disciplinare “M / PSI-02”

Dottorando

Dott. Alessandro Mattiello

matr. 14465

Tutor

Prof.ssa Nicoletta Berardi

Anni 2013 / 2016

A Vincenzo e Rosaria

Ad Anna

Contents

Abstract

It is generally considered that brain takes advantage of neural plasticity processes in order to modulate its response to different changes of internal and external environment. These variety of stimuli can induce a relevant shaping and strength of neural connections, influencing in a positive or negative manner the compensative response of the brain itself. The ability of neural networks to modulate their connectivity and functions in response of different stimuli usually decline proportionally to age, so that young neural system is considered more plastic and malleable rather than older ones.

Modulation of neural plasticity after a brain insult might be one of the most encouraging research and clinical approach to recover lost functions. For instance, rehabilitation protocols after ischemic stroke lesions are mainly focused on the plastic reorganization of altered connections through their active remodelling. In these cases, however, efficacy of such induced plastic modulation strongly depends upon timing, location, and extension of lesion, and also on both onset and duration of rehabilitative treatments. Moreover, plastic changes induced by brain injuries occurring during the development of a specific cerebral area seems to provoke a counterintuitive worsening of functions due to immaturity of these neural connections. Understanding the structural and molecular mechanisms underlying the "maladaptive" response of brain circuits can help to unveil and develop new therapeutic and rehabilitative targets, in order to promote a significant preservation or recovery of lost functions.

A paradigmatic example of developmental injury is the perinatal stroke, that is responsible for more than 70% of moderate-to-severe hemiplegic cerebral palsy in children and occurs

during the development of motor system. This process is characterized by an activity-dependent competition between ipsilateral and contralateral corticospinal projections, that evolves with the pruning of ipsilateral fibers and strengthening of contralateral ones. Recent studies have suggested that unilateral ischemic lesion occurring at early age in human favours a "maladaptive" strengthening of ipsilateral projections from the healthy hemisphere ("contralesional reorganization"), causing a worse motor outcome. Investigating the anatomical and molecular underpinnings of ischemic lesion timing effects on motor outcome in well characterized animal models would be useful to understand how plasticity mechanisms can promote or preclude motor recovery in an age-dependent manner.

Here I used the unilateral intracortical injection of the potent vasoconstrictor endothelin-1 (ET1) in the left forelimb motor cortex of rat with perinatal (P14) or juvenile (P21) age. These ages were chosen because they represent the higher and the final level, respectively, of developmental corticospinal axons remodelling. In order to assess behavioural long-term motor impairments induced by ischemic lesion, several general and fine motor tests were performed when animals reach adult age. ET1 lesion results in a comparable tissue damage both in P14 and P21 injured animals, but earlier lesioned rats show more prominent long term motor impairments. Taking advantage of well characterized viral vectors acting as anterograde tracers, I analysed, at the level of spinal cord, the anatomical alteration of corticospinal tract components (ipsilateral and contralateral) and plastic remodelling in terms of axonal sprouting from healthy side and their laminar distribution in the denervated side of spinal cord. These data suggest that ET-1 lesion dampens the normal development of corticospinal tract with an age-dependent effect: indeed, the earlier the lesion (P14) occurs, the more aberrant is sprouting of contralateral and ipsilateral components of CST onto the denervated spinal cord, with an abnormal targeting of dorsal and ventral laminae of denervated spinal cord. Interestingly, an early skilled training performed one week after lesion is sufficient to modulate this form of maladaptive plasticity, inducing a reduction of aberrant axonal sprouting coincident with a partial amelioration of long-term motor outcome.

1 Introduction

In this introduction, I will provide an overview of historical, molecular, and structural elements that characterize neural plasticity, with a particular focus on critical period regulation in the paradigmatic model of visual system. Afterwards, I will describe in details anatomy and development of motor system, in particular the corticospinal system. Moreover, I will discuss differences between adult and perinatal ischemic stroke pathophysiology, that have a fundamental influence on the correct choice of an appropriate treatment option. Finally, I will review recent works about the role of neural plasticity after an ischemic stroke in terms of axonal sprouting, cortical remodelling, molecular factors involved and examples of maladaptive plasticity processes.

1.1 *Neural Plasticity*

One of the leading features of the central nervous system (CNS) is neural plasticity, namely, the intrinsic ability to morphologically and physiologically modify itself in response to specific external stimuli, in particular during the developmental stage of life. Recalling both cheerful and melancholy events of our life, learning the better way to kick a ball to score a goal, or adapting our brain to new unexpected situations, all rely on neural plasticity. In the 19th century Ramon Y Cayal used, for the first time, the term *plasticity* to identify and characterize all the brain changes, induced by experience, that contribute to increase the structural and molecular complexity of neural circuitries. Experience is translated in patterns of electrical activity within neural circuits, and it is the pattern of electrical activity which drives the different forms of functional and structural plasticity, through

the spatially and temporally coordinated action of specific cellular and molecular factors. Neural plasticity may involve changes in the efficacy of already existing synaptic contacts, formation of new synaptic contacts or elimination of existing ones, large-scale changes in dendritic or axonal arborization, adding new neurons to a circuit.

1.1.1 Historical overview

The precision of the Cajal "Neuron Doctrine" (1894), that argued the contiguity but not continuity of neurons (in contrast with the "reticular theory" of Golgi), and the subsequent definition of *synapse* as "special connections from one nerve cell to another that facilitated the transmission of nervous impulses" [1] provided new inputs to better describe the process of neural plasticity, that was initially defined as

> "formation and multiplication of new synaptic junctions between the axon terminals of one nerve cell and the soma (i.e. the body and the dendrites) of the other" [2].

In the following year, Donald Hebb postulated that:

> "when an axon of cell A is near enough to excite a cell B and repeatedly or persistently takes part in firing it, some growth process or metabolic change takes place in one or both cells such that A's efficiency, as one of the cells firing B, is increased" [3].

introducing the concept of *synaptic plasticity*, the major component of neural plasticity. Hebb also introduced the idea that the pattern of electrical activity is important to induce plastic changes in synaptic efficacy, and in particular the notion that the presence of a correlated activity between pre- and postsynaptic neurons promotes the potentiation of synaptic transmission; as a corollary, decorrelated activity promotes depression of synaptic transmission. In Hebb's statement, it is already present also the notion that synaptic plasticity involves both functional and structural changes. Homosynaptic LTP at excitatory synapses consists indeed of a prolonged increase in synaptic efficacy which involves both functional and structural modifications of synaptic contacts and is induced by repeated bouts of correlated pre- and postsynaptic activity. The temporal requirements for the pattern of

pre- and postsynaptic activity has been now refined, since several studies have shown how synaptic efficacy can be increased (long term potentiation, LTP) or decreased (long term depression, LTD) according to the relative spike timing and firing rate of pre- and postsynaptic neurons (*spike-timing-dependent plasticity*, STDP). Also, the level of previous activity in the circuit affects the probability that a given change of activity in the same circuit induces LTP rather than LTD (*metaplasticity*). Non-Hebbian forms of synaptic plasticity have also been observed: for instance, monocular neurons in the visual cortex responding exclusively to the deprived eye increase their responsiveness following MD, as if they were trying to preserve their original drive. Therefore, in addition to plastic changes driven by synapse-specific electrical activity which follow hebbian rules, there seem to be forms of global feedback plasticity aimed at preserving neuronal total excitatory drive (*homeostatic plasticity*). First evidence surprisingly demonstrated that depriving visual input from one eye in mice increase the response of visual cortex from both eyes [4]. Interestingly, homeostatic plasticity processes are also showed in humans, where a protocol similar to previous one in mouse induce a paradoxical strengthening of activity from deprived eye [5]. Inhibitory circuits regulation underlies such homeostatic plasticity, because the boost of perception from deprived eye is correlated to a significant decrease of GABA concentration in the visual cortex [6].

1.1.2 Molecular and structural elements of synaptic plasticity

Until now, the molecular mechanisms underlying the plasticity of neural circuits are not completely understood and explored. Early studies, carried out by Eric Kandel using the gastropod Aplysia as a model, demonstrated that phenomena of habituation and sensitization after the execution of a simple gill-withdrawal reflex are mediated by plastic modifications of synaptic transmission, through an increase of glutamate release (short-term plasticity) or changing in gene expression (long-term plasticity). In mammals, the principal models for synaptic plasticity are *LTP* and *LTD*. LTP and LTD have been observed in many brain areas, both cortical and subcortical. The sequence of events leading to induction, expression, and consolidation of long-term changes of the LTP and LTD type has been recently reviewed

[7]. The first step, the trigger for induction of LTP and LTD at glutamatergic synapses is, in most cases, dependent on the activation of glutamate *N-methyl-D-aspartate receptors* (NMDARs), which have classically been thought of as coincidence detectors of pre- and postsynaptic activity. The opening of NMDARs during the induction of LTP leads to calcium entry that triggers a biochemical cascade involving intracellular kinases such as *extracellular signal regulated kinase* (ERK), *cAMP-dependent protein kinase* (PKA), *calcium-calmodulin kinase type II* (*α*CaMKII), the end product of which are the first, rapid post- and presynaptic effects towards the expression of synaptic potentiation, which include potentiation of the *2-amino-3-(3-hydroxy-5-methyl-isoxazol-4-yl)propanoic acid* (AMPA) receptor-mediated excitatory postsynaptic currents (EPSC). On the contrary, LTD process is induced by a small increase in intracellular [Ca^{++}] that stimulates a phosphatase activity in the cell, with a consequent internalization of AMPA receptors previously integrated in the plasmatic membrane. Therefore, Ca^{++} seems to be involved in a dual control of opposite plasticity mechanisms, depending on a threshold of intracellular concentration increase [8] (figure 1.1). One of the main important learning rule that seems to influence some types of experience-dependent plasticity *in vivo* is the so-called *spike timing-dependent plasticity* (STDP), where the plasticity is guided by the temporal sequence and interval between pre- and postsynaptic activity. The classic STDP is characterized by a double interval action: when presynaptic firing anticipates the postsynaptic one (interval 0-20 ms) induce LTP (tLTP), whereas the anticipation of the postsynaptic firing with respect to the presynaptic one (interval 0-20/50 ms) produce LTD (tLTD). In tLTP, NMDA receptors act as coincidence detector for pre- and postsynaptic spiking; the short duration of the time window seems to be due to the kinetics of Mg^{++} [9]. For tLTD, the coincidence detector can change depending on different synapses, but an important role is played by phospholipase C (PLC) in barrel cortex [10, 11], where its activation promoted by metabolic receptors of glutamate (mGluRs) increase intracellular [Ca^{++}] and activate several forward and reverse pathways [12, 13].

As introduced before, neural plasticity is exerted also in ways which do not follow the canonical Hebbian learning rules, as in the case of homeostatic plasticity [14]. Neural plas-

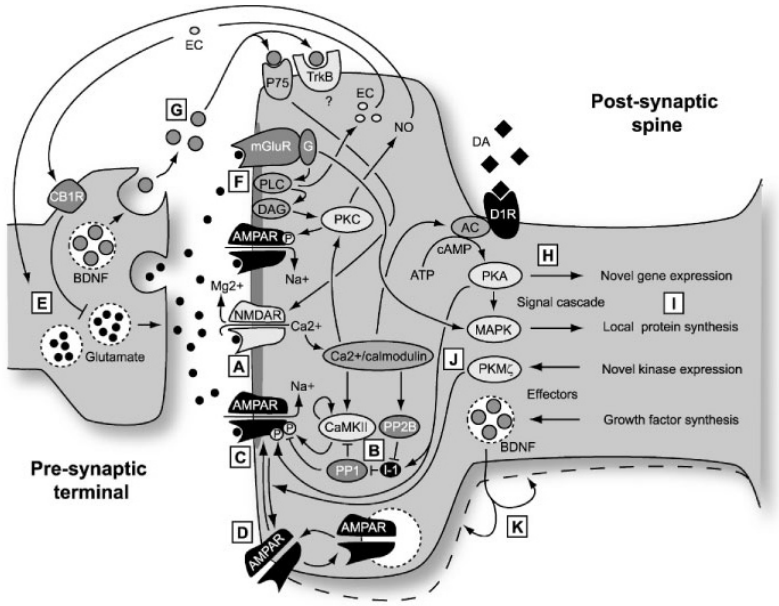

Figure 1.1. LTP and LTD: schematic of molecular mechanisms (modified from [7]).

ticity is exerted in several ways which do not follow the canonical Hebbian learning rules. Whereas Hebbian plasticity is considered a positive feedback loop that leads to a continuous strengthening of connections, there are other mechanisms that act as negative feedback loops and are able to preserve a physiological set point level of cellular activity; this form of plasticity is called *homeostatic* [14].

1.1.3 Critical periods

The plastic potential of CNS, in terms of susceptibility of the system to experience, is strongly limited by age. In many brain areas and species, it is possible to pinpoint a time window, called *critical period*, in which the plastic capability of a specific neural system is greatly enhanced. The first description of the critical period existence was the filial imprinting observed by Konrad Lorenz in the fledglings. This type of plasticity process underlies an innate capacity to learn (the fledglings closely follow the recognized mother around) and its critical window is very limited in time and well-defined; critical periods for many other systems last for longer time and their boundaries are not always clearly identified.

1.1.3.1 Sensory systems as models of critical period plasticity

The relevance of experience in the correct maturation of a neural system was confirmed by numerous experiments, performed particularly in the visual system, a paradigmatic model for studying plasticity. Early evidence showed that the deprivation of visual experience from one eye (*monocular deprivation*, MD) in kittens alters the electrophysiological response of primary visual cortical neurons in terms of rapid loss of responses to the deprived eye and gain of influence of the non-deprived ones [15]. This type of plasticity was maximal during a short period between four and eight weeks after birth in kittens, and then declined gradually until three months after birth [16]. A critical period for ocular dominance (OD) plasticity was also observed in other species such as monkeys [17], ferrets [18] and rodents [19, 20]. Currently, a massive improvement of knowledge about critical period plasticity, in terms of molecular and cellular mechanisms, was made possible thanks to mouse and rats studies.

A great deal of effort was done in recent years to unveil the molecular mechanisms underlying the opening and the closure of a critical period, using the visual system as a model. This issue is crucial for brain repair, considering that the induction of plasticity processes also in adults could promote the recovery from brain injuries. Hensch group demonstrated for the first time the role of *γ-aminobutirric acid* (GABA) inhibitory circuits in the shaping and re-finement of the critical period in the visual cortex; mice with a reduced expression of the 65-kD isoform of the GABA-synthesizing enzyme *glutamic-acid decarboxylase* (GAD65) do not show an evident OD plasticity [21] until they are treated with GABA agonists, such as *diazepam* [22]. Inhibitory circuit development in the visual cortex is strictly dependent from growth factor action. For instance, mice overexpressing *Brain-Derived Neurotrophic Factor* (BDNF) show a precocious development of intracortical inhibition, a premature closure of OD critical period and a precocious development of visual acuity [23]. Similarly, *Insulin-like Growth Factor 1* (IGF-1) can accelerate the development of inhibitory innervation and the increase of visual acuity [24, 25] and reactivates OD plasticity in adulthood [26], whereas the absence of the *orthodenticle homeobox 2* transcription factor

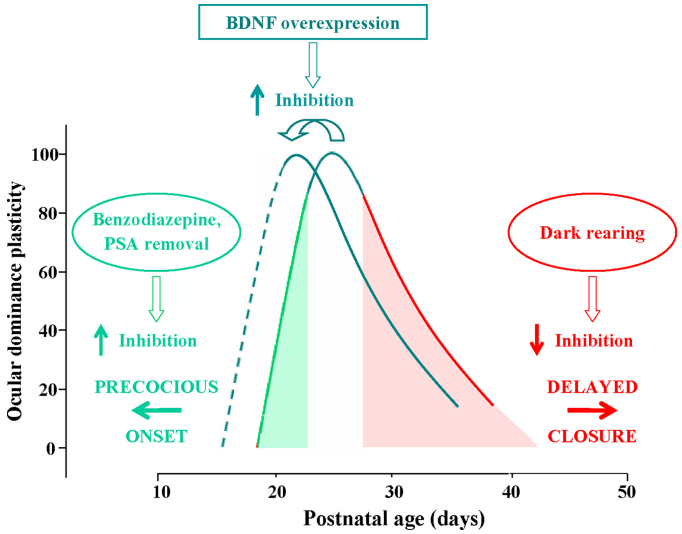

Figure 1.2. Time course of the critical period (CP) for ocular dominance (OD) plasticity in response to monocular deprivation in rodents; OD plasticity is normalized to the CP peak's level (modified from [30]).

(Otx2), which regulates intracortical inhibition development, the critical period does not start [27]. Interestingly, IGF-1 upregulates BDNF expression [28], suggesting that the interaction of several pathways could be fundamental for a correct regulation of the critical period onset (figure 1.2). These molecules mainly act on a specific subset of inhibitory GABA-ergic cortical cells, characterized by a basket morphology and a positive immunoreactivity for *parvalbumin* (PV^+). For instance, Otx2 is transcribed and translated in the retin, a, but it is also transported in an activity-dependent way to the visual cortex where control the maturation of PV^+ interneurons [27], through the interaction with elements of the *extracellular matrix* (ECM), the *chondroitin sulphate proteoglycans* (CSPGs), which are able to enwrap these neurons forming dense structures sheathing the somata and proximal dendrites known as *perineural nets* (PNNs) [29].

The closure of critical period seems to be guided by multiple mechanisms related in part to the stabilization of the previously formed connections (figure 1.3). In this way, the ECM covers a relevant role; indeed, first evidences demonstrate that the selective disruption of PNNs enwrapping the PV^+ cells injecting of the enzyme *chondroitinase-ABC* (ChABC) in the visual cortex, reactivates the OD plasticity in adult mice [31]. Moreover, knockout of the *cartilage link protein 1* (Crtl1), an important factor for the development of PNNs, shows

similar effects [32, 33]. Therefore, due to PNNs role in the development of PV^+ interneurons mediated by Otx2, ChABC treatment or Crtl1 deficiency may alter the function of PV^+ interneurons through the depletion of Otx2. Hence, it was developed a new two-threshold model for Otx2 action on the maturation of PV^+ interneurons, therefore on opening and closing of critical period, where the visual experience controls the accumulation of Otx2 in PV^+ cells, driving the onset of the critical period, and the subsequently formed PNNs promote the accumulation of Otx2 that results in a defined maturation and stabilization of circuits [27, 34, 35]. Other "stabilizing" factors whose depletion restore the OD plasticity in adult animals are the receptors for myelin-associated growth inhibitors, *Nogo-66 receptor* [36] and the *Paired immunoglobin-like receptor B* (Pir-B) [37, 38]. However, the closure of the critical period also involves (epi)genetic transcription reprogramming and modifications of neuromodulatory circuits (figure 1.3). In particular, it was demonstrated that a MD or a brief visual stimulation during the critical period strongly upregulates *cAMP responsive element binding-protein* (CREB) phosphorylation and CREB-dependent gene transcription [39, 40], whereas the overexpression of a dominant-negative CREB in V1 blocks OD plasticity [41]. Going upstream in the pathway, the regulation of CREB and CREB-dependent gene transcription is highly mediated by epigenetic mechanisms, through covalent modifications of histones or DNA, and action of *microRNAs* (miRNAs). In fact, applying drugs that inhibit or reduce the histone deacetylation restores the OD plasticity potential after a MD and the visual acuity in adult after a long-term MD [40, 42]; the specific ablation of *histone deacetylase 2* (HDAC2) on PV^+ interneurons reduces inhibitory driving in the adult visual cortex, delaying the closure of the critical period [43]. Moreover, DNA methylation of specific targets, such as BDNF promoter and *mir-132*, expressed in dependence of visual stimulation fundamental for OD plasticity [44, 45], is upregulated by a brief MD, and the inhibition of enzymes involved in DNA methylation revert the effect of MD [46]. Finally, both the increase in serotonin signalling, through treatments with the serotonin reuptake inhibitor fluoxetine, and the disinhibition of cholinergic circuits, promote an improved plasticity potential of the visual system [47, 48].

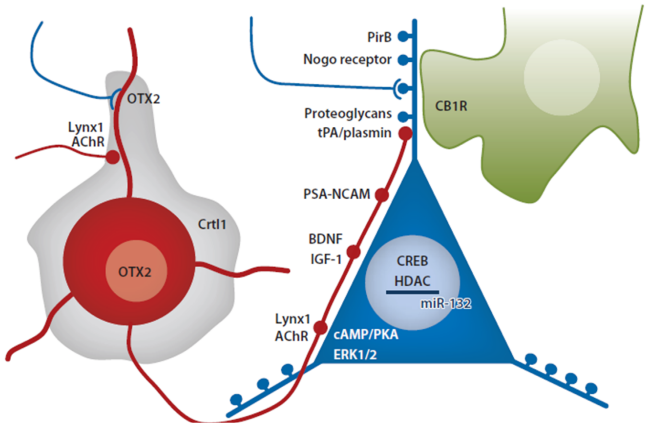

Figure 1.3. Principal molecules involved in regulating the critical period. Abbreviations: BDNF, brain-derived neurotropic factor; CB1R, cannabinoid receptor 1; Crtl1, cartilage link protein 1; ECM, extracellular matrix; HDAC, histone deacetylases; nAChR, nicotinic acetylcholine receptors; NCAM, neural cell-adhesion molecule; OD, ocular dominance: PirB, paired immunoglobulin-like receptor B; PSA, polysialic acid; PV, parvalbumin; tPA, tissue plasminogen activator (modified from [53]).

Another approach to study the molecular mechanisms underlying neural plasticity is the *environmental enrichment* (EE), conceived by Rosenzweig, Bennet and Diamond in the '60s, which consists in the rearing of large groups of animals in wide cages with numerous toys, tubes and wheels of various colours and shapes used to promote sensorial stimulation, exploration, motor exercise and sociability. EE can modulate the development of the visual system in young rats, with an acceleration mediated by the upregulation of BDNF [49] induced by improved maternal care [50]. Interestingly, EE exposure to adult animals upregulates BDNF levels and reactivates OD plasticity [51], with a crucial role of serotonin circuits and activity-dependent acetylation of histone H3 [51, 52].

Visual cortical synaptic plasticity described above has historically represented a prototypical model for sensorial and also motor mechanisms of activity- and experience-dependent plasticity. However, critical periods have been shown for every developing structure investigated. For instance, in the *primary somatosensory cortex* (S1), the tactile experience mediated by whiskers stimulation is anatomically represented by a one-to-one association of individual whiskers with well-defined cell clusters, called *barrels*, in cortical layer 4 [54]. Trimming or plucking a subset of whiskers causes S1 neurons to rapidly lose spiking responses to deprived whiskers and to more slowly increase responses to spared whiskers, thus weakening and

shrinking the representation of deprived whiskers and both strengthening and expanding the representation of spared whiskers within the map of the so-called *barrel cortex* [55, 56]. In contrast to the visual cortex plasticity, it is possible to identify at least three different critical periods for barrel cortex: early postnatal, adolescent and adult. Early postnatal stage (P0-7) is characterized by a strong degree of layer 4 plasticity, with thalamocortical afferents that show a form of LTP which involves conversion of silent synapses to active synapses [57, 58]. This layer 4 plasticity rapidly decrease during adolescence age (1-2 months), where layer 2/3 plasticity, also present previously, is maintained. In adolescence, plasticity is characterised by the potentiation of the spared whiskers or depression of the deprived ones. Depression of deprived whiskers appears to be limited to the first 2 months of life and has not yet been detected in older animals [56, 59]. However, potentiation of spared whiskers seems not to show a critical period in layers 2/3 of the barrel cortex, and is present in adult animals (6 months of age) [56]. As expected, also auditory abilities could be shaped by experience in a critical period-dependent manner. In fact, a continuous passive presentation of a single tone during development increase its tonotopic representation area in the cortex, and earlier is presented the tone, bigger will be this expansion [60]. Environmental noise (e.g. exposure at moderate intensity white noise) or deafness leads to a delay, but not a complete arrest, in the development and extends the sensitive period of experience dependent development of the tonotopic organization [61]. More recently, experience dependent developmental plasticity has been shown also for the motor system.

1.2 *Motor system: development, anatomy and function*

In mammals, execution and control of voluntary movements represent a fundamental evolutionary advantage in locating food, finding mates and avoiding predators, and help animals in the exploration of the environment. The motor system includes complex anatomical structures (motor cortex, cerebellum, basal nuclei, spinal cord) and circuits interacting themselves and with sensory inputs. In this section I will focus on the *corticospinal tract* (CST), the principal descending pathway involved in voluntary and skilled movements, that

starts from *primary motor cortex* (M1) and reaches its target on the *spinal cord*.

1.2.1 Anatomy of CST and spinal cord

In humans, approximately 40% of 1 million corticospinal (CS) axons originate from layer 5 of M1 (Brodman area 4), belonging to a subtype of subcerebral projecting cortical neurons (*corticospinal motor neurons*, CSMNs), also called *pyramidal neurons*, the biggest of the nervous system. It is possible to map regions controlling individual part of the body in M1; this map is called, in humans, motor *homunculus*. Using both anatomical and intracortical stimulation techniques it was possible to identify such *"musunculus"* or *"ratunculus"* also in rodents M1, that is identified in the fronto-medial cortex.

CST descend through the subcortical matter in the internal capsule, and the cerebral peduncle in the midbrain. Passing the pons, CST forms characteristic protuberances in the ventral part of medulla called *medullar pyramids*, that give to the CS projection the historical name of *pyramidal tract*. In humans, most CS fibers cross the midline to the opposite side at the level of the so-called *pyramidal decussation*, forming the *contralateral* CST. However, approximately 10% of fibers do not cross the midline and descend ipsilaterally (*ipsilateral* CST).

The *spinal cord* is the part of the CNS that controls voluntary muscles of limb and trunk, and receives sensory information from the periphery. It is divided into 4 different segments (cervical, thoracic, lumbar, and sacral), even separable into several levels (C1-C8, T1-T13, L1-L6 and S1-S4 in rat), identified by the emergence of dorsal and ventral roots. Spinal cord diameter is significantly enlarged in regions where limbs' nerves (the brachial and lumbosacral plexuses) appear, forming the so-called cervical and lumbar enlargements. Coronal section of spinal cord reveals the characteristic organization in two principal section, the external *white matter* that contains the myelinated sensory and motor fibers surrounding the peculiar butterfly- or (depending on the level) H-shaped *gray matter*, which includes neuronal cell bodies, axons, dendrites and glial elements. The dorsal parts of gray matter are called *dorsal horns*, and the ventral parts *ventral horns*, whereas the central region, which connects the dorsal and ventral horns, is called *intermediate gray* matter. Microscopic

analysis of the gray matter shows a complex cytoarchitectonic structure studied by Rexed in 1952 and 1954, who identified 10 different regions, or *laminae* [62]. Laminae 1-4 are located in the dorsal horn, and receive inputs from cutaneous receptors. Lamina 5, the "neck" of the dorsal horn, receive information from skin, muscles and viscera. Lamina 6, the most ventral layer of dorsal horn, and lamina 7, that includes the intermediate gray matter and the dorsal region of ventral horn, are involved in the regulation of posture and movement. In particular, lamina 7 contains interneurons connected to the motoneurons; the functional distribution of these interneurons is matched with the topographical distribution of motoneuron pools. Neurons in lamina 8 seem to play a pivotal role in the coordination of motor activity, whereas lamina 9 contains the α-motoneurons, which control the extrafusal fibers striated muscles of the axial skeleton and the limbs, and the γ-motoneurons, that innervate the intrafusal fibers. The arms of gray matter divide the white matter into three *columns*: dorsal, lateral and ventral. In rodents and many non-primate mammals, the most ventral part of the dorsal column contains the contralateral component of CST (*dorsal CST, dCST*), whereas the medial part of the ventral column is occupied by the ipsilateral component of CST (*ventral CST, vCST*) [63] (figure 1.5). In primates and carnivores, almost all the CS fibers are primarily found in the dorsal part of the lateral column, and a smaller tract in the ventral column.

1.2.2 Development of CST

CST is the last motor pathway to develop, and this process occur both prenatally and postnatally, lasting through the first years of life in humans and the first 2-3 weeks in rodents [66]. CST development consist of 4 major steps: a) differentiation of neuron precursors; b) growth of CS axons to reach their targets on spinal cord; c) refinement of spinal circuits, with axon myelination; d) development of cortical motor maps and skilled motor abilities. While genetic factors principally guide the first two steps, the latter two strictly correlate with activity-dependent processes.

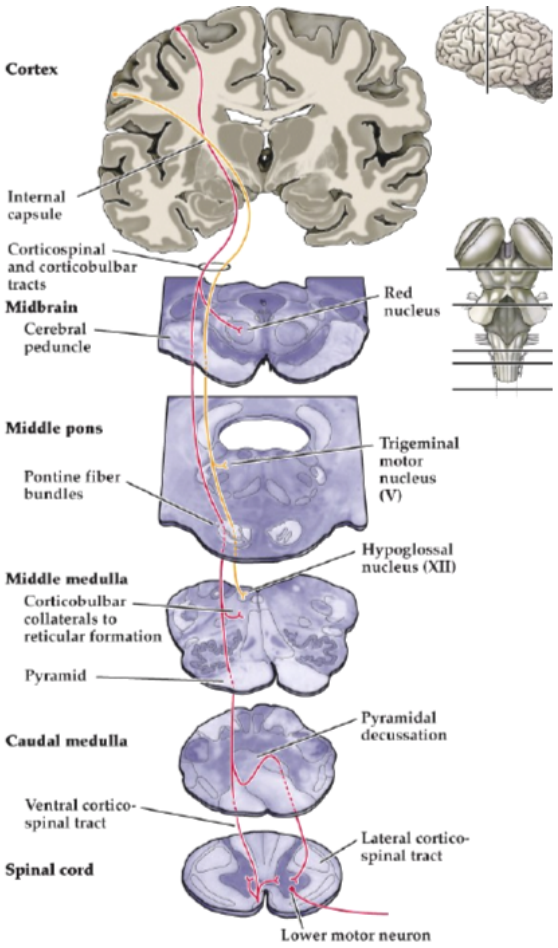

Figure 1.4. Corticospinal tract in humans (modified from [64]).

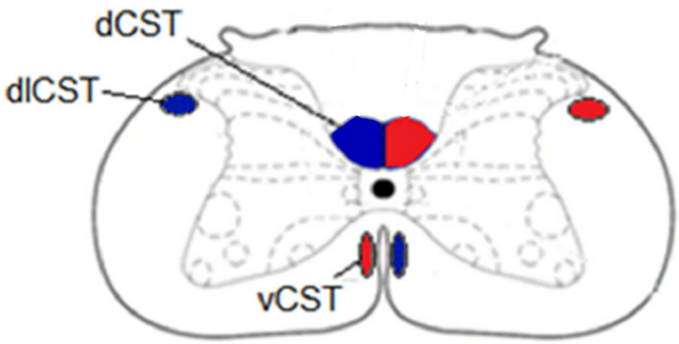

Figure 1.5. Scheme of a coronal section of the rat spinal cord with principal corticospinal descending pathways. dCST, dorsal corticospinal tract; vCST, ventral corticospinal tract; dlCST, dorsolateral corticospinal tract (modified from [65]).

1.2.2.1 Early development of CST

As described above, CSMNs are layer 5 cells mainly located in the primary motor cortex. In rodents, CSMNs are generated between embryonic days (E) 11–17 in the subventricular zone of the embryonic telencephalon [67]. During the subsequent radial migration, the neurons undergo several morphological modifications, with the acquisition of bipolar shape and axonal maturation. The specification and differentiation of CSMNs is a not really understood process, however big steps were done in recent years to unveil the molecular determinants of CSMNs development. The *Fez family zinc finger 2* transcription factor (Fezf2), was recently found to be required for the specification of all subcerebral projection neurons. The deletion of Fezf2 provoke the total ablation of subcerebral projection neurons and of other projection from the cerebral cortex to both spinal cord and brainstem; other cortical layers are less (L6) or no (L2-3, L4) affected [68, 69]. Moreover, the ectopic expression of Fezf2 in layer 2-3 post-mitotic cells is sufficient to promote the expression of CSMNs typical genetic programme [70, 71].

Fezf2 seems to act like an upstream factor that regulate neural differentiation; in fact, the deletion of the transcription factor *Ctip2* induce deficits in the fasciculation, outgrowth and pathfinding of subcerebral projection axons and a decrease in the number of fibers reaching the brainstem. Moreover, reduced expression of Ctip2 in Ctip2-heterozygous mice results in abnormal developmental pruning of corticospinal axons [72]. Other transcription factors involved in the target choice of subcerebral projection are *Otx1*, primarily expressed in the corticotectal neurons of the primary visual cortex [73], and *Sox5*, which is required for CSMNs generation in the appropriate temporal sequence [74, 75].

Once differentiated, CS axons must reach their target on spinal cord; for these neurons, the problem is not so tricky, because the distance to travel is the longest of any neuron in CNS. In general, *axon guidance* is mediated by the presence of different cues, mainly acting on the axonal growth cone and located on specific substrates; some cues are actively *attractive* and stimulate axon growth towards them, whereas others have an opposite effect, being *repulsive*. A great number of molecules are involved in this pathfinding process, that includes

the existence of many "check-point" stations. For instance, in the telencephalon, class 3 Semaphorins (*Sema3A* and *Sema3C*), through their repulsive effects, guide axons toward the internal capsule [76]; here, *Slit1* and *2* are implicating in the dorsoventral positioning of the corticofugal axons [77]. In rodents, CS axons enter in the upper brainstem in E16, whereas at birth (P0) they reach the rostral region of medulla, forming the above-mentioned medulla pyramids. Here the fibers achieve an important choice, because the mayor part of them cross the midline at the level of decussation and descend contralaterally. There are good evidences that *Netrin-1* signalling is involved in this process together with *Unc5* and *DCC* receptors [78], expressed in CSMNs at the time when the CS fibers cross the hindbrain boundary in the medulla and into the spinal cord [79]. In the absence of the Unc5c receptor, the CST splits into two bundles; a more lateral one that descend in the lateral white matter of the spinal cord, and a more medial bundle that turns dorsally, crosses the midline and is then deflected laterally into the dorsal grey matter [79]. Similarly, a spontaneous recessive mutation of DCC (DCCkanga/+) produce comparable deficits, with two altered bundles, one more lateral and one more ventral [80]. Another important factor involved in CST decussation is the cell-adhesion factor *L1-CAM*, expressed by CS axons, and its ligand *CD24*, expressed in the pyramidal decussation; L1-CAM knockout is responsible for an altered decussation of CS axons, and the fibers do not continue beyond the cervical level [81]. The repulsive Ephrin signalling is also involved in CS axons decussation, in particular the receptor *EphA4* and its ligand *EphrinB3*. EphA4 knockout mice decussate normally, but terminate bilaterally in the spinal cord region [82]; moreover, the expression of EphrinB3 is fundamental to prevent the recrossing of decussated fibers, favouring the unilateral motor control [83]. Interestingly, EphrinB3/EphA4 forward signalling is involved in both descending and ascending, that means sensory, axons in the spinal cord [84]. In rodents, pioneer axons of CST reach the cervical level of spinal cord at day P2, the thoracic level at P4 and the lumbar enlargement at P5 [85]; these fibers are followed by a several number of fasciculating axons, through the interaction of the cell-adhesion molecule N-CAM [86]. Instead, in humans CS axons reach caudal cervical levels at 24 weeks of fetal life, whereas they contact motor neurons and

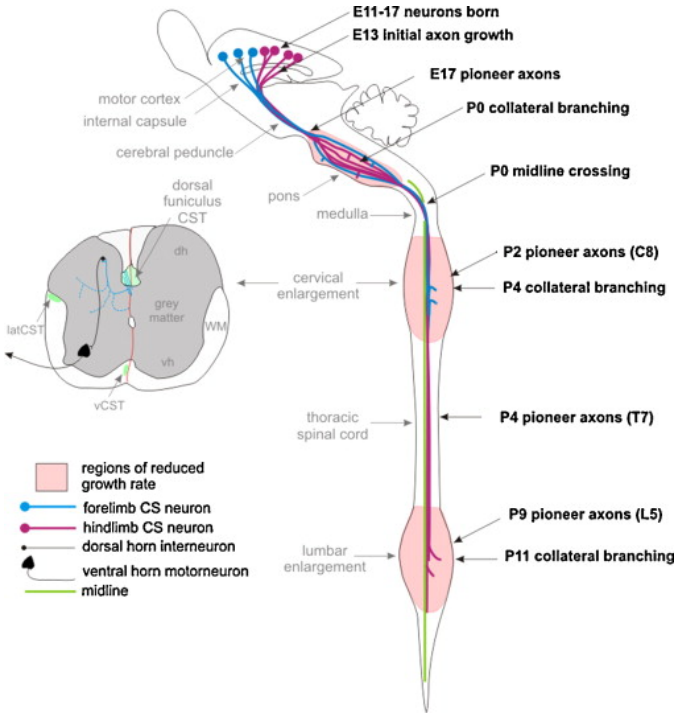

Figure 1.6. Scheme of CST development timeline in rodents. C, cervical spinal cord segment; CS, corticospinal; dh, dorsal horn; E, embryonic day; L, lumbar spinal cord segment; latCST, lateral corticospinal tract; T, thoracic spinal cord segment; vCST, ventral corticospinal tract; vh, ventral horn; WM, white matter (modified from [88]).

interneurons of spinal cord by birth [87].

1.2.2.2 Late development of CST

When CS axons reach the spinal cord, fiber terminations do not show the pattern distribution that we find in maturity. During development, CS fibers have a wide distribution that is progressively refined through a process called *pruning*. In immature kittens (5 weeks of age), CS fibers terminations are distributed bilaterally in the ventral horn and the intermediate laminae [89]; starting from 7-8 weeks, such pattern is refined, with the pruning of ipsilateral terminations and the strengthening of contralateral axons, that reach their target on the deeper dorsal horn laminae and the upper ventral horn [89]. The question is if the mechanisms underlying this refinement process are guided by genetic programmes or by environmental and neural activity influences. In the last fifteen years, the Martin lab answered this question using as experimental model the cat, in which CST development matches reasonably well, in timing and features, the human one [90, 91]. To test the role of

neural activity in shaping CS terminations, two different approaches were used, applied during the critical period (5-7 weeks); the use restriction of forelimb through the injection of *botulinum toxin A* (BTX) into a specific forelimb muscle [92] and the unilateral inactivation of M1 activity using the intracortical injection of *muscimol*, a GABA-A receptor agonist [93, 94] (figure 1.8). Both experimental interferences lead an aberrant pattern of CS axons distribution in the depressed side, where fibers are not able to reach territories occupied after a normal development, and have fewer branches and presynaptic boutons [94]; instead, the contralateral healthy side shows an extensive contralateral projection and preserves significant ipsilateral terminations in intermediate zone and dorsal horn. On the other hand, the unilaterally activation of one side of spinal cord through an electrical stimulation carried out during critical period promotes the maintenance of transient ipsilateral terminations, that are normally contralateral, and a dorsal displacement of non stimulated axons [95]. All findings strongly confirm a model in which the CS termination patter is determined by an *activity-dependent competition* between contralateral and ipsilateral axons, that induce, in presence of a normal neural activity, the strengthening of the former and the pruning of the latter. Interestingly, a bilateral CST inactivation induces a normal contralateral pattern distribution of axons [93], indicating that it is not important the absolute level alone, rather than the relative level of neural activity between the contralateral and ipsilateral components.

The refinement of cortical motor maps is strictly connected with the development of CST. Although development of motor control during this period likely depends on maturations of multiple cognitive, sensory and motor system, the role of CST is also important. Movement representation in M1, that integrates premotor and subcortical control signal to obtain output circuitry for controlling specific joints, is first detected at 7 weeks in the cat [96]. Prior to this stage, microstimulation of motor cortex is not able to induce a reliable movement in any muscle. In the following weeks, the developmental emergence of the map is characterized by an increase in the percentage of active sites, the progressive increase in distal muscles representations and a decrease in the current threshold [96], that suggest a strengthened

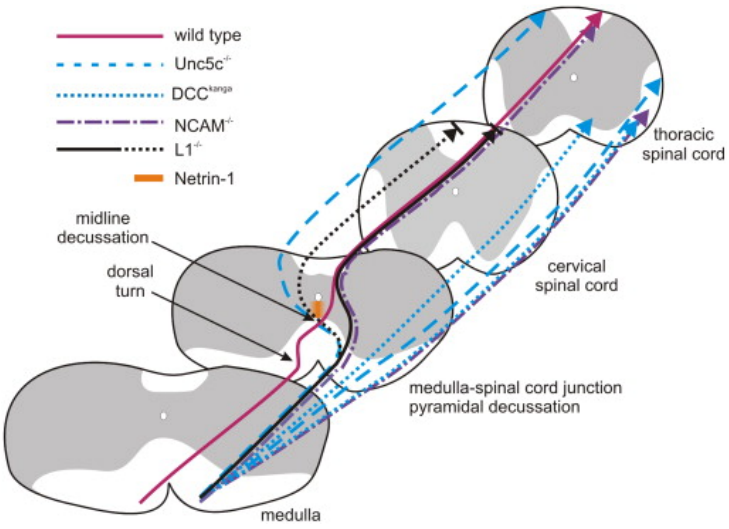

Figure 1.7. CST trajectory in wild-type and mutated animals (modified from [79]).

activation of spinal motor circuits and synapses [97]. Transcranial magnetic stimulation studies in humans exhibit a comparable reduction of intensity stimulation necessary to elicit motor-evoked potentials until adolescence [87].

1.3 *Ischemic stroke: from adult to newborn*

Ischemic stroke is a cerebrovascular disorder that occurs during a temporary or permanent interruption of blood flow in the brain caused by a thrombosis, an embolism or systemic hypoperfusion. This interruption induces a tissue damage primarily due to a loss of energetic and oxygen supply, which interfere with the normal cellular homeostasis. This pathology is etiologically distinct from by *hemorragic stroke*, that on the contrary is provoked by the rupture of a cerebral vessel.

Taken together, these pathologies are defined as *stroke*; ischemic stroke account for 87% of total stroke events. It is estimated that each year in the USA stroke approximately afflicts 700'000 subjects, and currently there are 2 million of people that survived from stroke event but are afflicted by several disabilities, are unable to work and represent an important health cost (approximately, 62 billion dollars annually [99]). In Italy, stroke represent the third cause of death after hearth ischemia and cancer (10-12% of annually total death are caused by stroke), and the first cause of disability; moreover, 75% of stroke survivors are

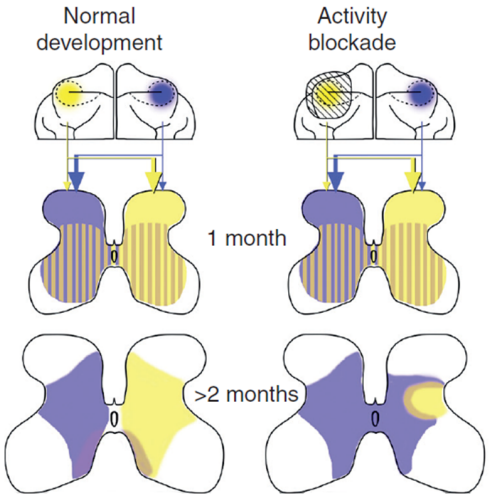

Figure 1.8. Activity-dependent refinement of corticospinal axon topography. Normally there are overlapping CS terminations in the spinal cord at 1 month in the cat (left). These terminations are refined into predominantly contralateral terminations after 2 months. After motor cortex inactivation between weeks 5 and 7 through muscimol intracortical injections (right), the silenced axons (yellow) failed to populate as much of the contralateral gray matter. In contrast, the active side (blue) has a bilateral termination pattern. The ipsilateral axons are largely maintained transient terminations (modified from [98]).

affected by some form of disability, and the half of this percentage lose its independence (Italian Ministry of Health, [100]).

Contrary to widely held assumption, ischemic strokes occur in different ages; for instance, *perinatal strokes* (figure 1.9), that occurs between the 20th week gestational age and the 28th day after birth, is considered the second group for stroke incidence, after adult age stroke group. It is estimated that the incidence of a perinatal stroke is 17-fold higher with respect to any other pediatric epoch [101], and ranges between 1 in 2300 to 1 in 5000 births [101, 102]). This pathology produces a significant morbidity and severe long-term neurologic and cognitive deficits, including epilepsy, language and visual defects, psychiatric disorders, and represent the leading cause of *hemiplegic cerebral palsy* in children; approximately 90% of affected children show this type of motor deficits [101, 102]. As result, a compromised use of the arm and hand to reach, grasp, release, and manipulate objects is the main deficit occurring after injury. The immediate and long-term effects of an ischemic insult are highly different between adult and newborn age, because of the different susceptibility of specific brain cells, blood brain barrier, inflammation and apoptosis. In order to differentiate and

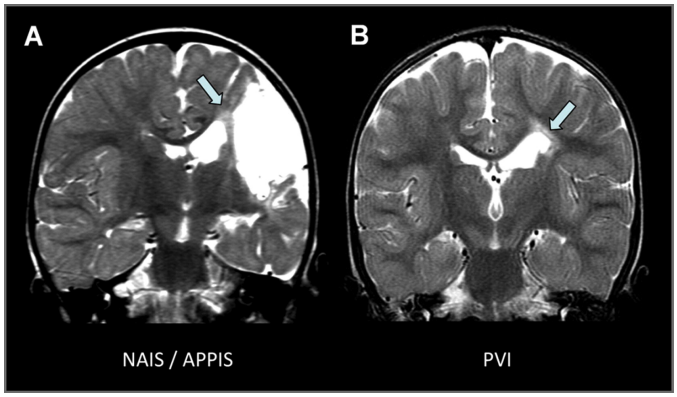

Figure 1.9. Perinatal stroke syndromes causing hemiplegic cerebral palsy. (A) Arterial perinatal strokes (neonatal arterial ischemic stroke or arterial presumed perinatal ischemic stroke) (B) Periventricular venous infarction results in isolated injury to the subcortical white matter. Both lesions damage corticospinal tracts, leading to contralateral hemiplegic cerebral palsy (modified from [103]).

specify the treatments for these divergent pathologies, it is crucial to understand the distinct pathophysiological mechanisms, diagnostic markers and long-term outcome.

1.3.1 Pathophysiology of ischemic stroke

Brain tissue is characterized by an elevated level of oxygen and glucose consumption, because its metabolism is almost exclusively dependent on oxidative phosphorylation mechanisms. This high energy level is fundamental for the maintenance of ionic gradients; it is estimated that neuronal Na^+/K^+ pump consumes 70% of energy supplied to the brain [104]. For this reason, the primary event of an energy depletion is the sudden loss of membrane potential with a strong depolarization that activates the voltage-dependent Ca^{++} channels (figure 1.10). The intracellular increase of $[Na^+]$ and $[Ca^{++}]$ induce the passive influx of water and a subsequent formation of intracellular *oedemas*. Membrane depolarization also leads to neurotransmitter release; in particular, the excitatory neurotransmitter *glutamate* plays a pivotal role in ischemic pathology, because the depolarization and the accumulation of Na^+ into the cells induce the reversal of Na^+/dependent glutamate transporters, located on both pre- and postsynaptic membranes, with an increase of glutamate in the extracellular space. This event generates a positive loop where glutamate excite nearby neurons, increasing their depolarization level; this phenomenon is called *excitotoxicity* (figure 1.10). Both ionotropic (NMDA, AMPA) and metabotropic (mGluRs) glutamate receptor are involved in

the exacerbation of excitotoxicity. Pharmacological blockade of mGlu1 receptors induce neuroprotection in both *in vitro* and *in vivo* models of ischemia [105], whereas blockade of mGlu5 limit excitotoxicity by reducing NMDA receptor activation [106]. In contrast, group II (mGlu2 and mGlu3) and III (mGlu4, 6, 7, 8) of mGlu receptors are located in the presynaptic terminals and mainly inhibit glutamate release; indeed, group II and II agonists are neuroprotective by limiting the induction of excitotoxicity and increasing production of neurotrophic factors from astrocytes, such as TGF-beta and NGF [105]. Intracellular [Ca^{++}] influx plays a crucial role in the generation of cellular damage, because activates proteolytic enzymes that degrade cytoskeletal proteins, *phospholipase-A2* (PLA2) and *cyclooxygenase* (COX) which generates *free-radical species* (Radical Oxygen Species, ROS). Moreover, Ca^{++} activates neuronal nitric oxide synthase (nNOS), with subsequent production of *nitric oxide* (NO), which has a vasodilating effect on nearby endothelial cells but also combines with *superoxide* (O_2^-) to produce *peroxynitrite* (ONO_2^-), a potent oxidant that promote tissue damage. NO also overactivates *poly(ADP-ribose) polymerase-1* (PARP-1), a DNA repair enzyme that in the ischemic milieu consumes high levels of NAD^+, impairing NAD^+ dependent processes such as glycolysis and mitochondrial respiration and leads to ATP deprivation, energy failure and neuronal death [107]. Finally, NO-mediated activation of *matrix metalloproteases* (MMPs) leads to the degradation of collagen and laminins in the basal lamina and disrupts the integrity of *blood brain barrier* (BBB). This event can cause parenchymal hemorrage, vasogenic brain oedema and neutrophil infiltration into the brain [108]. (figure 1.10). Cytotoxic oedema is also generated by the astrocyte swelling mediated by the water channels (*acquaporin-4*) present in the astrocyte end feet [109].

The ischemic event induces different damages with respect to preserved blood flow entity. The region where the blood flow is 20% below normal is called *core* and cells are rapidly killed by lypolysis, proteolysis, cytoskeleton disruption and total energetic failure. The region surrounding the core is called *penumbra*, where perfusion and bioenergetic metabolism is partially preserved. In these penumbra regions, the high level of depolarization induces a continuous release of K^+ and glutamate that spread through the brain and promote the

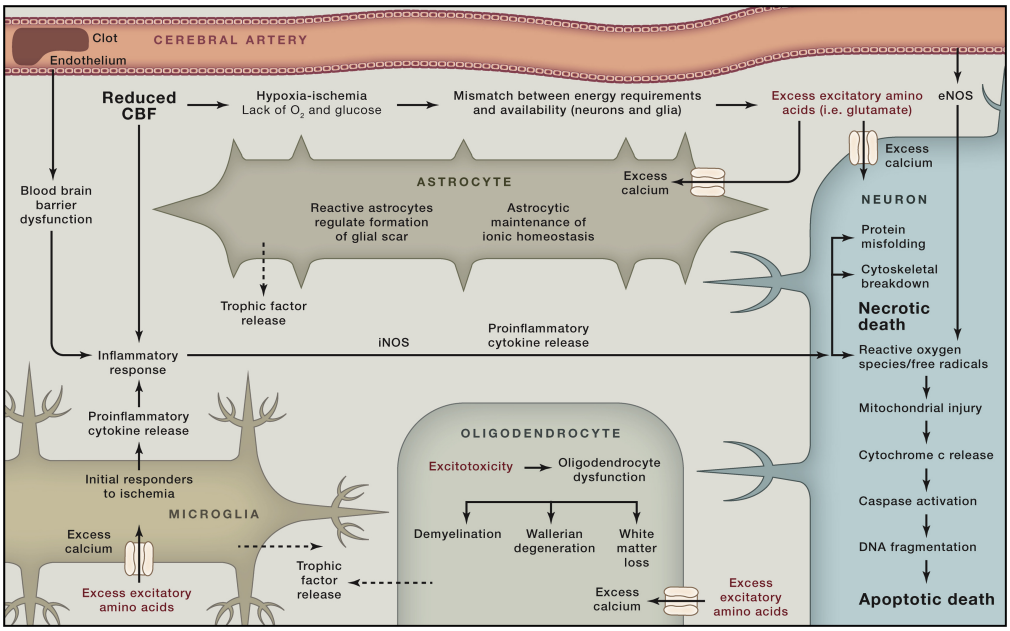

Figure 1.10. Pathophysiology of stroke (modified from [110]).

depolarization of other cells in a positive-loop way; these recurrent spontaneous waves are called *peri-infarct depolarizations* (PIDs), and are correlated with the volume of lesion; effectively, drugs that reduce the number of depolarizations decrease infarct size [111].

Hours after the ischemic event, the increase in intracellular [Ca^{++}] and [NO] mediates long-term expression of pro-inflammatory and pro-apoptosis factors in the penumbra region (figure 1.11). First of all, BBB disruption facilitates the infiltration of neutrophils and lymphocytes, that causes damage through the release of ROS, proteolytic enzymes and production of *cytokines* (IL-1, IL-6, TNF-alfa, TGF-beta) and *chemokines* (CINC, MCP-1). In particular, *IL-1* is involved in arachidonic acid release, recruitment and adhesion of neutrophils (also promoted by TNF-alfa), enhancement of NMDA mediated excitotoxicity and stimulation of NO synthesis [112]. In contrast, TGF-beta seems to play a neuroprotective role in the pathogenesis of stroke; administration of TGF-beta blockers increase the volume of excitotoxic lesion after focal cerebral ischemia [112]. Intracellular [Ca^{++}] increase, ROS, DNA damage and ionic imbalance are important triggers of *apoptosis*, starting from a severe mitochondrial damage characterized by *cytochrome c release* from the outer membrane. Cytochrome c release activates downstream caspases of the intrinsic pathway, whereas the activation of specific *death receptors* (Fas/CD95, TNFR1, TRAIL) promotes the extrinsic

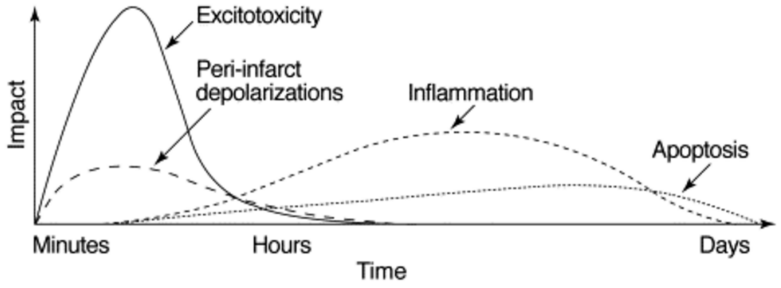

Figure 1.11. Putative cascade of damaging events in focal cerebral ischaemia (modified from [111]).

pathway; both pathways converge in the activation of effector caspases such as *caspase 3* and *7*, that cause cytoskeleton and DNA fragmentation [113].

1.3.2 Pathophysiology of perinatal ischemic stroke

Glutamate-dependent excitotoxicity represents the most common initial damage process after an ischemic injury in the immature brain too; however, it is more excitable and predisposed to oxidative stress with respect to the adult brain because of different glutamate and NMDA receptor subunit expression [114, 115], interaction with downstream signalling cascade [116], and different expression of several endogenous antioxidant enzymes [117]. Moreover, apoptosis is more readily activated in the immature brain, partly due to the high expression of many of the key components of apoptotic pathways related to the normal programmed neuronal death process during development. For this reason, apoptosis also contributes, coupled with necrosis, as a pivotal neuronal death mechanism in the infarct core after neonatal focal stroke [118]. However, it was demonstrated that caspase-3 deletion exacerbates injury through the activation of caspase-3 independent and necrosis pathways, suggesting that total elimination of caspase-3 can be detrimental rather than beneficial [119]. Inflammatory response also differs between adult and perinatal age, for example considering the underdeveloped no classical complement activation in term infants as well as in rat pups [120]. Moreover, deletion of inflammatory mediators, such as IL-1 [121], is not neuroprotective in immature brain, an effect opposite to that observed in adults. Finally, the role of BBB in ischemic injury, but also physiological functions, in immature CNS are different from the adult one [122]; in fact, BBB permeability in early postnatal age is lower than in adult (figure

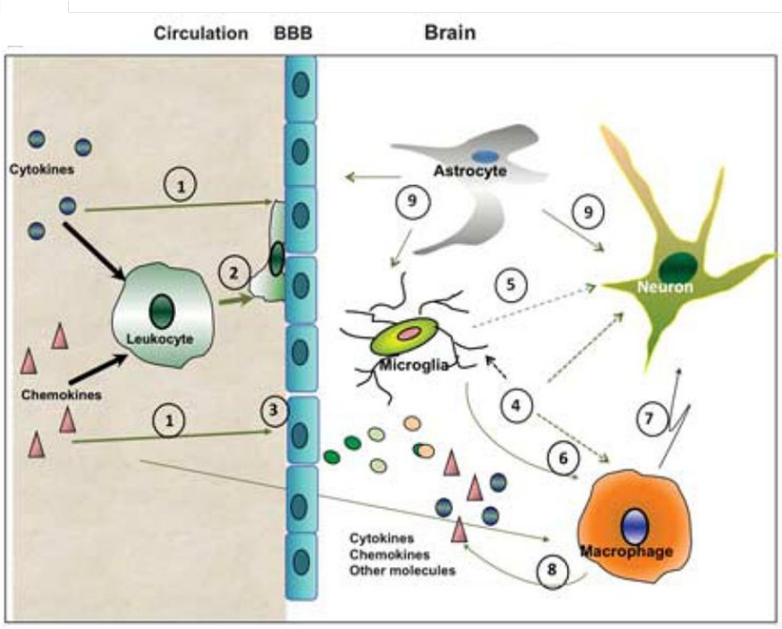

Figure 1.12. Events at the neurovascular interface after tMCAO in neonatal rats. In particular, the neutrophil leakage (2 and 3) is lower than in adult brain; moreover, cell–cell communications strongly differs in the newborn with respect to adult injury (4 to 9) (modified from [123]).

1.12). The BBB response after a perinatal ischemic injury is strongly influenced by this low permeability: for instance, extravasation of albumin at 2 hours after reperfusion is increased of 5 to 25-fold in rat adult injured brain but only of 2-fold in newborn [123]. Transcriptional analysis of endothelial cells isolated from lesioned and non lesioned adult and immature animals shows a higher expression of several tight junction and basal membrane components in neonates [123]. Neutrophil infiltration, that is both cause and effect of BBB disruption in adult ischemic injury, is negligible or limited in neonatal hypoxic-ischemic (HI) models [123, 124].

1.4 *Animal models of focal ischemic stroke*

It is widely accepted that research with animal models is crucial for developing and testing new treatments. Animal research allows to better understand the cellular mechanisms that underlie the organism's response to brain injury in the short and long term, and correlates it with specific behavioural and functional outcome induced by lesion. However, there are drawbacks to this approach, starting from the assumption that all mammals display the same cellular and physiological response to a specific injury, which is not always right.

Hence, researchers should be careful not only on the development and choice of reliable animal models, but also on the interpretation of experimental results. For ischemic stroke these points have a pivotal role on the improvement of knowledge and in the potential translational applications for promoting recovery of spared functions [125].

1.4.1 Focal stroke models in adult brain

Focal ischemic stroke models reproduce a condition of reduced energy supply that leads to the formation of the characteristic central ischemic core, with extensive necrosis, surrounded by the penumbra, a zone prone to plastic changes that promotes recovery [126].

The *middle cerebral artery* (MCA) is the most commonly affected blood vessel in human occlusive/ischemic stroke [127] and it is the artery most commonly targeted in rodent stroke models. The *occlusion of MCA* (MCAo) is a technique involving the transecting of the external carotid artery (ECA), and the insertion of a coated suture through the internal carotid artery to lodge in the junction of the anterior and middle cerebral arteries. The duration of suture occlusion of the MCA in the rat can range from 30 to 120 minutes, or permanent. Occlusion durations of 90–120 minutes are required to achieve reproducible tissue damage and result in very large infarcts that occupy much of the hemisphere. The advantages are that this technique does not require craniotomy, produces focal occlusion of a large cerebral artery as seen in human stroke and can be done in a high throughput manner. Disadvantages include the possibility to induce a hypothalamic injury, which can complicate the interpretation of histological and behavioural outcomes owing to impaired motivation and temperature regulation. Moreover, transecting of the ECA renders the muscles of mastication and swallow ischemic, producing difficulty in eating and weight loss [128].

The *distal occlusion of MCA*, consisting of local blood electrocoagulation [129] produce a permanent but more restricted damage to the cerebral hemisphere, avoiding the thalamic, hypothalamic, hippocampal, and midbrain damage seen in suture-occlusion of the MCAo of greater than 60 minutes. In this model, local collaterals from the anterior cerebral artery provide a zone of reflow in medial frontal and parietal cortex.

The occlusion of MCA can be also obtained through the production of an embolus. Micro- or macrospheres injected into the internal carotid artery lodge in the middle cerebral artery and produce an infarct of similar size and location as the permanent suture-occlusion of the MCA, without hypothalamic damage. Clots can undergo spontaneous thrombolysis, thereby causing multiple infarcts and high variability and mortality [126, 130].

Thromboembolism can be also induced injecting systemically a photosensitive dye (Rose Bengal or erythrosine B) in combination with irradiation through the exposed or thinned skull with light [131]. This technique, called *photothrombosis*, allows a precise stereotaxic location and generates highly circumscribed ischemic cortical lesions. The advantages of this model are the small size of the infarcts, the ability to place the infarct within distinct functional subdivisions of cortex, and the minimal surgical manipulation of the animal. The disadvantages of this model stem from the relatively little ischemic penumbra or region of local collateral flow and reperfusion. Moreover, the simultaneous development of both significant vasogenic and cytotoxic edema in MRI of photothrombotic stroke more closely resembles traumatic brain injury models than focal stroke [132].

The *endothelins* (ET1-2-3) are vasoactive peptides composed by 21 amino acids that act on two different G-coupled receptors (*ETA* and *ETB*). The physiological role of endothelins is the maintenance of vascular tone, and are considered the most powerful vasoconstrictors produced by human body. For this reason, they can be chosen for the localised vasoconstriction of cerebral cortex or deeper regions. In particular, intracortical injection of *endothelin-1 (ET1)* adjacent to the proximal MCA [133] is widely used to induce focal lesion in rat cortex [134]. Stereotaxic intracortical injection of ET1 induce a 60-92% blood flow reduction in the territory of MCA [135]; the lesion induced is similar to MCAo but more variable, and reperfusion occurs at a much slower rate [133, 134, 136]. Lesion size can be adjusted by varying the concentration or volume of ET1 to achieve reproducible injury. ET-1 model was mainly developed in rat, whereas in mice ET1 seems to have a much less potent effect for producing an infarct [137]. However, it was recently developed a reproducible stroke model of ET1 intracortical injection in mice useful for long-term analysis and neural repair studies [138].

1.4.2 Animal models of perinatal stroke

While several animal models of adult ischemic stroke have been developed so far, the search for reliable developmental model found a great number of obstacles. In particular, reliability of animal models, mainly rodents, to reflect ischemic stroke in the perinatal human period depends on matching the appropriate age between human and rodent neonates by correlating neuronal events that occur during maturation. These considerations represent an area of conflict in the literature, because different authors claimed that human term corresponds to either P7 [139] or P8–14 of rodent age, depending upon different criteria, such as white matter [140] or corticospinal system development [141] and EEG maturation [142].

The *hypoxic-ischemic model* (HI) was created by Rice and Vannucci in the 1981, and represent the better characterized model useful to analyse the short-term molecular and behavioural changes induced by an ischemic lesion in developmental age. In this model, rat pups (P7) underwent unilateral common carotid artery ligation followed by exposure to systemic hypoxia (8% oxygen) at a constant temperature of 37 °C. Brain damage, seen histologically, was generally confined to the cerebral hemisphere ipsilateral to the arterial occlusion, and consisted of selective neuronal death or infarction, depending on the duration of the systemic hypoxia [143]. The drawback is that although the lesion is reproducible and bears some resemblance to lesions observed in affected infants, the method for inducing it is artificial [144].

Because of human perinatal ischemic strokes mainly affect the MCA [145, 146], models developed for adult ischemic stroke were adapted to earlier ages. MCA temporary occlusion in young animals was explored for the first time by [147], who performed this technique in P14-P18 rats. 3 hours of occlusion are sufficient to induce a lesion that affect 40-50% of the total hemisphere and may resemble human stroke. MCAo was also performed in P7 rats, where it is evident the disruption of CBF and cytotoxic oedema formation in MCA territory and subsequent active microglia and astroglia infiltration after reperfusion [148]. However, this method produce an unacceptable high mortality rate, with only 21% of rats survive more than 28 days [149], making difficult any long-term assessment of outcomes.

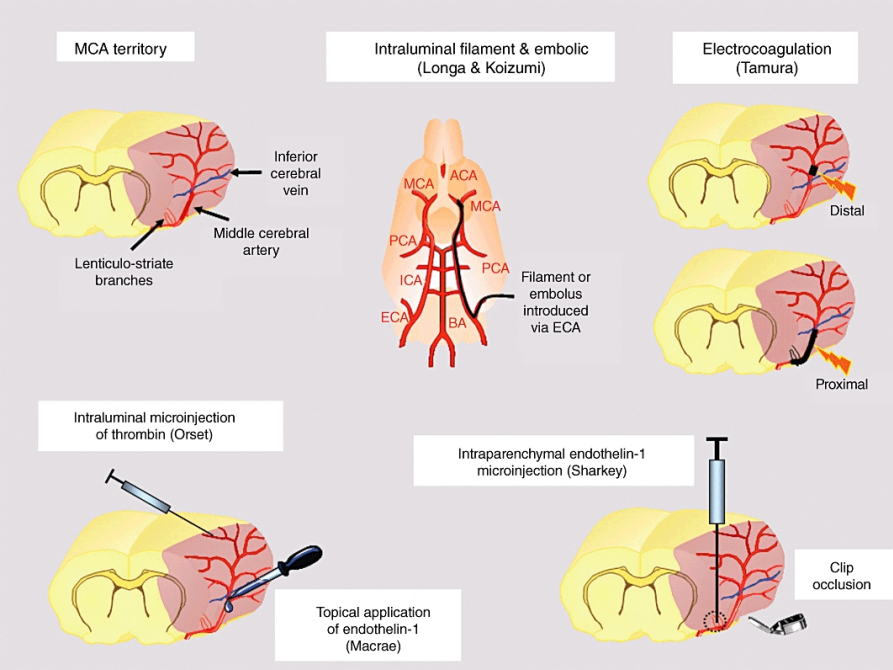

Figure 1.13. MCAo models in rat and mice (modified from [153]).

Embolic occlusion of MCA was also implemented [148]; embolus measure was designed according to rat's size and the infarct induced occupy 51-56% of the ipsilateral hemisphere [150]. Until now, phototrombotic models of perinatal stroke were used only in piglets, where is possible to induce a gray and white matter injury with 7.1-12.3% infarction volume [151]. Recently, ET1 was injected into the striatal area of juvenile (P21) rat brain to induce a reproducible focal lesion [152], but poor information are available about the long-term motor and cognitive outcomes.

1.5 *Treatments for perinatal ischemic stroke*

The diagnosis of perinatal ischemic events can be very diffcult and delayed because the initial symptoms are relatively nonspecific, including hypotonia, apnea, and focal seizures. For this reason, long-term outcome can be highly variable, depending on the time when the pathology is identified. The best treatment choice should take into account all of these considerations, and the timing of therapy application can strongly influence the degree of recovery. In general, for both adult and perinatal stroke events, there are at least two major categories of therapies currently used and investigated in clinics [154]:

1. *neuroprotective therapies*, that are functional in the acute phase of pathology, acting on biochemical and molecular events underlying the onset of ischemic event;
2. *neurorehabilitative therapies*, that are functional in the chronic phase of pathology, acting on the recovery of lost neuronal and motor functions.

Currently, several clinical trials are also being applied on safety and feasibility of *neural stem cells* treatments.

1.5.1 Neuroprotective therapies

Currently, the only FDA approved treatment for ischemic stroke is the *recombinant tissue plasminogen activator* (rtPA), which converts the plasminogen in plasmine, breaking down the fibrin and subsequently the thrombotic clot [155]. rtPA is delivered through an intravenous administration within 4.5 hours from ischemic event, despite some known collateral effects such as cerebral oedemas and hemorrhages [156]. Although antithrombotic interventions have neuroprotective potential that limits stroke volumes, in children affected by cerebral palsy there are very limited data on safety and efficacy of thrombolytic treatment [157].

Hypothermia is one of the most promising strategies for the acute ischemic stroke. Several models of ischemic stroke suggest that hypothermia confers neuroprotection through the preservation of metabolic activity, the reduction of glutamate release, inflammatory and apoptotic processes, and the maintenance and recovery of ionic gradients and physiological pH [158–160]. The first clinical study suggests a potential treatment effect of therapeutic hypothermia on perinatal stroke in terms of reduction of neonatal seizures [161]. However, studies on animal models also suggest that hypothermia is more effective if applied within 6 hours after ischemic event [162], highlighting the crucial problem of delayed diagnosis in perinatal stroke.

Other neuroprotective factors are also being explored in the context of neonatal brain injury, such as growth factors, antioxidants and anti inflammatory therapy [163]. For instance, treatment with *erythropoietin* (EPO) reduces the infarct volume [164], improves the neurogenesis in the SVZ and the behavioural motor outcome [165] in animal models. Interestingly, this

amelioration is also present if EPO treatment starts after 1 week from lesion [166]; furthermore, delayed treatment with *vascular endothelial growth factor* (VEGF) promote endogenous angiogenesis and ameliorates injury [167]. Instead, the antibiotic *minocycline*, a tetracycline derivative that crosses the blood-brain barrier and has general anti-inflammatory action [163], shows controversial effects on perinatal stroke, because in some models it seems to exert a transient positive effect on infarct volume and accumulation of cytokines and chemokines [168] but in another study, it is suggested a different effect of minocycline depending on the rodent species chosen [169] Another anti-inflammatory agent is the *Sildenafil*, a cyclic GMP phosphodiesterase inhibitor, that in a neonatal model of global ischemic stroke reduces the number and the activation of microglia [170, 171].

Considering all the benefits and pitfalls of these treatments, it could be possible that a combination of more than one neuroprotective agent or therapy may provide more long-lasting neuroprotection, preserving the brain from severe injuries and enhancing repair and regeneration processes [163].

1.5.2 Neural stem cells (NSCs) therapy

Neural stem cells (NSCs) therapy represent an exciting area of experimental and clinical research, with multiple possibility of intervention yet unexplored. Stem cells are mainly characterized by pluripotent or multipotent ability to develop in several cell types, depending on external environments and signals. Endogenous NSCs are produced, also in the adults, in the *subventricular zone* (SVZ), dentate gyrus of hippocampus and in the olfactory bulb.

It was demonstrated that brain ischemia induces an upregulation of endogenous NPCs and sometimes differentiation into the predominant cell type of the injured region [172, 173]. Therapeutic approaches have focused on augmenting the brain's normal endogenous reaction to injury, through several neurotrophins, growth factors or hormones, including GDNF, BDNF, G-CSF, IGF-1, or EPO [174–176]. Another research field is represented by the delivery of exogenous NSCs, that can originate from immortalized cell lines, human neural progenitor cells (NPCs), bone marrow-derived hematopoietic/endothelial progenitors and stromal cells [177]. It was demonstrated that these cells are able to improve recovery in

several models of stroke, even if it is necessary to reduce the risk of tumor formation [178]. Another intriguing stem cell type is represented by *induced-pluripotent stem cells* (iPSCs), that derive from adult differentiated fibroblasts that can be easily reprogrammed [179]. One of the main advantage is the possibility to generate patient-specific cell lines, minimizing the risk of immune rejection after transplant. In a recent study, the cortical or striatal transplantation of iPSCs in a rodent model of focal stroke effectively integrate in the circuit and promote a significant recovery of motor functions [180]. The mechanism underlying this recovery seems to be correlated to neurotrophic factor release and anti-inflammatory effects rather than neuronal and circuit replacement. Currently, phase I/II clinical studies are implemented, suggesting a good level of safety and feasibility of direct intracerebral transplantation of mesenchymal and bone marrow-derived stem cells [181, 182].

1.5.3 Neurorehabilitative interventions

1.5.3.1 Constraint-induced movement plasticity (CIMT)

This technique is a form of rehabilitation therapy that improves upper extremity function through the forced constraint of the healthy limb and the contemporary training of the affected one. Typically, CIMT involves immobilization of the unaffected arm in adult patients with hemiparetic stroke or hemiparetic cerebral palsy for 90% of waking hours while engaging the affected limb in a range of everyday activities coupled with intensive (about 6 h a day) task-oriented training of the affected arm [183]. Simplified version of CIMT is forced use therapy, which includes only immobilisation of the nonparetic arm to increase the amount of use of the paretic limb [184]. It has been shown that receiving CIMT early on (3–9 months post-stroke) will result in greater functional gains than receiving delayed treatment (15–21 months post-stroke) [185].

CIMT induces cortical plasticity: TMS studies have demonstrated a significant expansion of affected hand cortical representation in chronic hemiparetic patients after a CIM treatment [186]. Multiple paediatric trials support the effectiveness CIMT in hemiparetic cerebral palsy [103]. These studies likely include a high proportion of perinatal strokes, but

their results, while encouraging, remain clouded by disease heterogeneity. Moreover, other important limitations of constraint-induced movement therapy include a modestly invasive nature, particularly for young children, and the exclusion of bimanual learning [103].

1.5.3.2 Electrophysiological stimulations

It is widely demonstrated that therapeutic approaches based on non-invasive brain stimulation are powerful methods to modulate human brain function and to induce plastic changes during post-stroke recovery. One of these therapy is represented by *repetitive transcranial magnetic stimulation* (rTMS), used in wide research and clinical fields, including multiple sclerosis, ALS, movement disorders and ischemic stroke. The method consists of a magnetic coil placed near to the head of the subject; the coil produces trains of electromagnetic field pulses that induce small current changes in the brain. High frequency trains (10 Hz) induce the stimulation of motor cortex, whereas low-frequency repetitive transcranial magnetic stimulation (1 Hz) inhibits the cerebral cortex [187, 188]. Instead, *transcranial direct current stimulation* (tDCS) is a neuromodulatory technique that uses weak, direct electric currents delivered through the scalp to the neuronal tissue to induce changes in cortical excitability according to the parameters of stimulation. The procedure elicits focal reversible shifts in cortical excitability depending on the polarity, strength, and duration of stimulation; in particular, animal studies, also confirmed for humans [189], have established that *anodal* stimulation seems to increase neuronal excitability and spontaneous firing rate by depolarizing resting membrane potentials, whereas *cathodal* stimulation hyperpolarizes membrane potentials, leading to decreased neuronal firing rate and excitability [190]. tDCS is most commonly applied at 1–2 mA for 5–20 minutes using saline-soaked sponge electrodes and has been shown to have effects across various functions [191].

Although these two techniques can produce similar physiological and behavioural effects, TMS and tDCS are believed to operate by different mechanisms [190]. In humans, rTMS induce LTP-like and LTD-like plasticity effects in the neocortex, with significant changes in *motor evoked potential* (MEP) amplitudes; pharmacological evidence suggest a pivotal role of NMDA receptors [190]. Unlike rTMS, which is believed to induce action potentials in and

around the stimulated neuronal tissue, tDCS is considered to have a modulatory effect on cortical excitability [189].

Currently, both rTMS and tDCS are also applied in presence of perinatal or pediatric ischemic stroke [192]. The PLASTIC CHAMPS study [193] confirms safety, feasibility and suggest consistent functional gains across groups. In contrast to adult ischemic stroke, in case of perinatal event it is necessary to optimize the dosage; for instance, recent studies suggest a tDCS protocol adapted for perinatal stroke characterized by a 10-minute reduced current application (0.7 mA) [194].

1.6 *Neural plasticity in the recovery after stroke*

After a stroke event, the damaged circuits can undergo a relative small or great degree of remapping and functional restoration, that leads to a spontaneous recovery of impaired functions. These functional gains are mainly enclosed in a "critical period" window, that occupies few months in humans and few weeks in rodents after injury [195, 196]. Commonly used human and animal behavioural assessment protocols are not sensitive to distinguish, in the improvement of performances, between *"true" recovery* (restoration of original pre-lesion strategies), *behavioural compensation* (the restoration of function through alternative and novel strategies) or a combination of both. For instance, detailed post-injury kinematic analysis of rats reaching movements show that motor impairments are balanced by postural adjustments that allow a partial recovery of pre-stroke motor performances [197]. Moreover, forelimb lift, pronation and supination remain altered despite significant success in a skilled reaching task during a chronic phase after stroke injury, indicating the presence of compensatory mechanisms [198]. In general, long-lasting rewiring of damaged local or distant circuits represent a fundamental point of investigation in post-stroke recovery research. However, it is yet unclear whether these plastic processes invest only a positive or also a *maladaptive* role after a stroke event; in particular, the intrinsic characteristic of the lesion, the *timing* of its onset and also the therapeutic intervention window, can influence in different manners the ability to recovery of lost or altered neuronal functions [199, 200].

1.6.1 Synaptic learning rules after ischemic stroke

The presence of activity-dependent processes and critical periods effects suggest strong correspondence between stroke recovery and synapse-based learning rules that are involved in wiring and refining of brain connections [201]. As described above (see paragraph 1.1.2), the two main conceptual classes of synaptic plasticity mechanisms are the Hebbian and homeostatic plasticity. While Hebbian rules have a pivotal role in producing activity-dependent changes in synaptic strength in learning and memory [202], few evidences directly support this role in stroke recovery. However, specific forms of use-dependent rehabilitative training (such as reaching training for an impaired limb), based on typical Hebbian rules, can influence rewiring and functional outcome [203]. Also homeostatic plasticity may be involved in recovery. Post-stroke neuronal hyperexcitability of peri-infarct zone, often resulting in an increasing spontaneous activity, occurs within the first month after injury, and can be linked to an attempt of circuit to upscale its connectivity level in a compensatory manner [199]. In this way, also axonal sprouting and increase in dendritic spine production, events highly correlated with the onset of stroke, may be considered as homeostatic processes that help to return post-stroke synaptic activity to standard levels [199]. However, it could be also possible that the system could take advantage from a reduction of activity, rather than an hyperactivation. Clinical and experimental reports show that very early physical therapy, in particular if too intensive, might be detrimental for stroke recovery [204, 205]. For this reason, it is worth considering all of these factors in the implementation of effective rehabilitation protocols, and further studies are needed to unveil the role of homeostatic and hebbian plasticity in different type of stroke injuries.

1.6.2 Molecular determinants of axonal sprouting

Brain injury, and in particular ischemic stroke, leads to a dramatic change in the molecular expression programme of affected neurons, especially in those cells that survive lesion in the peri-infarct region.

Axonal sprouting represents one of the principal responses caused by this new molecular

pattern expression, and is triggered by several factors, including cytokines released by astrocytes, microglia and infiltrated neutrophils [206, 207]. However, activated astrocytes also block the axonal sprouting through the action of CSPGs or Ephrin-5 [126, 208]. These events mainly involve the peri-infarct area, where classical axonal growth markers such as GAP-43, CAP23 and the transcription factor c-Jun are expressed [126].

Peri-infarct regions release a great number of growth factors that promote axonal and dendritic sprouting, including BMP7 [209], IGF-1 and TGF-beta signalling factors; in particular, *GDF10* and *Activin* act through their respective cell surface receptors to the transcription factor Smad 2/3 [210, 211], activating *phosphatidilinositol-3* (PI3) kinase gene systems and inhibiting both *phosphatase and tensin homolog* (PTEN) and *suppressor of cytokine signalling* (SOCS3) action. PTEN is a well-known negative regulator of *mammalian Target of Rapamycin* (mTOR) signalling, and its deletion is essential to increase the CSNs regenerative ability after CNS lesion [212]. The involvement of PTEN and SOCS3 in axonal sprouting was also demonstrated in other contexts in the adult, such as in optic nerve and spinal cord injury [213–215]. Taken together, these data indicate that GDF10 is an important molecular trigger after stroke and activates parallel growth promotion cascades.

IGF-1, produced by microglia or delivered through intranasal pathway, is known to promote neurogenesis [216]. Unexpectedly, IGF1 delivery does not induce any significant change in motor cortical connections above the normal degree of post-stroke axonal sprouting; moreover, endogenous IGF-1 expression levels arise only after an adult ischemic stroke, but not during young age [217].

In peri-infarct cortex, gene profile of axon sprouting neurons reveals the specific activation of growth factor, cytokines, cell surface receptor, cytoplasmatic cascade and transcriptional and (epi)genetic modifications. The comparison between molecular profiling in young and adult lesioned animals shows that only few genes are commonly regulated by stroke in these two ages ([217], suggesting that the axonal transcriptome (also called "*sproutome*") could have a crucial role in the distinct response of an ischemic stroke in different ages. Expression of genes involved in epigenetic DNA control, such as *ATRX*, is up-regulated

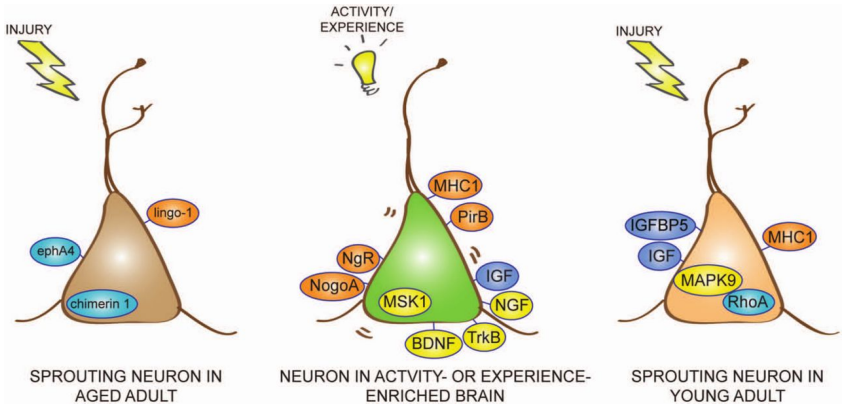

Figure 1.14. Molecules associated with injury-, activity-, and experience-induced plasticity (modified from [208]).

in both young and adult sprouting neurons. Axonal sprouting neurons in the aged brain paradoxically upregulate genes that block axonal growth, such as EphA4 and *Lingo-1* [217]. Lingo-1 is part of the Nogo Receptor 1 (NgR1) signalling complex, which includes NgR1/p75 or TROY/Lingo-1 [218]. Blockade of NgR1 signalling either directly by genetic knockout or pharmacologically with a Lingo-1 antagonist, also causes more robust axonal sprouting after stroke [217]. Finally, it has been shown that other molecules can restrict structural plasticity after injury: for example, PirB and MHCI ligands limit axonal outgrowth in development and regeneration after injury both *in vitro* and *in vivo* [38] (1.14).

1.6.3 Function of cortical remapping after an ischemic stroke

Recovery after small strokes mostly involve peri-infarct tissue remapping [219], whereas in larger lesions similar function lesion can only be found in more distant sites, such as premotor cortex or contralateral hemisphere [220, 221]. This contralateral axonal sprouting has been reported in rodents and non-human primates after cortical lesions [222–224] and is associated with remapping of motor representations of the ipsilateral limb in this motor cortex. These findings suggest that the recovery of sensorimotor functions after stroke and brain remapping involve changes in the temporal and spatial spread of sensory information processing across local and distant sites. Recently, Muprhy and colleagues have implemented novel optogenetic approaches for mapping motor maps in mice after stroke [225–227]. Optogenetics represents an important technical progression in neuroscience that

allows the selective activation or inhibition of neurons, *in vivo*, through genetical expressed channels or pumps activated by light (for review, [228, 229]). For instance, it is possible to express the cation light-activated *channelrhodopsin-2* (ChR2) in layer V pyramidal neurons using transgenic mice models; laser stimulations at specific blue wavelengths induce the firing of these corticospinal neurons, that results in a clear movement of the contralateral forelimb [230]. Using this approach, it was demonstrated that motor output is strongly reduced in the area immediately adjacent to the lesion, counterbalanced by an increased excitability of other peri-infarct areas, suggesting that surviving regions of cortex are able to assume functions from stroke-damaged areas, although this is also correlated to an alteration of motor maps [231]. The combination of optogenetics and *voltage sensitive dyes* (VSDs) techniques allows the coupled cortical stimulation and imaging of activated areas, in order to define a clear "*connectome*" pattern in physiological and pathological conditions with high temporal resolution and large-scale recording of neural activity [232]. In rodents, a unilateral photothrombotic stroke induces an alteration of the normal symmetry between hemispheres, with a depression of activity that involve not only the lesioned but also the healthy hemisphere after 1 week [233] (figure 1.15).

Ischemic strokes also induce strong modifications in the dendritic plasticity, in terms of formation and retraction of dendritic spines. The onset of this remodelling is fast; in fact, a series of *in vivo* studies demonstrated dynamic changes to dendrites in layer 1 during the onset of ischemic depolarization [234–236], that generally occurs upon first 2 minutes from ischemic event [234]. After stroke, there is initially a net loss of dendritic spines in peri-infarct cortex within 24 h after photothrombotic stroke [237, 238] and in the first week after middle cerebral artery occlusion [239]. Interestingly, dendritic remodelling occurs in regions with a normal blood flow [239], indicating that spine loss is mostly due to neuronal network damage from loss of axonal connections and not due to partial ischemia in peri-infarct regions.

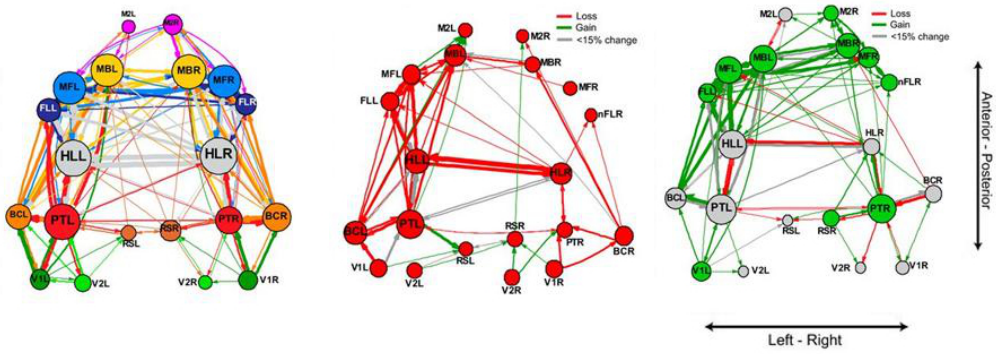

Figure 1.15. Network diagrams of connectivity changes over time reveal interhemispheric asymmetries after phototrombotic stroke. It was used optogenetic stimulation of multiple sites on the brain coupled with voltage-sensitive dye (VSD) relative responses. *Left*, connectivity map in sham animals. *Center*, connectivity map in lesioned animals after 1 week post-stroke; note the strong interhemispheric asymmetry and general depression of neural activity. *Right*, after 8 weeks post-stroke the network diagram appears to be returning toward sham levels (modified from [233]).

1.6.4 Experimental modulation of structural plasticity after stroke

Both positive and negative effectors can modulate the plastic response of the post-stroke brain. Moreover, the combinatorial approach of coupled pharmacological plasticizing treatment and physical rehabilitation protocols are widely studied in experimental research.

Pioneer studies from Schwab's laboratory investigated the role of the blocking of NogoA inhibitory activity on axonal sprouting through the injection of specific antibodies (*anti-NogoA*, [240–242] or *inosine* [243, 244] or both treatments coupled with environmental enrichment [245], showing a positive effect of cortical and subcortical sprouting on behavioural motor outcome. More recently, it was demonstrated that intrathecal injection of anti-NogoA after focal stroke in adults promote a rewiring of the CST in terms of augmented sprouting of fibers from the intact hemisphere into the denervated side of the spinal cord [223] (1.16). In another pivotal study, anti-NogoA treatment was coupled with an intensive physical rehabilitation training. When physical rehabilitation follows the pharmacological treatment (*sequential* protocol), there is a dramatic and progressive recovery of motor function, accomplished by a strong and well directed sprouting at spinal cord level from healthy to denervated side. Interestingly, if these treatments are applied together (*parallel* protocol) the recovery is significantly slower, with misdirected sprouting at spinal cord

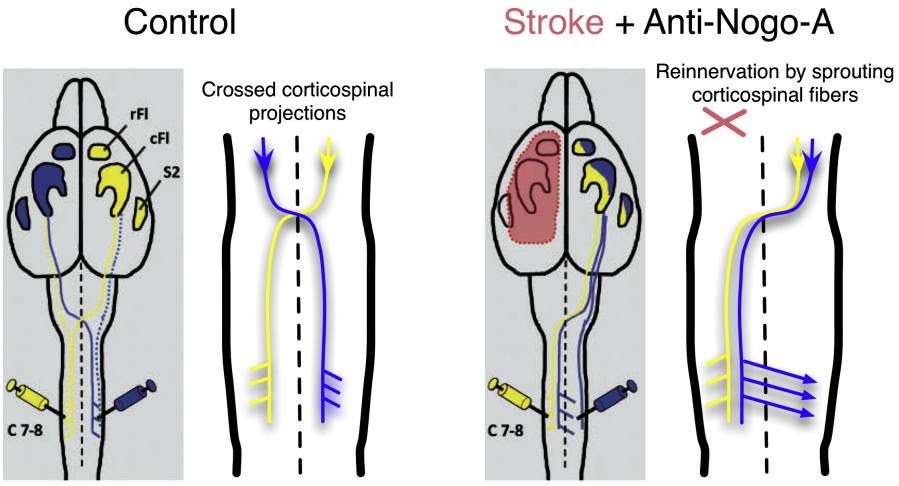

Figure 1.16. Anti-NogoA treatment promotes functional sprouting of fibers originating from healthy hemisphere to the denervated side of spinal cord (modified from [223]).

level, even if the overall sprouting level is higher with respect to sequential control [246] (1.17). Other studies confirm that genetic deletion of Nogo-A, or Nogo-A antagonism coupled with motor training leads to enhanced recovery from stroke [241, 247]. These findings suggest the importance of intervention timing and reinforce the role of physical rehabilitation in the stabilization of circuits modified by plasticity processes.

Several studies have been focused on the role of PNNs in stroke recovery and the plastic effect induced by their remodelling. As described above, ChABC is an enzyme that digest the side chains of CSPGs that form the PNNs surrounding PV^+ inhibitory neurons, modifying visual cortex plasticity (see paragraph 1.1.3.1). In a similar way, intraspinal injection of ChABC after a focal ischemic stroke in elderly rats effectively remove CSPGs from the extracellular matrix, promoting the sprouting of the contralesional CST and recovery of motor function [248]. ChABC is also effective in peri-infarct area, where, in combination with a skilled motor training, induces an amelioration of motor outcome after a focal stroke through a counterbalance of the excitatory inputs [249].

1.6.5 Maladaptive plasticity

As shortly described above, ischemic stroke events can spontaneously induce molecular and structural changes in neural circuits, and clinicians can take advantage of these process to drive the appropriate therapy for the treatment of this pathology. However, neural plasticity

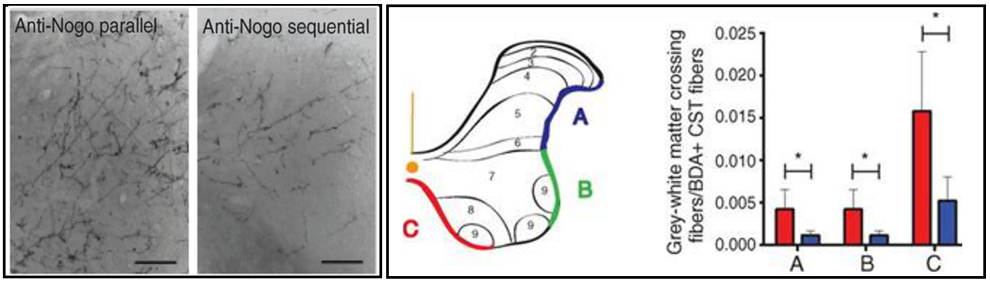

Figure 1.17. CST sprouting after unilateral stroke depends on timing of rehabilitative and pharmacological training. *Left*, sprouting patterns of ipsilateral fibers to the denervated side of spinal cord in animals with different rehabilitative protocol. Note the substantial increase in axonal projections when behavioural activity is manipulated at the same time as axonal growth is pharmacologically stimulated. *Right*, scheme of the spinal cord gray matter, included laminae. Red columns indicate simultaneous Nogo blockade and behavioural activity; blue columns indicate first Nogo blockade then behavioural activity. When Nogo is blocked and skilled reach training implemented simultaneously, there is axonal sprouting throughout the spinal cord gray matter, including to non-motor areas (modified from [246]).

does not only exerts a positive effect in the improvement of motor recovery, on the contrary can lead to adverse outcomes; this aberrant form of neural plasticity, called *maladaptive plasticity*, characterizes in particular developmental injuries, where the affected corticospinal tract does not assume a primary role in movement control in the first few months after birth [91], and as a consequence, an abnormal bilateral pattern of innervation is established (figure 1.18). Several studies have reported its involvement in alteration and limitation of motor function after stroke. First, the implementation of compensatory motor strategies is a crucial trigger for the alteration of motor functions; for instance, the dominant use of the healthy side (i.e. the nonparetic limb) induces the phenomenon of *learned non-use* of the paretic limb, which limits the capacity for subsequent gains in motor function of the paretic limb [250].

An important role in maladaptive plasticity process after stroke is carried out by ipsilateral projection from the healthy hemisphere. In hemiplegic children, the abnormal persistence of ipsilateral corticospinal projections, that normally withdraw during postnatal development through activity-dependent processes (see paragraph 1.2.2.2), is associated with a poor motor recovery [251, 252]. These clinical evidences contrast the *Kennard principle*, that states how the physiological outcome after a brain lesion is negatively correlated with age; in particu-

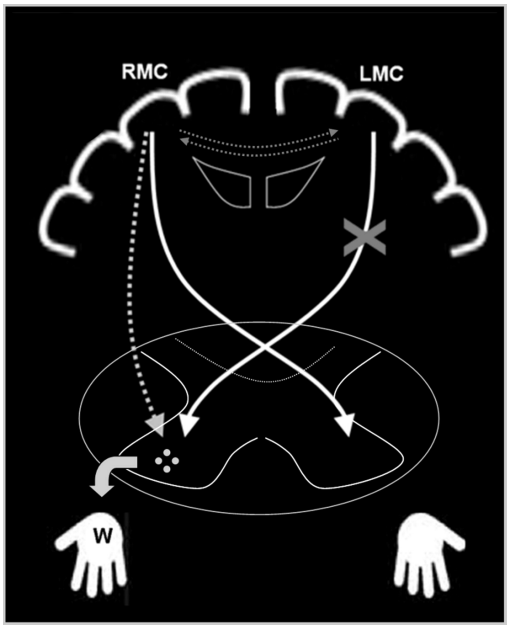

Figure 1.18. Developmental plastic motor organization after perinatal stroke. Control of the weak right hand (W) often relies on both contralateral corticospinal pathways from the left (lesioned) primary motor cortex (LMC) and ipsilateral projections from the unlesioned right primary motor cortex (RMC, dashed line). These two inputs compete to establish synapses. The relative balance of control determines motor outcome, with contralateral control associated with better function (modified from [103]).

lar, Kennard described better outcomes in younger primates after unilateral motor cortex lesions [253]. Despite it appears counterintuitive that activity driven maintenance of ipsilateral projections from the non-infarcted hemisphere is not associated with preservation of function, several studies confirm this hypothesis. For instance, Eyre et al. demonstrated that children affected by unilateral perinatal stroke loss MEPs responses from TMS stimulation of lesioned cortex, whereas the same stimulation in children with bilateral perinatal stroke does not reduce MEPs amplitude [254]; these results clearly resemble experimental data from cats described above (see paragraph 1.2.2.2). All of these data suggest a vicious circle of maladaptive activity-dependent competition, where the less competitive spared corticospinal projections provokes the gain of ipsilateral axons activity, with reciprocal influences from these competitions [255].

1.7 *Aim of the thesis*

Developmental stroke (perinatal or pediatric) represents a rare cerebrovascular disorder and a frequent cause of hemiplegia in children. Despite the high plastic potential of developing brain, a unilateral ischemic lesion at early stage of development deeply affects the normal functional refinement of motor pathways. Strengthening of CST ipsilateral projections from the healthy hemisphere (otherwise pruned with normal development) in favor of the contralateral ones has been pointed at the cornerstone of maladaptive plasticity mechanism after developmental injury. The occurrence of this "maladaptive plasticity" could be responsible for driving the long term functional outcome towards a moderate or severe motor impairments. Studies in rodent might effectively help detection of axonal sprouting, and may reveal to which degree injury affects axonal terminal fields and shed light on the molecular and anatomical basis of this maladaptive phenomenon. In this study, I investigated the anatomical underpinnings of ischemic lesion timing effects on motor outcome to understand how plasticity mechanisms can promote or preclude motor recovery in an age-dependent manner.

The aims of the thesis are:

1. Characterization of rat models of focal ischemic stroke during the development of corticospinal tract, through the intracortical injection of endothelin-1 (ET-1) at P14 and P21 pre-weaning ages;
2. Analysis of structural modifications, in terms of axonal sprouting and laminar distribution onto the denervated side of spinal cord, induced by lesion at different ages, taking advantage from AAV-GFP anterograde tracer injected in rat pups;
3. Studying the effects of an early activity-dependent modulation, by means a skilled motor learning paradigm in P14 injured animals, on corticospinal structural plasticity and functional recovery after a developmental ischemic lesion.

2 Materials and Methods

2.1 *Experimental design*

All procedures were performed in accordance with the Italian Ministry of Health guidelines for care and maintenance of laboratory animals (law 116/92) and in strict compliance with the European Communities Council Directive 86/609/EEC.

Long Evans rats from P1 until to P60 of both sexes were used. Animals were housed with a 12 h/12 h light/dark cycle with food and water *ad libitum* access. After weaning at P20, animals were reared in a standard environment (3 rats in 30 cm × 40 cm × 20 cm laboratory cages). During Montoya Staircase test, rats were fed 20 g of Purina® rat chow once a day after the daily tests [256] in addition to the food pellets they obtained while performing the test (Bio-Serv® dustless precision pellets product F0021). The weight of the rats was maintained at about 90–100% of their expected body weight. All behavioural and anatomical analysis were performed in a blinded fashion.

2.2 *Injection of viral tracer into rat pups*

AAV1-hSynap-eGFP-WPRE-bGH (titre 10^{11} copies/ml, Addgene®) was used as anterograde tracer of CST, because it was demonstrated a strong tropism for CSMNs of these serotype and promoter [257]. P1-3 rat pups were taken from their cages and anesthetized through hypothermia, covering them under approximately 6 cm of crushed ice for a duration of 1 min/g of body weight. Once anesthetized, pups were positioned and blocked on an adapted stereotaxic apparatus (Cunningham, Stoelting Co.©) previously cooled with dry ice. An head

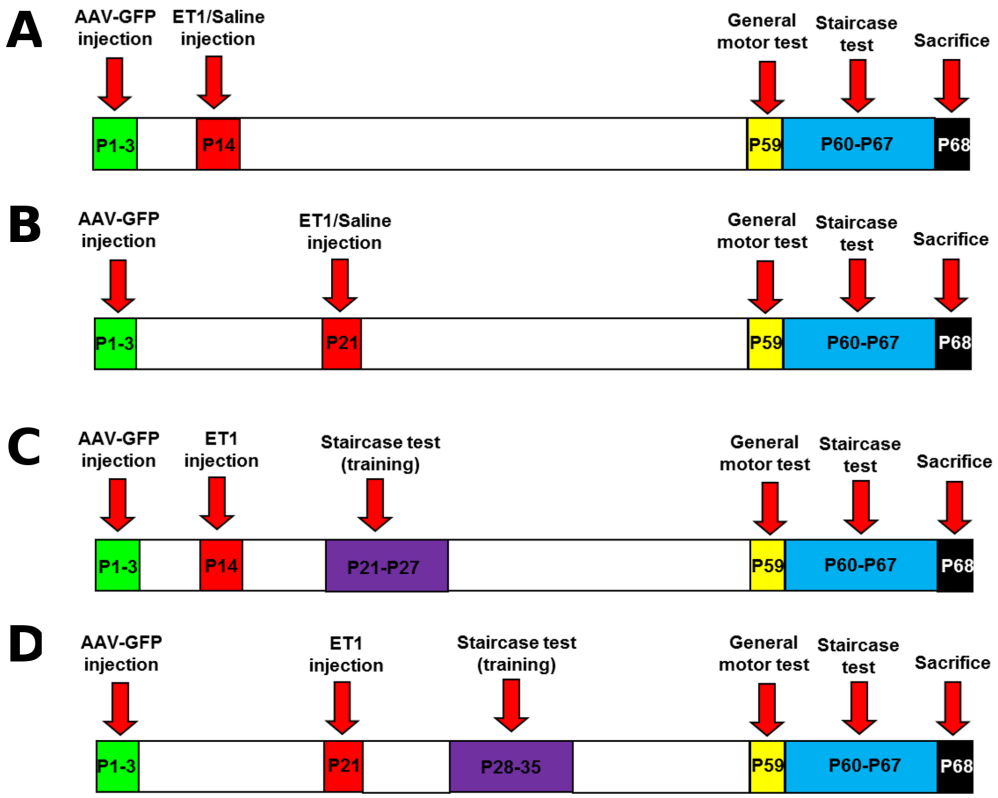

Figure 2.1. (A) and (B). Experimental design for behavioural and anatomical assessment of ET-1 or saline intracortical injections in P14 and P21 animals, respectively. (C) and (D). P14 and P21 animals, respectively, performed an early training protocol 1 week after lesion.

skin incision through the midline was made, and 4 holes were produced through a modified 30-gauge needle at specific stereotaxic coordinates for somatosensory right cortex (with respect to Bregma: 1) 1.5 mm ML : 0.7 mm AP; 2) 1 mm ML : 0.3 mm AP; 3) 1 mm ML : 0.0 mm AP; 4) 2 mm ML : 0.5 mm AP). A previously pulled glass micropipette was filled with 1 μl of AAV solution and was connected to a pneumatic ejection pump (PDES-02TX, npi®). The micropipette was held perpendicular to the skull surface and slowly inserted on each injection site, at a depth of 0.5 mm. Once the pipette was in place, 0.25 μl/site of viral solution was gradually injected into each hole (pressure 1 bar, time of pressure 0.3-4 ms). At the end of each injection, the micropipette was left in place for 2 minutes to allow the viral vector diffusion from the injection site. After the injections were completed, pups were placed under a heating lamp until they regained normal colour and resume both breathing and movements. Finally, injected animals were transferred to the home cage with their mothers.

2.3 *Induction of ischemic lesion in P14 or P21 rats*

ET-1 unilateral intracortical injection was used to induce a focal ischemic lesion in the forelimb area of primary motor cortex (fM1) in P14 or P21 rats, with a protocol modified from [249]. Prior to surgery, animals were anesthetized globally through intraperitoneal injection of avertin (200 mg/Kg) and locally through a subcutaneous injection of lidocaine (100 mg/Kg) under the scalp. The head was then blocked on a stereotaxic frame using adapted ear bars. Body temperature was monitored and maintained at 37 °C with a homothermic blanket (Harvard Apparatus Ltd©, UK). To perform unilateral lesions in the left hemisphere, we performed an incision to the scalp and displaced the periosteum to reveal anatomical landmarks on the skull. The 2 sites of injection were identified in correspondence to the left fM1 (with respect to Bregma: 1) 1.5 mm ML : 0.0 mm AP; 2) 1.5 mm ML : 0.5 mm AP) [258], and the skull was gently drilled cooling the area with sterile saline. A previously pulled glass micropipette was filled with 2 μl of ET-1 solution (Sigma-Aldrich®, 120 pmol/μl in sterile saline) for experimental groups, and 2 μl of vehicle for control groups, and connected to a manual pump. The micropipette was held perpendicular to the skull surface and slowly

inserted on each injection site, at a depth of 0.5 mm for P14 and 0.7 mm for P21 animals. Once the micropipette was in place, 1 μl/site of ET-1 solution or vehicle was gradually injected into each hole. ET-1 was delivered at a rate of 0.5 μl/min with a 2-minute interval before retracting the micropipette from the tissue. Immediately after surgery animals were given local antibiotic (Aureomicina® 3% cream) on the surgical suture and analgesic (Tachipirina® gocce, 10 mg/kg) administered in drinking water. Animals were kept under a heating lamp until they recovered from anaesthesia. P14 animals returned to their mothers in the home cage.

2.4 *Behavioural assessment of motor function and motor training*

All behavioural tests were carried out by an operator blind to group membership of the animals. Animal motor profiles, including locomotion analysis and evaluation of muscles strength were assessed the day before injury, P20, and at adult age, P59. Reaching skills were assessed from P60.

Vertical ladder test allows the assessment of motor coordination (figure 2.2A). Animals were encouraged to climb a vertical ladder of 100 cm length with 1 cm distance between rungs [259]. Three trials per animals were video recorded and analysed offline. Average time taken to climb the full vertical ladder length was quantified.

Grip strength test allows a reliable measure of forelimb muscle strength (figure 2.2B). Animals were placed over a base plate, in front of a trapeze-shaped grasping bar. Animals were lifted over the base plate by the tail so that their forepaws were allowed to grasp onto the steel grip of and gently pulled backward by the tail until the grip was released. Three trials were performed for each animal with a 1-minute resting period between trials. Muscular strength was assessed by sensing the peak amount of force that was required to make animals release their grip, conveyed in grams (Ugo Basile® Grip-Strength meter). Forelimbs grip strength was measured as average tension force of the three trials per animal.

Gait analysis was performed to assess animals' locomotor pattern and forelimb posture during walking (figure 2.2C). Limb rotation and inter-limb coordination were considered

the most descriptive parameters [260, 261]. The fore and hind paws were painted with inks of different colours (red the former and black the latter) and rats were encouraged to walk in a straight line along a 100 cm long runway over absorbent paper (10 cm width) toward home cage. Since this task is aimed at assessing the rat spontaneous walking pattern, no training was required before baseline recording. Footprint patterns were then digitalized and analysed using MetaMorph® software (Molecular Devices©, USA). Limb rotation score was estimated by the angle formed by the intersection of the line through the print of the third digit and the central pad (the print representing the metatarsophalangeal joint) and the line through the metatarsophalangeal print parallel to the walking direction, was used as an indication of limb rotation. Inter-limb coordination was measured as the distance between the central pads of the forelimb and hind limb on each side of the body. Three trials for each animal were performed and a series of at least 10 sequential steps printed in the same session was used to determine the mean values of each measurement.

To assess long lasting reaching and grasping impairments, animals were trained for 7 days from P60 in *Montoya Staircase* skilled reaching task [262] (figure 2.2D). The Staircase apparatus consists of seven steps located to the left and right of the animal, where pellets can only be obtained by the respective left and right forelimbs (three pellets/step). Animals were handled every day for 3 days before the onset of the experiment while let familiarizing with the staircase box and were food restricted in their home cage from 1 week before the experimental recordings. After habituation, rats were trained to remove and eat as many food pellets as possible from the staircase (Bio-Serv® dustless precision pellets product F0021). Two parameters were measured: 1) number of pellets retrieved and eaten; 2) number of step reached on each side of the staircase during the task. Animals were trained to reach for pellets once/day for 15 minutes.

To investigate the effects of a specific early motor training in skilled reaching on motor outcome and CST axon plastic remodelling, a group of animals treated with ET-1 at P14 or P21 were trained once/day for 7 days in the Staircase apparatus starting 1 week after lesion induction. Afterwards the effect of this specific early training on general movement

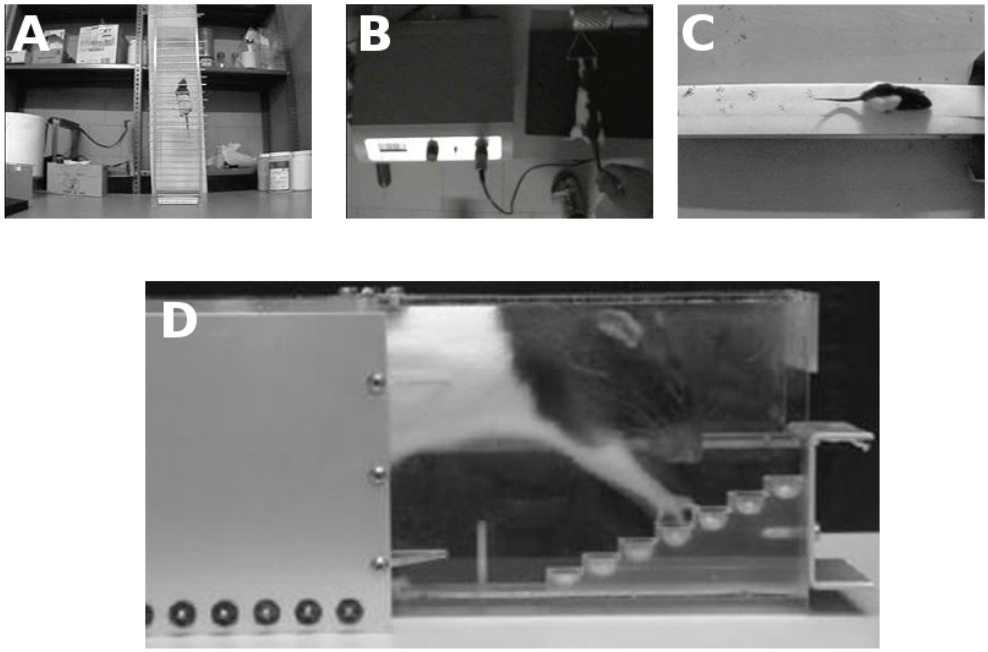

Figure 2.2. Behavioural motor battery. (A) Vertical ladder test. (B) Grip test. (C) Gait test. (D) Montoya Staircase test.

performance and on reaching capability was assessed up to adulthood, from P59, and the results were compared with those of control groups consisting of untrained P14 and P21 ET-1 or saline injected animals.

2.5 *Histology and lesion volume measurement*

After behavioural assessment, animals were deeply anhaestetized with chloralium hydrate (10%) and transcardially perfused with PBS (pH 7.4) followed by paraformaldehyde 4% (PFA) 0.1 M phosphate buffer. Both brain and spinal cord was extracted and post-fixed in the same fixative overnight at 4 °C, then immersed in a dehydrating solution of sucrose 30% and sodium azide 0.05% for at least 3 days. Dehydrated tissues were embedded with Tissue-Tek® OCT™, snap-frozen in −80 °C cooled isopentane, and 50 μm coronal sections of brain and cervical spinal cord were cut with a cryostat (Leica®).

To allow a reliable measure of the lesion volume, coronal slices of entire motor cortex were collected; 1 out of 2 slices were then stained with propidium iodide (5 μ/ml, Sigma-Aldrich® and later mounted and cover slipped. Images were acquired with Leica® fluorescence micro-

scope and lesion area was measured using the MetaMorph® software (Molecular Devices©, USA). The lesion volume was calculated by computing individual lesion areas multiplied by the interslice distance.

1 out of 10 slices of medullar pyramids (at the level of caudal cerebellum) were also collected and mounted. Cervical spinal cord was sectioned from C5 to T1 levels; a total number of 4 sections/level were obtained, collecting 1 out of 6-8 consecutive slices.

2.6 *Analysis of axonal sprouting at spinal cord level*

For analysis of GFP^+ axonal sprouting from labelled dorsal CST (dCST) and ventral CST (vCST), spinal cord slices were analysed online through a fluorescence microscope (Leica®), magnification 20x, using the software Stereo Investigator (MBF Bioscience ©). At least 3 sections per level were measured for each rat. For all slices, GFP signal was detected without immunohistochemistry procedures. GFP^+ axonal fibers originating from labelled dCST and reaching contralateral denervated spinal cord were counted as fibers crossing the spinal cord midline (M) and branching through 4 different distance lines (D1-4), with each line 100 μm apart. GFP^+ axonal fibers originating from labelled vCST and reaching ipsilateral denervated spinal cord were counted as fibers crossing the boundary between white-gray matter of the medial part of ventral horn [246]. dCST and vCST fiber sprouting were expressed as the number of GFP^+ axons in the spinal cord divided by the number of GFP^+ fibers counted in the medullar pyramids.

To measure the fluorescence integrated density of dCST and vCST, 10x magnification images were acquired at a fluorescence microscope (Zeiss©) and analysed with ImageJ software. For each animal, at least 3 sections per level were analysed, and both time exposure and fluorescence intensity were maintained constant in order to reduce the variability due to different transduction efficiency. Integrated density values were divided by the number of GFP^+ fibers counted in the medullar pyramids.

To normalize axonal sprouting and fluorescence analysis for viral transduction efficiency, the total number of GFP labelled corticospinal axons were counted on at least 3 coronal

sections of medullar pyramids. Images were acquired at a fluorescence microscope coupled with the structural illumination system ApoTome (Zeiss©). ApoTome setup provides an axial resolution in the z-axis that is comparable to that achieved by confocal microscope [263]. To quantify the total number of GFP labelled corticospinal axons, 63x magnification images of two regions of interest (ROI) in the medullar pyramid were acquired and then extrapolated to the total area of pyramid per slice, measured from 5x magnification images. Acquired images were analysed offline using the dedicated software Imaris (Bitmap®). GFP^+ axons were detected as "spots", with a minimum diameter settled on 1 μm and a double "quality" filter (intensity at the center of the spot in the channel the spot was detected) optimized to include only reliable axons.

2.7 *Laminar pattern distribution of sprouted axons*

Z-stack images of 3 C6-C8 spinal cord sections per animal were obtained using ApoTome module (Zeiss©), with a magnification of 10x. Images were acquired both in brightfield and in green channel fluorescence, in order to recognize anatomical landmarks of spinal cord gray matter.

The analysis of laminar pattern distribution of GFP^+ sprouted axons was performed using a custom-made MATLAB® script, based on *mathematical morphology* theory (figure 2.3). Briefly, 15 square ROIs (129x129 μm) per section were selected on standardized positions located using brightfield cues, in order to sample all spinal cord laminae (figure 2.3A). ROIs 1 to 5 identify *dorsal* sensory laminae (1 to 6), ROIs 6 to 10 the *intermediate* lamina 7 and ROIs 11 to 15 the *ventral*, motor laminae 8 and 9 (figure 2.3B). The algorithm acts on ROIs, through background subtraction, application of sharpen filter and binarization. Sharpen radius (size of the region around the edge pixels that is affected by sharpening) was maintained constant (15), whereas sharpen amount (strength of the sharpening effect) ranges from 0.1 to 3, depending on imaging quality. Using the MATLAB® functions `bwmorph` and `strel` several morphological operations that operate on detected objects ("remove", "bridge", "thicken", "close") were applied (figure 2.3C1 and 2). To perform branchpoints and endpoints computa-

tions the image is further skeletonized and shrinked, using the same function `bwmorph`. It is possible to calculate the number of objects per ROI and to extrapolate different parameters from these objects, such as number of branchpoints and endpoints, complexity (sum of branchpoints and endpoints per object), area (total number of pixel per object), perimeter, length (the number of pixel of the major axis of an ellipse containing the object), orientation (angle between X axis and the major axis of an ellipse containing the object), fluorescence intensity. Laminar pattern distribution is measured as "*axonal complexity index*":

$$Axonal\ Complexity\ Index\ = N_a\ *\ C_a$$

where N_a is the mean number of detected axons per laminae (normalized for the number of GFP^+ axons in medullar pyramids) and C_a is the mean axonal complexity per laminae.

2.8 *Statistical analysis*

All data are presented as mean ± standard error of the mean (SEM), except for anatomical analysis of ET1-P21 TRAINING group, presented only as mean because represents preliminary data from 2 animals. *n* denotes numerosity of indicated group. Significant level was settled as 0.05. Lesion volume between injured groups, general motor behaviour, integrated density measures, sprouting from vCST and laminar distribution were analysed using Two-Way ANOVA. Factors considered are lesion (saline or ET1 injection) and age (P14 or P21), or training (with or without) and age. Normality assumption was validated using Shapiro-Walk test; when rejected, data were transformed on ranks and then analysed with the appropriate statistic test. Number of GFP^+ axons on medullar pyramids was analysed through non-parametric Kruskal-Wallis test. Behavioural data of Montoya Staircase test and axonal sprouting from dCST were analysed using Two-Way repeated measure ANOVA, with number of days and sequential distances, respectively, as within-subject factors. Post-hoc multiple comparison using Holm-Sidak test was performed, when appropriate. SigmaPlot®12.0 was used to perform the analysis.

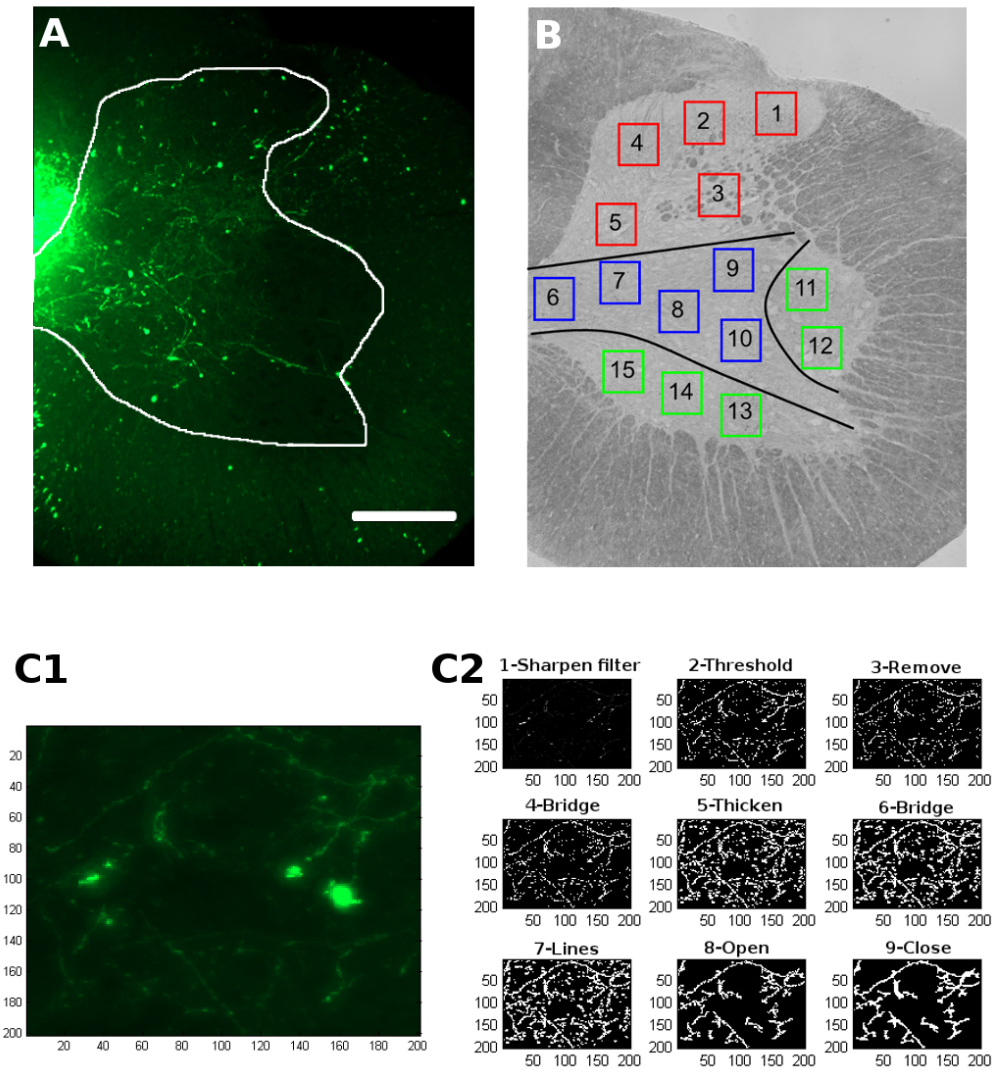

Figure 2.3. ROIs selection and position for complexity analysis of sprouted axons. Coronal section of a denervated C8 spinal cord in fluorescence (A) and brightfield (B) acquisition modes from a SAL-P14 animal. In (B) is also indicated the standardized position of ROIs for MATLAB® analysis: red squares sample dorsal laminae (1 to 6), blue squares samples intermediate lamina (7) and green squares sample ventral laminae (8-9). Scale bar: 250 μm. (C1) Morphological imaging processing and operations carried out on a typical sampling ROI (C2) using MATLAB® function `bwmorph` for the detection of axonal morphology. First, sharpen filter and thresholding were applied in order to minimize signal-to-noise ratio, then "remove" operator sets interior pixels as 0, thus leaving only pixels on the boundary. "Bridge" and "thicken" operators allow the connection of neighbouring unconnected pixels and add pixels to the exterior of objects, respectively. Using the function `strel` it is possible to create structural elements of a specific shape, in this case lines on different orientation (0°, 30°, 60°, 90°). Finally, typical morphological operators such as opening (dilation followed by an erosion) and closing (erosion followed by a dilation) refine detected objects for an optimal skeletonization and extrapolation of desired parameters. For further information, see MATLAB® documentation (https://it.mathworks.com/help/matlab/) for `bwmorph` and `strel` functions.

3 Results

3.1 *ET1 intracortical injections in fM1 of P14 and P21 animals provoke similar focal ischemic lesions*

ET1 (120 pmol/μl, 1 μl/site) was intracortically delivered in left fM1 of P14 or P21 rats previously injected with AAV1-GFP when pups. Once adults, fM1 slices were stained with propidium iodide (PI) in order to observe tissue integrity. Ischemic lesion appeared as multiple black spots of loss tissue diffused for all cortex depth (figure 3.1). There was not statistical significance between lesion volumes in ET1-P14 and ET1-P21 injured animals, with or without lesion (Two-Way ANOVA, factor treatment x age $F_{1,19}$=0.892, p=0.359), indicating that ET1 injection produces the same tissue loss degree in both ages, and that training do not have neuroprotective effect on the lesion volume. Saline injected animals do not exhibit any or few sign of damaged tissue (data not shown).

3.2 *ET1 lesion induces different general motor deficit in P14 and P21 rats*

Long-term general motor performance after an ischemic lesion was assessed through both general and motor task in young-adult rats (P59-P68). General movements were analysed through vertical ladder, grip and gait test at P59, whereas skilled abilities of lesioned forelimb were verified using Montoya Staircase test, applied for 7 days starting from P60 (see paragraph 2.1).

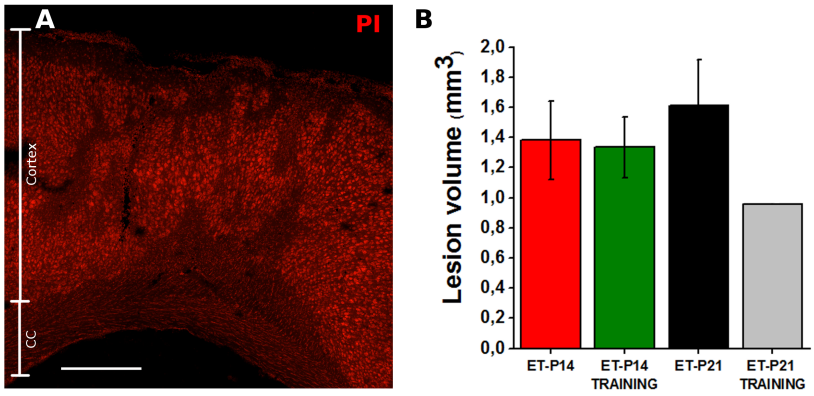

Figure 3.1. ET1 induces an equal focal lesion in P14 and P21 rats. (A) Coronal section of M1 cortex with a unilateral ischemic lesion through ET-1 intracortical injection, stained with propidium iodide (PI). Scale bar: 500 μm. CC: corpus callosum. (B) Lesion volume. Two-Way ANOVA, factor treatment x age p=0.359. ET1-P14 n=7; ET1-P14 TRAINING n=5; ET1-P21 n=6; ET1-P14 TRAINING n=2.

3.2.1 ET1 lesion produces an age-independent deficit on climbing a vertical ladder and on muscle strength

To assess long-term motor coordination deficits after ischemic lesion, we used vertical ladder test. In this task, ET1-P14 (n=11) and ET1-P21 (n=5) animals showed a significant increase in the time of climbing a vertical ladder, with respect to relative controls injected with saline (n=10 and n=8, Two-Way ANOVA, factor treatment $F_{1,34}$=48.367, p<0.001; post-hoc Holm-Sidak test p<0.001) (figure 3.2A). However, early lesion did not induce a worse outcome (Two-Way ANOVA, factor age $F_{1,34}$=0.242, p=0.626), indicating that the same focal lesion induced at different ages affects motor coordination at the same degree. Similarly, ET1 lesion induced long-term deficit in forelimb muscle strength. ET1-P14 (n=8) and ET1-P21 (n=9) animals showed a significant decrease in the forelimb muscle strength, with respect to relative controls injected with saline (n=11 and n=7, Two-Way ANOVA, factor treatment $F_{1,41}$=48.541 p<0.001, post-hoc Holm-Sidak test p<0.001) (figure 3.2B). However, there was only a slightly non significant tendency for reduced strength in ET1-P14 lesioned animals with respect to ET1-P21 group (Two-Way ANOVA, factor age p=0.112), indicating that the same focal ischemic lesion induced at different ages affects forelimb muscle strength in a similar degree.

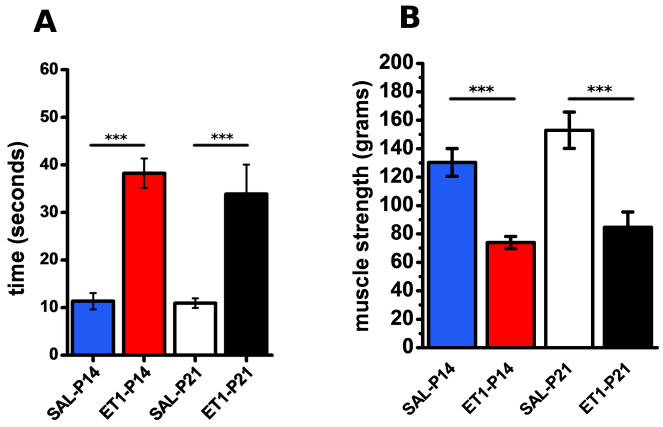

Figure 3.2. ET-1 lesion induces an age-independent deficit on climbing a vertical ladder and on muscle strength. (A) Vertical ladder test. Two-Way ANOVA, factor treatment $p<0.05$, post-hoc Holm-Sidak. (B) Grip test. Two-Way ANOVA, factor treatment $p<0.001$, post-hoc Holm-Sidak. Asterisks denote significance between groups: *** $p<0.001$.

3.2.2 ET1 lesion produces an age-dependent abduction of lesioned forelimb and walking alterations

To examine long-term locomotor alteration after ischemic injury, two gait parameters were analysed. Animals were encouraged to walk in a straight platform over absorbent paper, with paws differentially inked (figure 3.3A). In this test, ET1-P14 (n=9) and ET1-P21 (n=9) rats showed a significant abduction of the lesioned (contralateral) forelimb, with respect to relative controls injected with saline (n=11 and n=7, Two-Way ANOVA, factor treatment $F_{1,35}=38{,}721$, $p<0.001$; post-hoc Holm-Sidak test $p<0.001$). Moreover, ET1-P14 animals exhibited a strong tendency, despite non significant, for a greater abduction of injured forelimb compared to ET1-P21 group (Two-Way ANOVA on ranks, factor age x treatment $F_{1,35}=3.845$, $p=0.059$; figure 3.3B, right). ET1-P14 lesion also affected the interlimb coordination between injured forelimb and hindlimb of the same side (Two-Way ANOVA, factor treatment $F_{1,35}=12.500$, $p=0.001$, post-hoc Holm-Sidak ET1-P14 vs SAL-P14, $p<0.001$). This alteration was not present in ET1-P21 lesioned animals (factor treatment x age $F_{1,35}=11.158$, $p=0.002$; figure 3.3C, right). Both analysis did not show any alteration in healthy (ipsilateral) forelimb (figure 3.3B and C, left). Taken together, these data suggest that a focal ischemic lesion induced at different ages strongly alters locomotion in an age-dependent manner, because it is mainly affected in P14 injured animals.

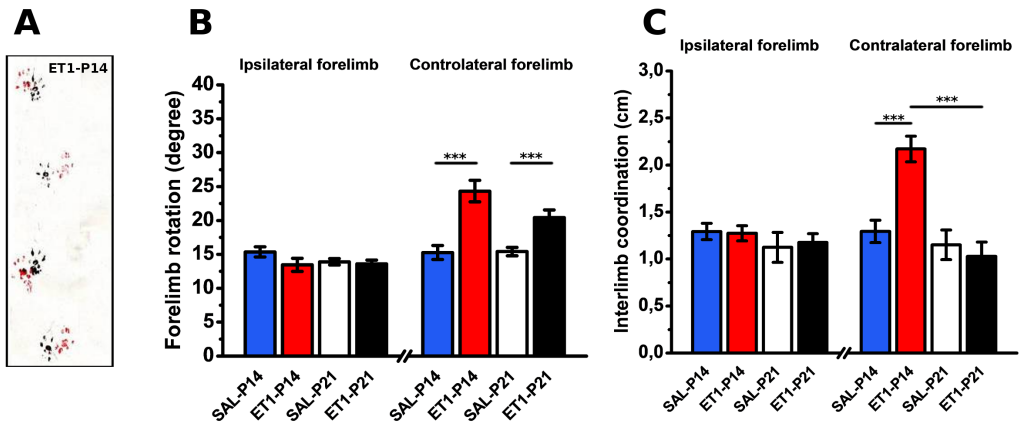

Figure 3.3. ET1 lesion produces an age-dependent abduction of lesioned forelimb and walking alterations. (A) Typical example of inked paws from a ET1-P14 animal. Red inks indicate forelimbs, black inks indicate hindlimbs. (B) Forelimb rotation. Two-Way ANOVA for affected forelimb, factor treatment $p<0.001$, factor treatment x age $p=0.059$, post-hoc Holm-Sidak. (C) Interlimb coordination. Two-Way ANOVA for affected side, factor treatment $p=0.001$, factor treatment x age $p<0.01$, post-hoc Holm-Sidak. Asterisks denote significance between groups: *** $p<0.001$.

3.3 *ET1-P14 lesion provokes long term fine motor deficit, particularly in grasping abilities, and a delayed learning of task.*

Long-term fine motor abilities after ischemic injury induced in P14 or P21 rats were assessed through the Montoya Staircase test, applied for 7 days from P60 in order to compare grasping, reaching and motor learning skills in different age lesion models. Grasping abilities were measured as the number of eaten pellets, whereas forelimb extension as the number of step reached. P14 and P21 lesion produced a general decrease in grasping performance of lesioned forelimb compared to relative controls (Two-Way repeated measure ANOVA, factor group x age $F_{3,377}=6.503$, $p<0.001$; figure 3.4A). Moreover, P14 lesion induced a stronger long-term impairment comparing to P21 injury (Two-Way repeated measure ANOVA, post-hoc Holm-Sidak ET1-P21 vs ET1-P14 $p=0.021$), whereas no statistical difference is showed between saline injected controls. Considering only the mean value of eaten pellets in last 3 days (where learning curves reach plateau levels), ET1-P14 and ET1-P21 groups exhibited a significant deficit in grasping abilities with respect to controls; in addition, the earlier lesion group showed a significant worse outcome compared to the later one (Two-Way ANOVA, factor

treatment x age $F_{1,54}$=6.279, p=0.015, post-hoc Holm-Sidak p=0.006; figure 3.4B). Learning curves analysis indicated that ET1-P21 and control groups are able to learn the motor task starting from 2nd or 3rd day of behavioural test, except for ET1-P14 group, which started to significantly increase the number of eaten pellets only in the 5th day of task (Two-Way Repeated Measure ANOVA, factor days $F_{6,377}$=66.622, p<0.001, post-hoc Holm-Sidak) (figure 3.4A).

Similarly, P14 and P21 lesion induced an overall reduction in reaching and extension abilities of lesioned forelimb compared to relative controls (Two-Way repeated measure ANOVA, factor group x age $F_{3,377}$=5.198, p<0.001, post-hoc Holm-Sidak; figure 3.5A). In addition, P14 lesion induced a significant stronger long-term impairment compared to P21 injury (Two-Way repeated measure ANOVA, post-hoc Holm-Sidak ET1-P21 vs ET1-P14 p=0.041), whereas no difference is showed between saline injected controls. However, plateau level of measured step reached (as a mean of last 3 days of task) did not highlight a significant difference between ET1-P14 and ET1-P21 (Two-Way ANOVA, factor treatment x age p=0.279), whose performances are in any case significantly worst respect to controls (Two-Way ANOVA, factor treatment p<0.001; figure 3.5B). As assessed for grasping analysis, learning curves indicated that all groups are able to learn the reaching motor task starting from 2nd or 3rd day of behavioural test, except for ET1-P14 group, which started to significantly increase the number of step reached only in the 6th day of task (Two-Way Repeated Measure ANOVA, factor days $F_{6,377}$=93.544, p<0.001, post-hoc Holm-Sidak; figure 3.5A).

Taken together, these data suggest a worse long-term motor performance exhibited by ET1-P14 lesioned animals compared to ET1-P21 in reaching and, particularly, grasping abilities, with a significant delay on motor learning.

3.4 *AAV1-GFP is well expressed in fM1 and all CST*

In order to anterogradely trace pyramidal neurons of uninjured side, rat pups were intracortically injected with AAV1-GFP viral vector. The injection resulted in the wide transduction of fM1 cells, counterstained with propidium iodide (PI; figure 3.6A and B). It was previously

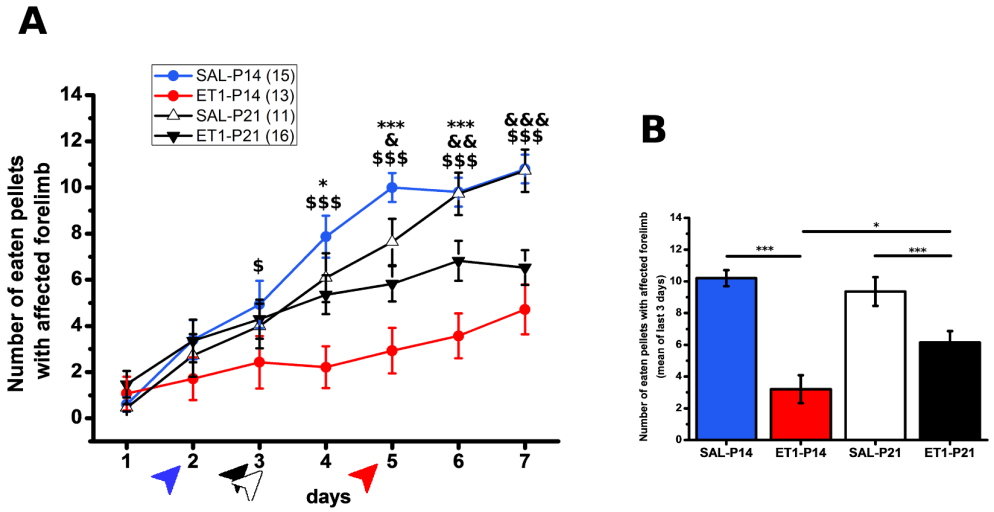

Figure 3.4. Montoya Staircase test: number of eaten pellets with lesioned forelimb. (A) Number of eaten pellets along 7 days of task. Two-Way repeated measure ANOVA, factor group x days $p<0.001$. Multiple comparison between days were performed through post-hoc Holm-Sidak test. Arrows indicate the day in which animal performances are significantly improved with respect to the first day of test: ET1-P14: 5 vs 1 * $p<0.05$; ET1-P21: 3 vs 1 *** $p<0.001$; SAL-P14 2 vs 1 ** $p<0.01$; SAL-P21: 3 vs 1 *** $p<0.001$. Multiple comparison within days were performed through post-hoc Holm-Sidak test: ***** denote comparison between ET1-P14 and ET1-P21; **$** denote comparison between ET1-P14 and SAL-P14; **&** denote significance between ET1-P21 and SAL-P21. (B) Mean number of eaten pellets as a mean of last 3 days values. Two-Way ANOVA: factor treatment $p<0.001$, factor age $p>0,169$, factor treatment x age $p=0.015$. Multiple comparisons were performed through post-hoc Holm-Sidak test. Asterisks denote significance between indicated groups: * $p<0.05$, *** $p<0.001$. SAL-P14 n=15; ET1-P14 n=13; SAL-P21 n=12; ET1-P21 n=16.

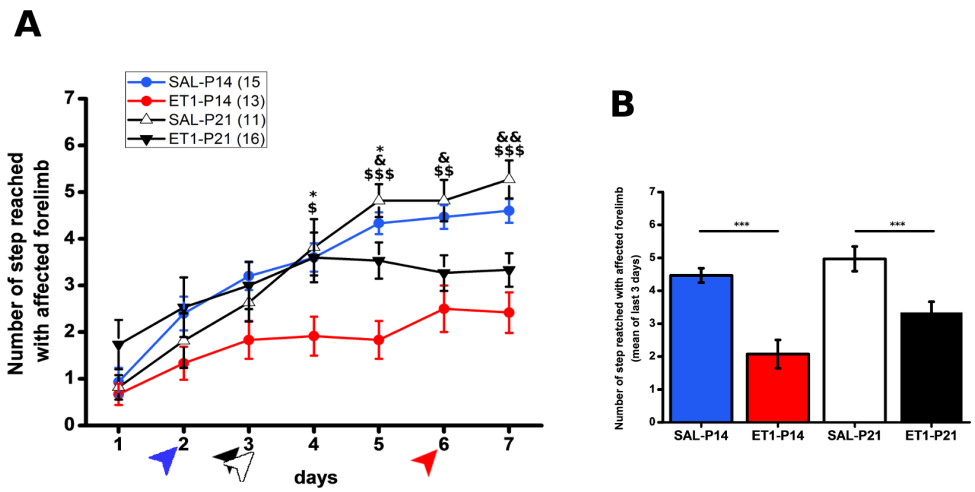

Figure 3.5. Montoya Staircase test: number of step reached with lesioned forelimb. (A) Number of step along 7 days of task. Two-Way repeated measure ANOVA, factor treatment x age p<0.001. Multiple comparison between days were performed through post-hoc Holm-Sidak test. Arrows indicate the day in which animal performances are significantly improved with respect to the first day of test: ET1-P14: 6 vs 1 * p<0.05; ET1-P21: 3 vs 1 ** p<0.01; SAL-P14 2 vs 1 *** p<0.001; SAL-P21: 3 vs 1 *** p<0.001. Multiple comparison within days were performed through post-hoc Holm-Sidak test. ***** denote comparison between ET1-P14 and ET1-P21; **$** denote comparison between ET1-P14 and SAL-P14; **&** denote significance between ET1-P21 and SAL-P21. (B) Mean number of eaten pellets as a mean of last 3 days values. Two-Way ANOVA: factor treatment p<0.001, factor age p=0,014, factor treatment x age p=0.279. Multiple comparison were performed through post-hoc Holm-Sidak test. Asterisks denote significance between indicated groups: *** p<0.001. SAL-P14 n=15; ET1-P14 n=13; SAL-P21 n=12; ET1-P21 n=16.

demonstrated that the viral vector used in this work has a high tropism for CSMNs and a very low tropism for astrocytes [257].

GFP^+ signal was detected in all uninjured corticospinal tract, including medullar pyramids (figure 3.6C and D), where it is possible to count GFP^+ descending axons in coronal slices (figure 3.6E). Number of GFP^+ axons counted in labelled medullar pyramid were similar between groups (Kruskal-Wallis test, p=0.485; figure 3.6E). Moreover, GFP signal was clearly evident at cervical spinal cord level (figure 3.7), where all components of uninjured CST are labelled: the contralateral *dorsal CST* (dCST), located in the most ventral part of dorsal funiculus, and the ipsilateral *ventral CST* (vCST), located in the medial part of the ventral funiculus.

3.5 *P14 and P21 ischemic lesion alter the normal pattern of CS fibers in cervical spinal cord*

To evaluate if early ischemic lesions provoke an alteration of normal CST pattern, fluorescence integrated density of dCST and vCST was extrapolated from coronal sections of cervical (C6-C8) spinal cord of P14 and P21 lesioned animals and respective controls (figure 3.8A). C6-C8 segments are chosen because mainly receive inputs from fM1 and their motoneuronal pools are connected with forelimb muscles [264].

As expected, no significant differences on fluorescence integrated density were detected in dCST (figure 3.8B), confirming that animals receive a similar strong amount of viral vector. Instead, vCST fluorescence intensity of ET1-P14 and ET1-P21 was significantly higher with respect to control groups (Two-Way ANOVA, factor treatment $F_{1,20}$=5.023, p=0.039, post-hoc Holm-Sidak; figure 3.8C), even if no differences were detected between lesioned rats. This data suggests that both P14 and P21 ischemic lesion induce an alteration of normal CST development, in terms of more prominent ipsilateral ventral tract, that should be normally pruned and reduced.

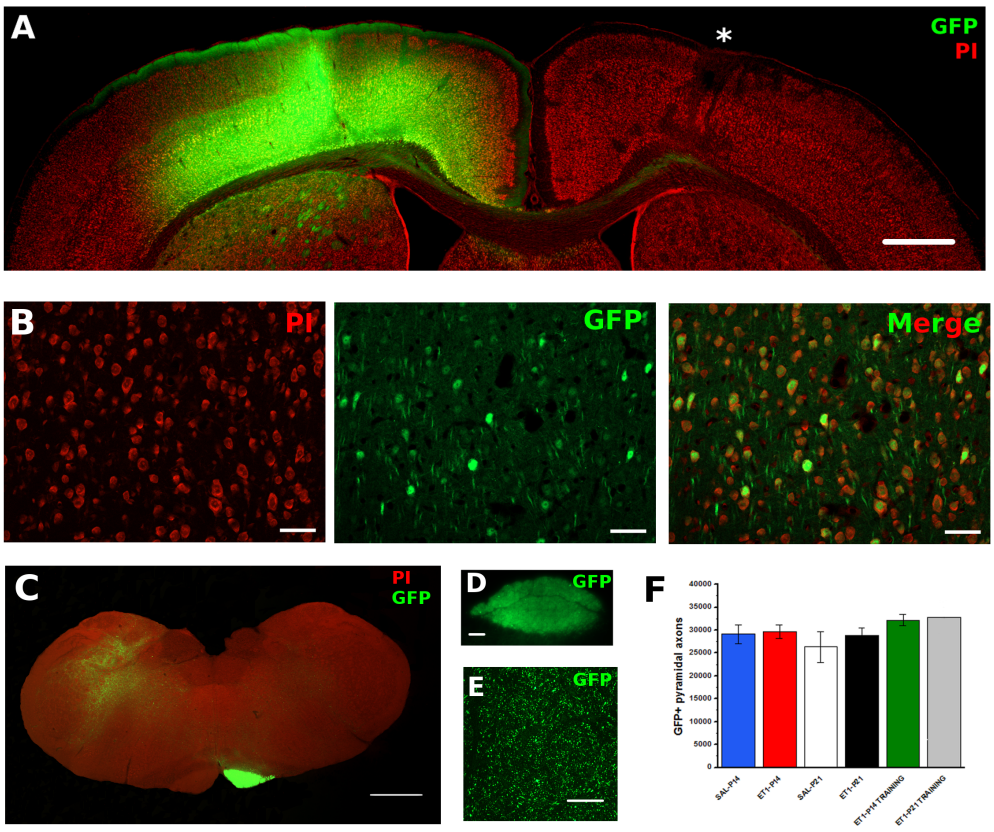

Figure 3.6. AAV1-GFP viral vector label injected motor cortex and pyramidal tract. (A) Coronal section of motor cortex characterized by a clear ischemic lesion in the left cortex (*) and a strong GFP labelling of cortical deep layers. Scale bar, 500 μm. (B) 20X magnification of GFP labelled cortex. Scale bars: 50 μm. (C) Coronal section of caudal medulla oblongata with a strong GFP labelling of left medullar pyramid. Scale bar: 1 mm. (D) and (E) 5X and 63X magnifications of labelled medullar pyramid. Green puncta are identified as GFP^+ axons. Scale bars: 100 μm and 50 μm, respectively. (F) Number of GFP^+ pyramidal axons in different groups does not significantly change. SAL-P14 n=5, ET1-P14 n=6, SAL-P21 n=4, ET1-P21 n=6, ET1-P14 TRAINING n=5, ET1-P21 TRAINING n=2.

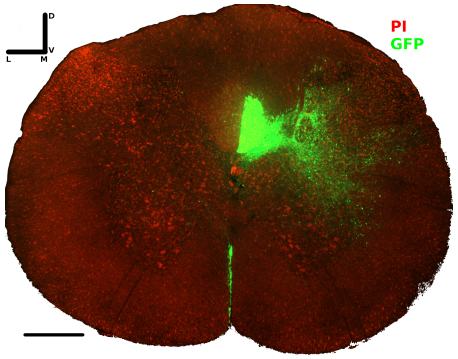

Figure 3.7. AAV1-GFP viral vector labelling of contralateral dorsal CST (dCST) and ipsilateral ventral CST (vCST). Coronal section of spinal cord stained with PI. Note the ventral part of dorsal funiculus (dCST) and the medial part of ventral funiculus (vCST) labelled with GFP. Scale bar, 500 μm.

3.6 *P14 ischemic lesion induces abnormal sprouting from both dCST and vCST to the denervated side of spinal cord*

To test the presence of anatomical correlates of worse motor outcome exhibited by ET1-P14 animals, the number of sprouted GFP^+ axon fibers from uninjured dCST to the denervated side of spinal cord was counted on midline (M) and on different distanced (D1-4) (figure 3.9A, left). Ischemic lesion induced a significant increase in spontaneous axonal sprouting from dCST to the denervated side of spinal cord (Two-Way repeated ANOVA, factor group x distance $F_{3,104}$=2.606, p<0.001); interestingly, ET1-P14 rats showed a significant greater number of sprouting axons compared to ET1-P21 animals, in particular at D2 and D3 distances (Two-Way repeated measure ANOVA, post-hoc Holm-Sidak) (figure 3.9B).

To check the effect of ischemic lesion in the axonal sprouting originating from vCST, the number of GFP^+ fibers crossing the border between white and gray matter in the ventral horn of spinal cord was counted (figure 3.9A, right). Similarly to dCST sprouting, ischemic lesion *per se* induced structural plasticity from vCST (Two-Way ANOVA, factor treatment $F_{1,20}$=30.051, p<0.001); such plasticity was significantly enhanced in ET1-P14 rats with respect to ET1-P21 animals (Two-Way ANOVA, factor treatment x age $F_{1,20}$=4.548, p<0.05) (figure 3.9C).

Taken together, these data shows, only for P14 lesioned animals, the coincidence of worse motor outcome and increased axonal sprouting from both dCST and vCST to denervated spinal cord.

3.7 *P14 ischemic lesion alters the laminar distribution of sprouted axons in the denervated side of spinal cord*

In order to better understand where axonal sprouting induced by ischemic lesion in ET1-P14 rats is mainly directed, it was implemented a semi-automated analysis of axonal distribution on different spinal cord laminae. This technique uses custom-made MATLAB® algorithm based on mathematical morphology theory. Selection of specific ROIs (figure 2.3) with

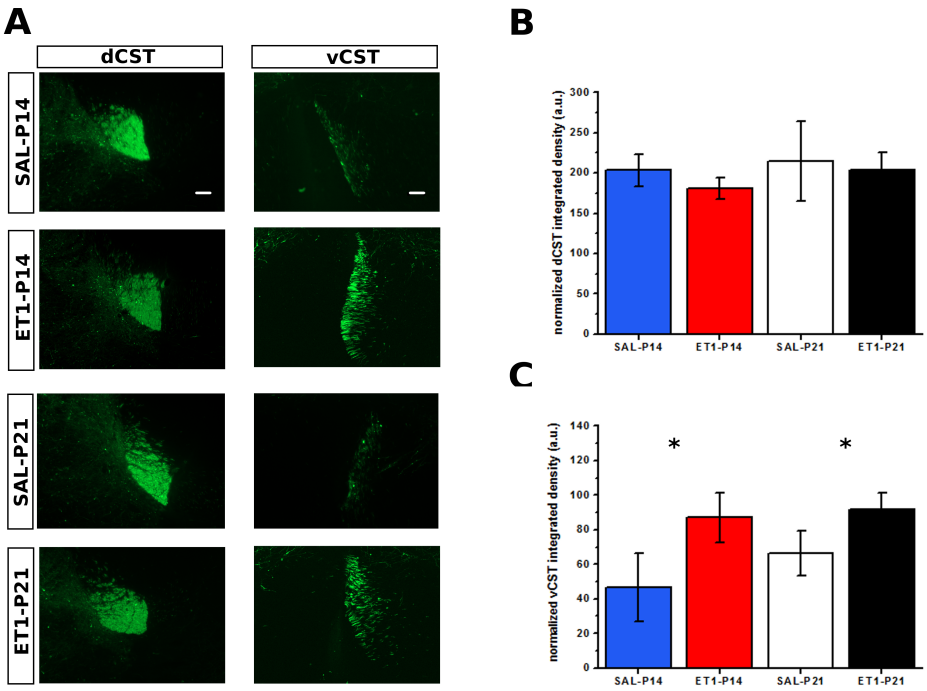

Figure 3.8. Fluorescence integrated density of dCST and vCST. (A) Representative images of dCST (left) and vCST (right) from animals of different groups. Scale bar: 200 μm. (B) Fluorescence integrated density of dCST. No differences were evident between groups. (C) Fluorescence integrated density of vCST. ET1 lesioned groups showed a significant increase in fluorescence intensity with respect to relative controls (Two-Way ANOVA, factor treatment * $p<0.05$). SAL-P14 n=5; ET1-P14 n=6; SAL-P21 n=4; ET1-P21 n=6.

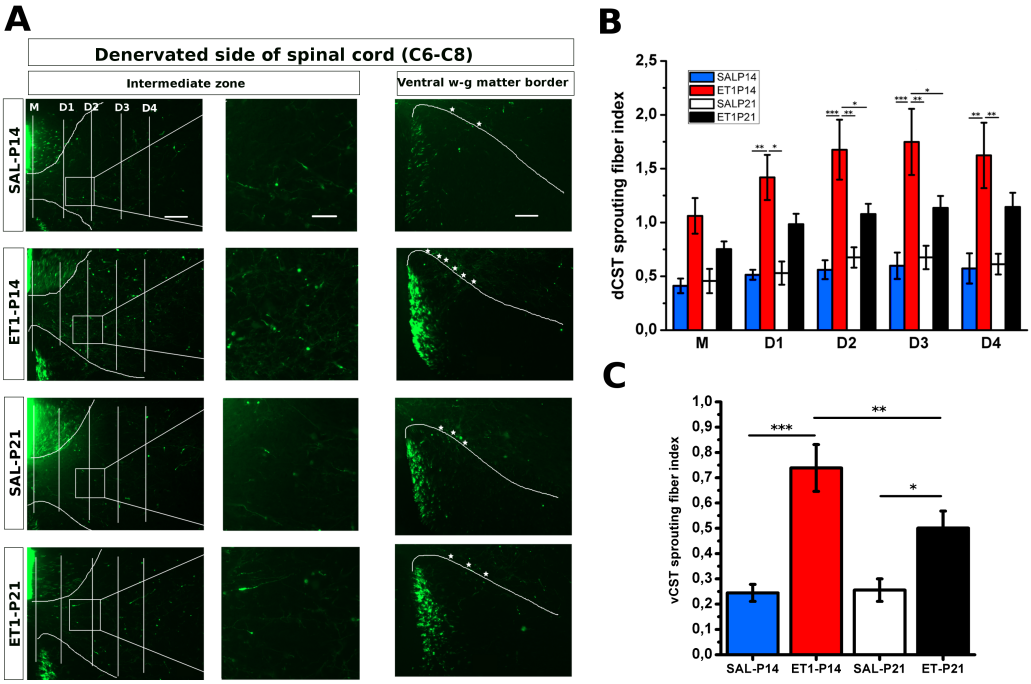

Figure 3.9. dCST and vCST axonal sprouting induced by ischemic lesion. (A) Representative images of denervated side of spinal cord. Sprouted axons from dorsal labelled CST are counted at 100 μm of distance (D1-4) from midline (M). Sprouted axons from ventral labelled CST are counted on the boundary between white and gray matter on the ventral horn. Scale bars, from left to right: 100 μm, 20 μm, 100 μm. (B) dCST axonal sprouting. ET1-P14 animals show more axonal sprouting from GFP labelled dCST compared to ET1-P21 rats. Two-Way repeated measure ANOVA, factor group x distance $p<0.001$. Multiple comparison within distance were performed through post-hoc Holm-Sidak test. Asterisks indicates significance between groups: * $p<0.05$, ** $p<0.01$, *** $p<0.001$. (C) vCST axonal sprouting. ET1-P14 animals showed a greater degree of axons crossing white-gray matter border and originating from GFP labelled vCST compared to ET1-P21 rats. Two-way ANOVA, factor treatment x age $p<0.001$, post-hoc Holm-Sidak. Asterisks indicates significance between groups: * $p<0.05$, ** $p<0.01$, *** $p<0.001$. SAL-P14 n=5; ET1-P14 n=6; SAL-P21 n=4; ET1-P21 n=6.

a precise distribution into the gray matter (dorsal, intermediate and ventral) allows the detection of sprouted axons in different regions of the denervated spinal cord (figure 3.10A). Laminar pattern distribution is measured as "*axonal complexity index*", where the mean number of detected axons in a specific lamina (normalized for the number of GFP^+ axons in medullar pyramids) was multiplied by the mean axonal complexity (number of branchpoints and endpoints of axons) of the same lamina (see 2.7). Evaluation of axonal laminar distribution can be crucial to understand if spontaneous sprouted axons reaches typical CST targets, mainly localized on intermediate laminae, or other off-targets, located in dorsal or ventral laminae (see paragraph 2.7).

On dorsal laminae, ET1-P14 rats exhibited an increased axonal sprouting complexity compared to relative control and ET1-P21 lesioned animals (Two-Way ANOVA on ranks for dorsal laminae, factor treatment x age, $F_{1,20}$=10.016, p<0.01, post-hoc Holm-Sidak; figure 3.10C). The same effect was also present on ventral laminae (Two-Way ANOVA on ranks for ventral laminae, factor treatment x age, $F_{1,20}$=8.686, p<0.01, post-hoc Holm-Sidak; figure 3.10E). Moreover, axonal complexity in ET1-P14 animals was significantly increased compared to control also in intermediate lamina, without effects between lesioned groups (Two-Way ANOVA on ranks for intermediate lamina, factor treatment x age, $F_{1,20}$=4.479, p<0.05, post-hoc Holm-Sidak; figure 3.10D). Interestingly, ET1-P21 animals' axonal complexity did not change compared to relative controls.

Taken together, these results suggest that a P14 focal ischemic lesion leads to an increased axonal sprouting and complexity from the uninjured to the denervated side of spinal cord, which is spontaneously misdirected to sensorial dorsal targets rather that intermediate or ventral motor targets. This "maladaptive" structural plasticity occurs in coincidence with a worse motor outcome compared to animals lesioned at P21, that do not exhibit the same altered spontaneous axonal sprouting.

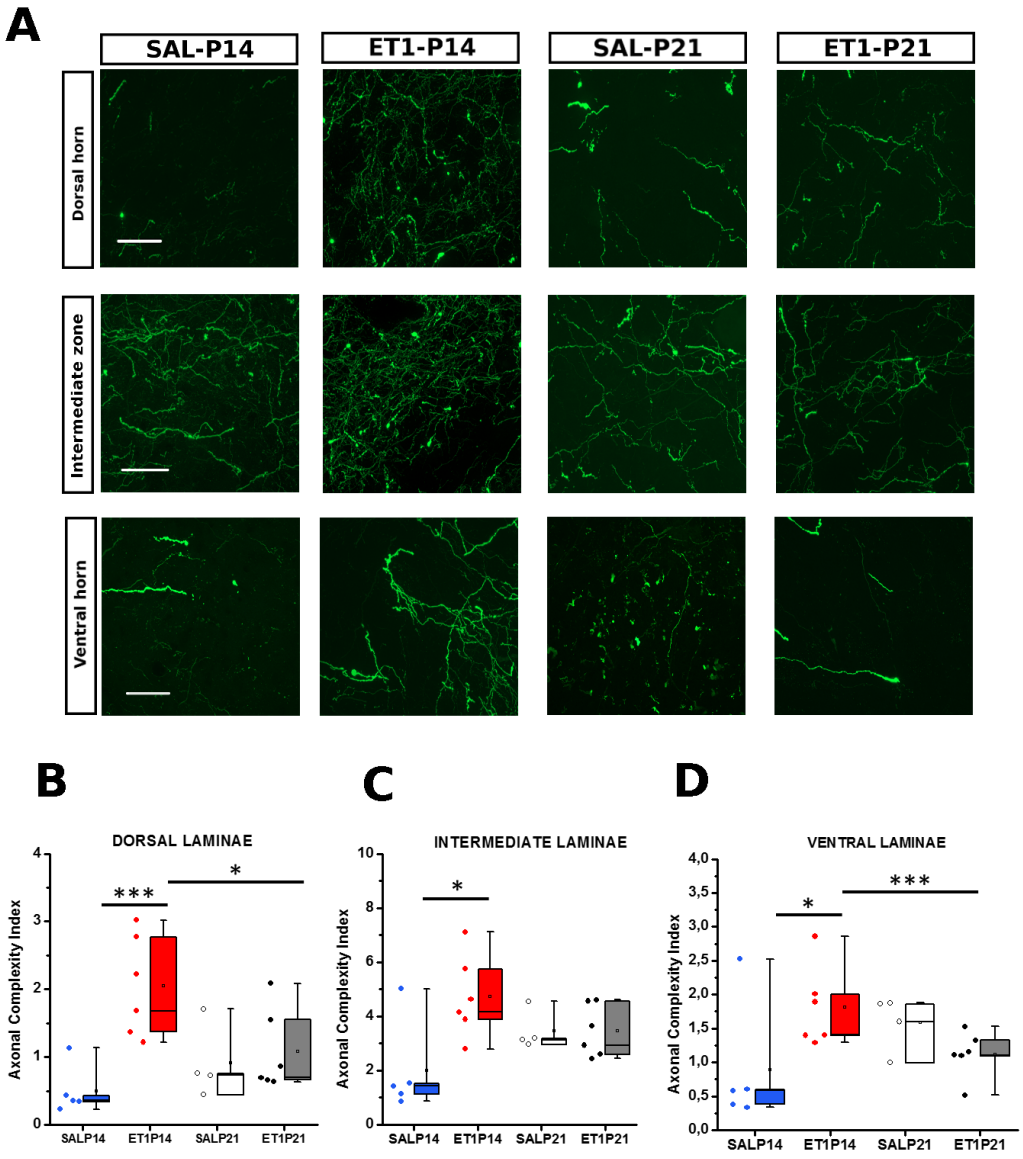

Figure 3.10. P14 ischemic lesion alters the laminar distribution of sprouted axons in the denervated side of spinal cord. (A) Micrographs (40x magnification) showing different sprouting patterns of GFP+ fibers from the contralesional cortex towards dorsal (left), intermediate (middle) and ventral (right) zones of the denervated cervical spinal cord (C7) in different groups. Scale bars, 50 μm. (B-D) Axonal Complexity Index. ET1-P14 animals exhibits a stronger axonal complexity in dorsal and ventral laminae compared to control and ET1-P21 animals. (C) Two-Way ANOVA on ranks for dorsal laminae, factor treatment x age $p<0.01$, post-hoc Holm-Sidak. (D) Two-Way ANOVA on ranks for intermediate lamina, factor treatment x age $p<0.05$, post-hoc Holm-Sidak. (E) Two-Way ANOVA on ranks for ventral laminae, factor treatment x age $p<0.01$, post-hoc Holm-Sidak. Asterisks indicates significance between groups: * $p<0.05$, ** $p<0.01$, *** $p<0.001$. SAL-P14 n=5; ET1-P14 n=6; SAL-P21 n=4; ET1-P21 n=6.

3.8 *Early training partially ameliorates general and skilled long-term motor abilities in P14 and P21 lesioned animals*

To investigate whether an early activity-dependent modulation of CST plasticity might correct the maladaptive contralesional rewiring observed after P14 lesion, P14 and P21 lesioned rats were administered at P21 and P28, respectively, with a skilled motor training (using Montoya Staircase test) twice/day till the plateau level of learning was achieved (see paragraph2.1). To understand whether the effects of training were long-lasting, motor assessment was performed in adult P59 rats. To verify whether this training exerts specific effects on trained ability or more general improvement in motor performance, we used the same battery of tests previously described in untrained rats. The analysis was done comparing P14 and P21 lesioned groups that have performed or not the early training.

Motor training produced an age-independent amelioration of motor coordination, measured through vertical ladder test, and forelimb muscle strength (Two-Way ANOVA, factor training $F_{1,37}$=13.122 and $F_{1,37}$=20.823, $p<0.001$; figure 3.11A and B). Moreover, the specific alteration in interlimb coordination on the affected side exhibited by P14 lesioned animals is reverted if they perform the low-intensity early training described before (Two-Way ANOVA, factor training x age $F_{1,31}$=9.061, $p<0.01$; figure 3.11C). No statistical differences were detected in the affected forelimb rotation (Two-Way ANOVA, factor training $p>0.05$, data not shown).

Motor training ameliorated grasping abilities for both P14 and P21 lesioned animals. In particular, ET1-P14 trained animals reached the performances of ET1-P21 non-trained rats, with a significant improvement respecting to ET1-P14 non-trained animals (Two-Way repeated measure ANOVA, factor age $F_{3,234}$=8.576, $p<0.001$, post-hoc Holm-Sidak between groups ET1-P14 TRAINING vs ET1-P21, p=310, ET1-P14 vs ET1-P14 TRAINING, $p<0.05$; figure 3.11D). Moreover, early motor training also exerted an effect on P21 lesioned animals, that improved their performances with respect to ET1-P21 lesioned only (Two-Way repeated measure ANOVA, ET1-P21 vs ET1-P21 TRAINING, $p<0.05$). In contrast, early low-intensity

training did not ameliorate reaching abilities in ET1-P14 animals, but exerted its positive effect only on ET1-P21 injured rats (Two-Way repeated measure ANOVA, factor group x days $F_{3,234}$=1.802, p<0.05, post-hoc Holm-Sidak between groups ET1-P21 TRAINING vs ET1-P21, p<0.05 in all days except for day 1; figure 3.11E).

3.9 *Early training restores normal anatomical CST features, sprouting pattern and laminar distribution in P14 lesioned animals: preliminary data*

To verify the effects of early training on structural maladaptive plasticity processes occurred in the spinal cord after a perinatal lesion, we performed the same anatomical analysis on fluorescence integrated density of CST components, sprouting from healthy dCST and vCST to the denervated side of spinal cord and laminar distribution of sprouted axons onto denervated grey matter, described above. The analysis was done comparing P14 and P21 lesioned groups that have performed or not the early training.

Fluorescence integrated density analysis indicated no significant differences in dCST anatomy (figure 3.12A), whereas vCST fluorescence intensity of ET1-P14 TRAINING and ET1-P21 TRAINING were significantly lower with respect to lesioned only groups (Two-Way ANOVA, factor treatment $F_{1,18}$=4.836, p=0.044, post-hoc Holm-Sidak; figure 3.12B), despite no difference was detected between trained rats.

Counts of axonal sprouting from dCST revealed that early training reduced spontaneous axonal sprouting after a perinatal (P14) ischemic lesion, compared to P14 lesioned group only (Two-Way repeated measure ANOVA, factor group x distance $F_{2,94}$=3.840, p<0.001; multiple comparison ET1-P14 TRAINING vs ET1-P14 p=0.031); this effect is not present comparing ET1-P14 TRAINING and ET1-P21 animals (Two-Way repeated measure ANOVA, multiple comparison p>0.05; figure 3.12C). Moreover, counts of axonal sprouting from vCST revealed that early training reduced spontaneous axonal sprouting after a perinatal (P14) ischemic lesion, compared to P14 lesioned group only (Two-Way ANOVA, factor age x training $F_{1,18}$=6.799, p=0.020; multiple comparison ET1-P14 TRAINING vs ET1-P14 p<0.001, figure 3.12D).

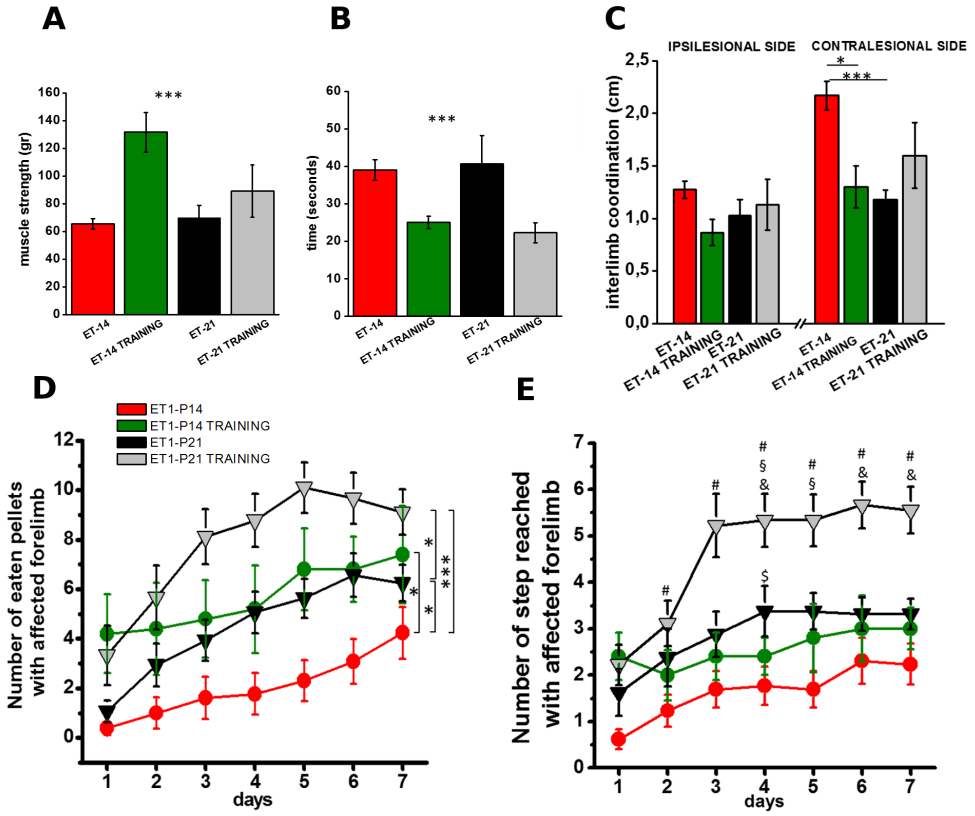

Figure 3.11. Behavioural motor ameliorations promoted by early training in P14 and P21 lesioned animals. (A) Grip test. Two-Way ANOVA, factor training *** p<0.001. ET1-P14, n=15; ET1-P14 TRAINING, n=5; ET1-P21, n=9; ET1-P21 TRAINING, n=9. (B) Vertical ladder test. Two-Way ANOVA, factor training *** p<0.001. ET1-P14, n=11; ET1-P14 TRAINING, n=5; ET1-P21, n=9; ET1-P21 TRAINING, n=9. (C) Interlimb coordination. For contralateral forelimb, Two-Way ANOVA, factor training x age p<0.01, post-hoc Holm-Sidak, * p<0.05, *** p<0.001. No statistical differences were detected in ipsilateral forelimb. ET1-P14, n=9; ET1-P14 TRAINING, n=5; ET1-P21, n=9; ET1-P21 TRAINING, n=9. (D) Number of eaten pellets with affected forelimb along 7 days of task. Two-Way repeated measure ANOVA, factor age p<0.001, factor training p<0.001, interaction p=0.071. Overall multiple comparison for factor group were performed through post-hoc Holm-Sidak test: ET1-P21 TRAINING vs ET1-P14 ***p<0.001, ET1-P21 TRAINING vs ET1-P21 *p<0.05, ET1-P14 TRAINING vs ET1-P14 *p<0.05, ET1-P21 vs ET1-P14 *p<0.05. (E) Number of step reached with affected forelimb along 7 days of task. Two-Way repeated measure ANOVA, factor group x days p<0.05. Multiple comparison within days were performed through post-hoc Holm-Sidak test. **$** denote comparison between ET1-P14 and ET1-P21; # denote comparison between ET1-P14 and ET1-P21 TRAINING; **&** denote significance between ET1-P21 and ET1-P21 TRAINING; § denote significance between ET1-P14 TRAINING and ET1-P21 TRAINING. For Montoya Staircase test, ET1-P14, n=13; ET1-P14 TRAINING, n=5; ET1-P21, n=16; ET1-P21 TRAINING, n=9.

Finally, axonal complexity was also evaluated for lesioned animals treated with early training protocol, compared to lesioned only animals. In ET1-P14 rats, early training promoted a significant reduction of complexity and axonal branching in dorsal (Two-Way ANOVA, factor age x training $F_{1,18}=7.404$, $p<0.05$), intermediate (Two-Way ANOVA, factor age x training $F_{1,18}=5.134$, $p<0.05$) and ventral (Two-Way ANOVA, factor age x training $F_{1,18}=9.850$, $p<0.01$) laminae; on the contrary, training did not influence ET1-P21 animals axonal complexity and branching.

Overall, these anatomical data, although preliminaries, strongly confirm the idea that maladaptive plasticity mechanism, influencing a poor motor outcome after a focal perinatal ischemic injury, can be positively modulated through an early specific low-intensity training.

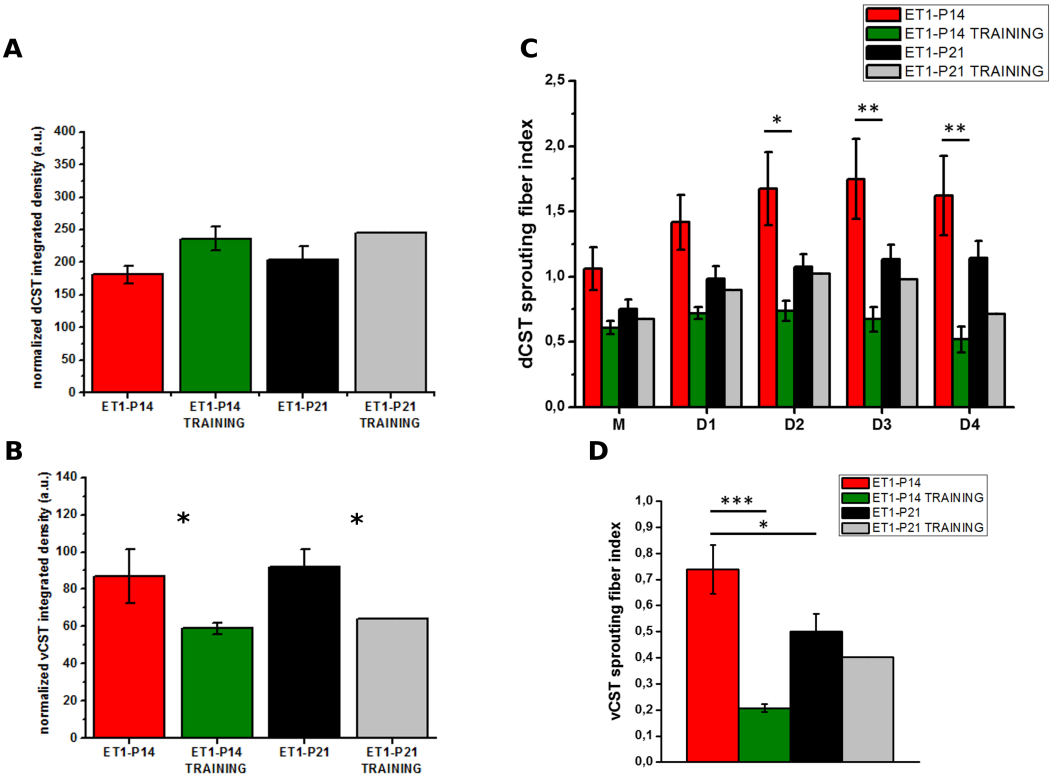

Figure 3.12. Early training effects on CST components distribution and axonal sprouting. (A) Fluorescence integrated density of dCST. No differences were evident between groups. (B) Fluorescence integrated density of vCST. Trained lesioned groups showed a significant decrease in fluorescence intensity with respect to lesioned only groups. Two-Way ANOVA, factor treatment *p<0.05. (C) dCST axonal sprouting. ET1-P14 TRAINING animals show a lower degree of axonal sprouting from GFP labelled dCST compared to ET1-P14 lesioned only rats. Two-Way repeated measure ANOVA, factor group x distance p<0.001, post-hoc Holm-Sidak. (D) vCST axonal sprouting. ET1-P14 TRAINING animals show a lower degree of axonal sprouting from GFP labelled vCST compared to ET1-P14 lesioned only rats. Two-Way ANOVA, factor age x treatment p<0.05, post-hoc Holm-Sidak. Asterisks indicates significance between groups: * p<0.05, ** p<0.01, *** p<0.001. ET1-P14 n=6; ET1-P14 TRAINING n=6; ET1-P21 n=6; ET1-P14 TRAINING n=2.

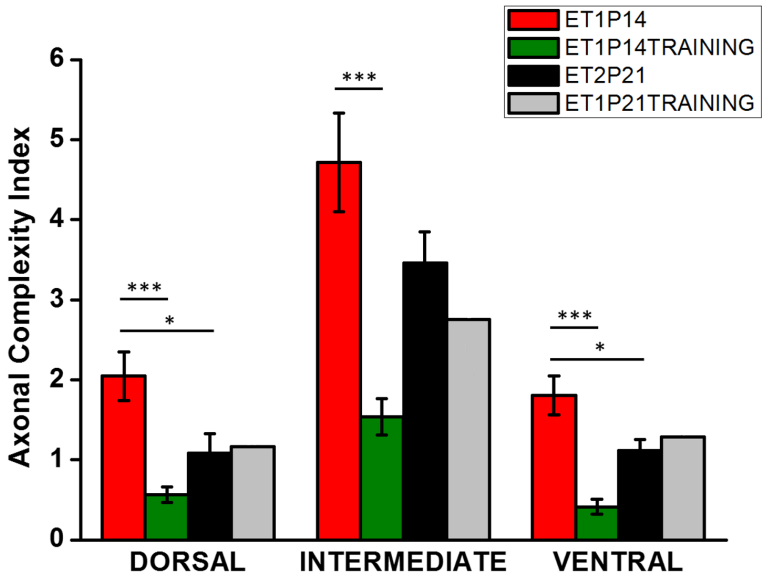

Figure 3.13. Early training effects on laminar distribution of sprouted axons. Axonal Complexity Index. ET1-P14 TRAINING animals shows a decreased axonal complexity and branching in dorsal, intermediate and ventral laminae compared to P14 lesioned only animals. Two-Way ANOVA: for dorsal laminae, factor age x training p=0.016; for intermediate laminae factor, age x training p=0.039; for ventral laminae, factor age x training p=0.007. Post-hoc Holm-Sidak. Asterisks indicates significance between groups: * p<0.05, ***p<0.001. ET1-P14 n=6; ET1-P14 TRAINING n=6; ET1-P21 n=5; ET1-P14 TRAINING n=2.

4 Discussion

In this study, we produced two rat models of perinatal and juvenile focal ischemic stroke, through intracortical injections of ET1 in fM1 of P14 or P21 aged rats, respectively. ET1 lesion resulted in a comparable degree of tissue damage between P14 and P21 injured animals. However, ET1-P14 rats showed more prominent long term motor impairments, on both general walking and skilled reaching abilities. Moreover, in coincidence with a poorer motor outcome, ET1-P14 lesion produced an aberrant axonal sprouting from both contralateral (dorsal) and ipsilateral (ventral) components of healthy CST onto the denervated spinal cord. These fibers display an altered laminar distribution into the spinal cord gray matter. Such maladaptive plasticity can be reverted if animals undergo an early skilled reaching training protocol; indeed, ET1-P14 rats showed a better motor outcome coupled with a significant reduction of aberrant sprouting and laminar distribution following early training.

ET-1 perinatal and juvenile models of ischemic stroke

Histological analysis show that ET1 ischemic lesion are closely similar between experimental groups, without any difference dependent on age of lesion. The strongest advantage of ET1 is the production of a reliable focal ischemic lesion, restricted to the forelimb area of motor cortex [134, 249]. The available models of perinatal and juvenile stroke, mostly based on global ischemia or global ischemia-anoxia [143, 151, 152, 265], lack the ability to recapitulate those fine features, such as consequential activation of plastic remodelling and functional compensation, that characterize focal stroke occurrence in children. For example, in a recent paper where an ischemic stroke model induced through permanent unilateral carotid

ligation was performed in P12 mice, the lesion affects a wide cerebral area, including both cortical and subcortical regions and determines a general spectrum of neurological deficits [266]. On the contrary, the model used in our work provokes a specific ischemic tissue damage that provides a well-defined impairment on forelimb motor outcome.

ET1-P14 lesion induces a long-term poorer general and skilled motor outcome

General motor performances, assessed at adult age, were significantly affected in both models of early stroke we developed. In particular, we found that both P14 and P21 injured animals display an overall decrease of forelimb strength, significant difficulties to climb a vertical ladder and the abduction of lesioned forelimb. Interestingly, P14 injured animals exhibit an increased deficit in forelimb-hindlimb coordination, that is not found in P21 lesioned animals. Interlimb coordination is a locomotor pattern strictly dependent on the interplay between motor cortex, cerebellum and central pattern generators (CPGs) located in the brainstem and spinal cord [267]. Previous studies suggest that different adult CNS injury models [268–270] found conflicting results for locomotor abilities damage after lesion, so that the presence of locomotor deficits resulted controversial and not well-defined. It could be conceivable that an early lesion, even if focal, can permanently alter the normal locomotion pattern because of its action during a critical period for the development and implementation of correct locomotor abilities.

With the same logic, we expected skilled motor abilities to be affected for the forelimb contralateral to the lesion. Indeed, long-term skilled reaching task revealed a significant deficit for both models, and in particular for ET1-P14 lesioned animals. These data strongly suggest the presence of maladaptive plasticity processes acting mainly after a perinatal lesion, and also confirm the strong specificity of ischemic injury induced. Moreover, this procedure of perinatal lesion induction may be potentially used to study mechanisms underlying the onset and the evolution of motor deficits and to design and test treatments aimed at promoting recovery after perinatal injury.

Validation of viral anterograde tracing

In this work, we took advantages of a well characterized adeno-associated virus tracer, with an high tropism and specificity for CSMNs [257], to finely assess the presence of sprouting of CST axons in the spinal cord. The number of labelled axons, used to normalized all anatomical measures, was counted on coronal section of medulla oblongata, at the level of the pyramids. In general, estimations of pyramidal axons number ranged from ~70-80.000 [271, 272] to ~100-150.000 [273], depending on visualization methods (light or electron microscopy, respectively). Recently, great attention was payed to the use of viral anterograde tracing in substitution of typical biotinylated dyes; in particular, there were used HIV-GFP lentivectors [274], AAV-8 [275] and AAV-2 [276], with axons number ranging from 1000 to 4000. Serotype 1 seems to be more effective in the trasduction of CSMNs compared to AAV2, AAV8 and also lentiviral vectors [257]. Concurrently with a more sensitive acquisition method, this is consistent with the high number of pyramidal axons that we are able to label and detect.

Aberrant CST anatomy and sprouting after a perinatal ischemic lesion

In most mammals, included primates and rodents, two main pathways compose CST, one of these crosses the midline and reaches contralateral spinal cord targets, whereas the other one do not cross the midline and reaches ipsilateral spinal cord targets. In rodents, these components are respectively called *dorsal* and *ventral CST* (dCST, vCST), referring to the location in the spinal cord white matter. vCST represent the minor component, in a percentage ranging between 2 and 5% in rodents [144, 277, 278] and 8-18% in humans of total CST [66]. Fluorescence intensity analysis on P14 and P21 lesioned animals reveals a significant alteration of CST anatomy, with an increase of ipsilateral, vCST component, and that early training preserve the correct CST pattern. Our fluorescence measures do not replicate the percentage of dCST and vCST distribution present in the literature, probably because GFP fluorescence measure produce a signal scattering that alter the analysis. Another reason might be the presence of a third minor component of CST, the *dorsolateral* one (dlCST) that

we do not consider in these analyses because of the difficulty of a reliable detection.

Axonal sprouting of survived neurons has been described as the principle plastic mechanism serving spontaneous [279] and treatment-induced recovery after stroke [240, 244, 246, 248, 280] that leads to the rewiring of denervated hubs at various levels of motor pathways. However, this structural plasticity can also exert a maladaptive role in worsening motor functions; clinical evidences suggest, in hemiplegic children after a perinatal stroke, that sprouting of ipsilateral projection from non-infarcted cortex compete with healthy survived corticospinal projections, providing a poorer motor outcome [254]. In accordance with these data, we found, in our model of ET1-P14 ischemic lesion, a spontaneous exacerbated axonal sprouting to the denervated spinal cord and an increased miss-targeting of sprouted axons in more dorsal or ventral regions.

Possible molecular mechanisms of maladaptive plasticity

It could be conceivable that a cortical unilateral lesion induced at this age alters the excitation/inhibition balance between hemispheres but also at spinal cord level, enhancing the activity of healthy CST and reducing the activity of the denervated one [281]. Recent efforts were done to identify molecular factors involved in the differentiation and development of CSMNs, both in prenatal and postnatal age [72]. The identification of molecular factors inducing specific axonal sprouting after a perinatal lesion can be crucial to better understand the underlying mechanism and to conceive new treatment approaches. Despite mechanisms of this maladaptive process is unclear, there are various examples of factors involved in adaptive or maladaptive sprouting induced in different injury models. For instance, it is known that co-deletion of PTEN (*phosphatase and tensin homolog*) and SOCS3 (*suppressor of cytokine signalling 3*) induces an increase of axonal sprouting in animals with a unilateral pyramidotomy, with a restoration of motor functions [282]. In contrast, in a spinal cord injury model, augmented sprouting induced by an overexpression of the transcription factor Sox11 worsen functional motor outcome [283] without any evident alteration in synaptogenesis or axonal laminar distribution [284]. Until now, we cannot confirm that sprouted axons

after a perinatal injury form functional synapses in the denervated spinal cord. However, laminar distribution analysis might suggest that a perinatal lesion results in an altered connectivity with off-target dorsal and ventral regions; therefore, maladaptive plasticity can be also related to a mistaken or aberrant connections of sprouted axons with propriospinal neurons [285] or sensory excitatory interneurons (*RORα*, [286]) mainly located in the dorsal gray matter of spinal cord. Moreover, failure of synaptogenesis or mis-targeting of axonal sprouting are not the only mechanisms that can be involved in maladaptive plasticity [284].

Searching for one or more molecular factors involved in maladaptive plasticity processes, we can speculate, on the basis of our results, on the characteristics that these factors should have: 1) expression profile of this factor(s) should deeply change between P14 and P21 age, because of the specific presence of maladaptive plasticity in the earlier age [72]; 2) expression or function of this factor(s) should be strictly dependent on neural activity, because of the reduction of maladaptive plasticity process after a low-intensity motor training; 3) factor(s) involved in maladaptive plasticity might interact in a different manner with spinal cord ECM (*extracellular matrix*), or in general with the external environment characteristic of the spinal cord and CST postnatal development [88].

Effects of early training after a perinatal ischemic lesion

Early training (performed one week after lesion in both P14 and P21 injury models) reduces the exacerbated sprouting and, in general, all the abnormal features of CST exhibited as a consequence of a perinatal (P14) lesion, with a slight improvement of motor functions. Training has also positive effects on P21 lesioned animals, despite the absence of a significant reduction of sprouting. This result is consistent with other works where a skilled motor training improves performances on reaching abilities without any effect on axonal sprouting at the level of spinal cord [287, 288]. Moreover, in our perinatal ischemic model, early training promotes only a partial motor recovery, suggesting in any case the importance of rehabilitation timing for a functional rescue [289]. To better understand the optimal timing of internvention, it might be interesting to compare the effects of a late training with respect

to an earlier one in a perinatal ischemic injury model [290]. It could be also conceivable that treatments including pharmacological or cell based therapies in combination with an optimized motor rehabilitation protocol [246, 249, 291] can further increase recovery of functions.

Conclusions

Spontaneous plasticity of corticospinal tract after an ischemic injury can exert a double-face effect, depending on lesion timing. This work demonstrates how an ischemic stroke at perinatal age strongly interferes with CST development with a consequent poorer long-term motor impairment, compared to a juvenile injury. Harnessing post-stroke neural plasticity via motor training can promote a significant recovery of motor function that is coupled to a reduction of induced aberrant sprouting. This study gives a proof-of-principle about the crucial role of an early intervention after perinatal ischemic stroke on the prevention of altered structural plasticity maturation. Future works should be directed on a better understanding of the mechanisms underlying this maladaptive plasticity process, in order to implement more effective therapeutic strategies aimed at regaining or preserving motor functions.

Bibliography

1. Foster, M. & Sherrington, C. *Textbook of Physiology* 7th ed., 929 (Macmillan, London, 1897).
2. Konorsky, J. *Conditioned reflexes and neuron organization* 89 (Cambridge University Press, 1948).
3. Hebb, D. *The organization of behaviour* (Wiley & Sons, 1949).
4. Mrsic-Flogel, T. D. *et al.* Homeostatic regulation of eye-specific responses in visual cortex during ocular dominance plasticity. *Neuron* **54,** 961–972. (2007).
5. Lunghi, C., Burr, D. C. & Morrone, M. C. Long-term effects of monocular deprivation revealed with binocular rivalry gratings modulated in luminance and in color. *Journal of vision* **13,** 1–1. (2013).
6. Lunghi, C., Emir, U. E., Morrone, M. C. & Bridge, H. Short-term monocular deprivation alters GABA in the adult human visual cortex. *Current Biology* **25,** 1496–1501. (2015).
7. Bliss, T. V. P. & Cooke, S. F. Long-term potentiation and long-term depression: a clinical perspective. *Clinics* **66,** 3–17. (2011).
8. Yang, S., Tang, Y.-G. & Zucker, R. S. Selective induction of LTP and LTD by postsynaptic [Ca2+] i elevation. *Journal of neurophysiology* **81,** 781–787. (1999).

9. Kampa, B. M., Clements, J., Jonas, P. & Stuart, G. J. Kinetics of Mg2+ unblock of NMDA receptors: implications for spike timing dependent synaptic plasticity. *The Journal of physiology* **556,** 337–345. (2004).

10. Bender, V. A. A., Bender, K. J., Brasier, D. J. & Feldman, D. E. Two coincidence detectors for spike timing-dependent plasticity in somatosensory cortex. *The Journal of neuroscience* **26,** 4166–4177. (2006).

11. Nevian, T. & Sakmann, B. Spine Ca2+ signaling in spike-timing-dependent plasticity. *The Journal of neuroscience* **26,** 11001–11013. (2006).

12. Hashimotodani, Y. *et al.* Phospholipase Cβ serves as a coincidence detector through its Ca 2+ dependency for triggering retrograde endocannabinoid signal. *Neuron* **45,** 257–268. (2005).

13. Maejima, T. *et al.* Synaptically driven endocannabinoid release requires Ca2+-assisted metabotropic glutamate receptor subtype 1 to phospholipase Cβ 4 signaling cascade in the cerebellum. *The Journal of neuroscience* **25,** 6826–6835. (2005).

14. Turrigiano, G. G. & Nelson, S. B. Homeostatic plasticity in the developing nervous system. *Nature Reviews Neuroscience* **5,** 97–107. (2004).

15. Wiesel, T. N. & Hubel, D. H. Single-cell responses in striate cortex of kittens deprived of vision in one eye. *J Neurophysiol* **26,** 1003–1017 (1963).

16. Hubel, D. H. & Wiesel, T. N. The period of susceptibility to the physiological effects of unilateral eye closure in kittens. *The Journal of physiology* **206,** 419 (1970).

17. Harwerth, R. S., Smith, E. L., Duncan, G. C., Crawford, M. L. & Von Noorden, G. K. Multiple sensitive periods in the development of the primate visual system. *Science* **232,** 235–238. (1986).

18. Issa, N. P., Trachtenberg, J. T., Chapman, B., Zahs, K. R. & Stryker, M. P. The critical period for ocular dominance plasticity in the ferret's visual cortex. *The Journal of neuroscience* **19,** 6965–6978. (1999).

19. Fagiolini, M., Pizzorusso, T., Berardi, N., Domenici, L. & Maffei, L. Functional postnatal development of the rat primary visual cortex and the role of visual experience: dark rearing and monocular deprivation. *Vision research* **34,** 709–720. (1994).

20. Gordon, J. A. & Stryker, M. P. Experience-dependent plasticity of binocular responses in the primary visual cortex of the mouse. *The Journal of neuroscience* **16,** 3274–3286. (1996).

21. Hensch, T. K. *et al.* Local GABA circuit control of experience-dependent plasticity in developing visual cortex. *Science* **282,** 1504–1508. (1998).

22. Fagiolini, M. & Hensch, T. K. Inhibitory threshold for critical-period activation in primary visual cortex. *Nature* **404,** 183–186. (2000).

23. Huang, Z. J. *et al.* BDNF regulates the maturation of inhibition and the critical period of plasticity in mouse visual cortex. *Cell* **98,** 739–755. (1999).

24. Ciucci, F. *et al.* Insulin-like growth factor 1 (IGF-1) mediates the effects of enriched environment (EE) on visual cortical development. *PLoS One* **2,** e475. (2007).

25. Baroncelli, L. *et al.* Early IGF-1 Primes Visual Cortex Maturation And Accelerates Developmental Switch Between NKCC1 and KCC2 Chloride Transporters in Enriched Animals. *Neuropharmacology*. (2016).

26. Maya-Vetencourt, J. F. *et al.* IGF-1 restores visual cortex plasticity in adult life by reducing local GABA levels. *Neural plasticity* **2012.** (2012).

27. Sugiyama, S. *et al.* Experience-dependent transfer of Otx2 homeoprotein into the visual cortex activates postnatal plasticity. *Cell* **134,** 508–520. (2008).

28. Carro, E., Nuñez, A., Busiguina, S. & Torres-Aleman, I. Circulating insulin-like growth factor I mediates effects of exercise on the brain. *The Journal of neuroscience* **20,** 2926–2933. (2000).

29. Sugiyama, S., Prochiantz, A. & Hensch, T. K. From brain formation to plasticity: insights on Otx2 homeoprotein. *Development, growth & differentiation* **51,** 369–377. (2009).

30. Sale, A., Berardi, N., Spolidoro, M., Baroncelli, L. & Maffei, L. GABAergic inhibition in visual cortical plasticity. *Front Cell Neurosci* **4** (2010).

31. Pizzorusso, T. *et al.* Reactivation of ocular dominance plasticity in the adult visual cortex. *Science* **298,** 1248–1251. (2002).

32. Carulli, D. *et al.* Composition of perineuronal nets in the adult rat cerebellum and the cellular origin of their components. *Journal of Comparative Neurology* **494,** 559–577. (2006).

33. Carulli, D. *et al.* Animals lacking link protein have attenuated perineuronal nets and persistent plasticity. *Brain* **133,** 2331–2347. (2010).

34. Beurdeley, M. *et al.* Otx2 binding to perineuronal nets persistently regulates plasticity in the mature visual cortex. *The Journal of Neuroscience* **32,** 9429–9437. (2012).

35. Spatazza, J. *et al.* Choroid-plexus-derived Otx2 homeoprotein constrains adult cortical plasticity. *Cell reports* **3,** 1815–1823. (2013).

36. McGee, A. W., Yang, Y., Fischer, Q. S., Daw, N. W. & Strittmatter, S. M. Experience-driven plasticity of visual cortex limited by myelin and Nogo receptor. *Science* **309,** 2222–2226. (2005).

37. Syken, J., GrandPre, T., Kanold, P. O. & Shatz, C. J. PirB restricts ocular-dominance plasticity in visual cortex. *Science* **313,** 1795–1800. (2006).

38. Atwal, J. K. *et al.* PirB is a functional receptor for myelin inhibitors of axonal regeneration. *Science* **322,** 967–970. (2008).

39. Pham, T. A., Impey, S., Storm, D. R. & Stryker, M. P. CRE-mediated gene transcription in neocortical neuronal plasticity during the developmental critical period. *Neuron* **22,** 63–72. (1999).

40. Putignano, E. *et al.* Developmental downregulation of histone posttranslational modifications regulates visual cortical plasticity. *Neuron* **53,** 747–759. (2007).

41. Pham, T. A. *et al.* A semi-persistent adult ocular dominance plasticity in visual cortex is stabilized by activated CREB. *Learning & memory* **11,** 738–747. (2004).

42. Silingardi, D., Scali, M., Belluomini, G. & Pizzorusso, T. Epigenetic treatments of adult rats promote recovery from visual acuity deficits induced by long-term monocular deprivation. *European Journal of Neuroscience* **31,** 2185–2192. (2010).

43. Nott, A., Cho, S., Seo, J. & Tsai, L.-H. HDAC2 expression in parvalbumin interneurons regulates synaptic plasticity in the mouse visual cortex. *Neuroepigenetics* **1,** 34–40. (2015).

44. Mellios, N. *et al.* miR-132, an experience-dependent microRNA, is essential for visual cortex plasticity. *Nature neuroscience* **14,** 1240–1242. (2011).

45. Tognini, P., Putignano, E., Coatti, A. & Pizzorusso, T. Experience-dependent expression of miR-132 regulates ocular dominance plasticity. *Nature neuroscience* **14,** 1237–1239. (2011).

46. Tognini, P. *et al.* Experience-dependent DNA methylation regulates plasticity in the developing visual cortex. *Nature neuroscience* **18,** 956–958. (2015).

47. Morishita, H., Miwa, J. M., Heintz, N. & Hensch, T. K. Lynx1, a cholinergic brake, limits plasticity in adult visual cortex. *Science* **330,** 1238–1240. (2010).

48. Vetencourt, J. F. M., Tiraboschi, E., Spolidoro, M., Castrén, E. & Maffei, L. Serotonin triggers a transient epigenetic mechanism that reinstates adult visual cortex plasticity in rats. *European Journal of Neuroscience* **33,** 49–57. (2011).

49. Cancedda, L. *et al.* Acceleration of visual system development by environmental enrichment. *The Journal of Neuroscience* **24,** 4840–4848. (2004).

50. Sale, A. *et al.* Enriched environment and acceleration of visual system development. *Neuropharmacology* **47,** 649–660. (2004).

51. Baroncelli, L. *et al.* Experience-dependent reactivation of ocular dominance plasticity in the adult visual cortex. *Experimental neurology* **226,** 100–109. (2010).

52. Baroncelli, L. *et al.* Experience Affects Critical Period Plasticity in the Visual Cortex through an Epigenetic Regulation of Histone Post-Translational Modifications. *The Journal of Neuroscience* **36,** 3430–3440. (2016).

53. Levelt, C. N. & Hübener, M. Critical-Period Plasticity in the Visual Cortex. *Annu. Rev. Neurosci.* **35,** 309–330. (June 2012).

54. Woolsey, T. A. & Van der Loos, H. The structural organization of layer IV in the somatosensory region (SI) of mouse cerebral cortex: the description of a cortical field composed of discrete cytoarchitectonic units. *Brain research* **17,** 205–242. (1970).

55. Fox, K. A critical period for experience-dependent synaptic plasticity in rat barrel cortex. *The Journal of neuroscience* **12,** 1826–1838. (1992).

56. Glazewski, S. & Fox, K. Time course of experience-dependent synaptic potentiation and depression in barrel cortex of adolescent rats. *Journal of neurophysiology* **75,** 1714–1729. (1996).

57. Crair, M. C. & Malenka, R. C. A critical period for long-term potentiation at thalamocortical synapses. *Nature* **375,** 325–328. (1995).

58. Isaac, J. T. R., Crair, M. C., Nicoll, R. A. & Malenka, R. C. Silent synapses during development of thalamocortical inputs. *Neuron* **18,** 269–280. (1997).

59. Skibinska, A., Glazewski, S., Fox, K. & Kossut, M. Age-dependent response of the mouse barrel cortex to sensory deprivation: a 2-deoxyglucose study. *Experimental brain research* **132,** 134–138. (2000).

60. Stanton, S. & Harrison, R. Abnormal cochleotopic organization in the auditory cortex of cats reared in a frequency augmented environment. *Aud. Neurosci* **2,** 97–107 (1996).

61. Chang, E. F. & Merzenich, M. M. Environmental noise retards auditory cortical development. *Science* **300,** 498–502. (2003).

62. Watson, C., Paxinos, G. & Kayalioglu, G. *The spinal cord: a Christopher and Dana Reeve Foundation text and atlas* (Academic press, 2009).

63. Brosamle, C. & Schwab, M. E. Ipsilateral, ventral corticospinal tract of the adult rat: ultrastructure, myelination and synaptic connections. *Journal of neurocytology* **29,** 499–507. (2000).

64. Purves, D., Cabeza, R., Huettel, S. A. & Platt, M. L. *Principles of cognitive neuroscience* (Sinauer Associates Sunderland, MA, 2008).

65. Kathe, C. *et al.* Unilateral pyramidotomy of the corticospinal tract in rats for assessment of neuroplasticity-inducing therapies. *Journal of visualized experiments: JoVE* (2014).

66. Eyre, J. A. Corticospinal tract development and its plasticity after perinatal injury. *Neuroscience & Biobehavioral Reviews* **31,** 1136–1149. (2007).

67. Takahashi, K. & Yamanaka, S. Induction of pluripotent stem cells from mouse embryonic and adult fibroblast cultures by defined factors. *cell* **126,** 663–676. (2006).

68. Chen, B., Schaevitz, L. R. & McConnell, S. K. Fezl regulates the differentiation and axon targeting of layer 5 subcortical projection neurons in cerebral cortex. *Proceedings of the National Academy of Sciences of the United States of America* **102,** 17184–17189. (2005).

69. Molyneaux, B. J., Arlotta, P., Hirata, T., Hibi, M. & Macklis, J. D. Fezl is required for the birth and specification of corticospinal motor neurons. *Neuron* **47,** 817–831. (2005).

70. De la Rossa, A. *et al.* In vivo reprogramming of circuit connectivity in postmitotic neocortical neurons. *Nature neuroscience* **16,** 193–200. (2013).

71. Rouaux, C. & Arlotta, P. Direct lineage reprogramming of post-mitotic callosal neurons into corticofugal neurons in vivo. *Nature cell biology* **15,** 214–221. (2013).

72. Arlotta, P. *et al.* Neuronal subtype-specific genes that control corticospinal motor neuron development in vivo. *Neuron* **45,** 207–221. (2005).

73. Weimann, J. M. *et al.* Cortical neurons require Otx1 for the refinement of exuberant axonal projections to subcortical targets. *Neuron* **24,** 819–831. (1999).

74. Kwan, K. Y. *et al.* SOX5 postmitotically regulates migration, postmigratory differentiation, and projections of subplate and deep-layer neocortical neurons. *Proceedings of the National Academy of Sciences* **105,** 16021–16026. (2008).

75. Lai, T. *et al.* SOX5 controls the sequential generation of distinct corticofugal neuron subtypes. *Neuron* **57,** 232–247. (2008).

76. Bagnard, D., Lohrum, M., Uziel, D., Puschel, A. W. & Bolz, J. Semaphorins act as attractive and repulsive guidance signals during the development of cortical projections. *Development* **125,** 5043–5053. (1998).

77. Bagri, A. *et al.* Slit proteins prevent midline crossing and determine the dorsoventral position of major axonal pathways in the mammalian forebrain. *Neuron* **33,** 233–248. (2002).

78. Barallobre, M. J., Pascual, M., Del Rio, J. A. & Soriano, E. The Netrin family of guidance factors: emphasis on Netrin-1 signalling. *Brain Research Reviews* **49,** 22–47. (2005).

79. Finger, J. H. *et al.* The netrin 1 receptors Unc5h3 and Dcc are necessary at multiple choice points for the guidance of corticospinal tract axons. *The Journal of neuroscience* **22,** 10346–10356. (2002).

80. Fazeli, A. *et al.* Phenotype of mice lacking functional Deleted in colorectal cancer (Dcc) gene. *PROBE* **1** (1997).

81. Itoh, K. *et al.* Brain development in mice lacking L1-L1 homophilic adhesion. *The Journal of cell biology* **165,** 145–154. (2004).

82. Coonan, J. R. *et al.* Development and reorganization of corticospinal projections in EphA4 deficient mice. *Journal of Comparative Neurology* **436,** 248–262. (2001).

83. Kullander, K. *et al.* Ephrin-B3 is the midline barrier that prevents corticospinal tract axons from recrossing, allowing for unilateral motor control. *Genes & Development* **15,** 877–888. (2001).

84. Paixão, S. *et al.* EphrinB3/EphA4-mediated guidance of ascending and descending spinal tracts. *Neuron* **80,** 1407–1420. (2013).

85. Joosten, E. & Bar, D. Axon guidance of outgrowing corticospinal fibres in the rat. *Journal of anatomy* **194,** 15–32. (1999).

86. Joosten, E. A. J. Developmental expression of N-CAM epitopes in the rat spinal cord during corticospinal tract axon outgrowth and target innervation. *Developmental brain research* **78,** 226–236. (1994).

87. Eyre, J. A., Miller, S., *et al.* Functional corticospinal projections are established prenatally in the human foetus permitting involvement in the development of spinal motor centres. *Brain* **123,** 51–64. (2000).

88. Canty, A. J. & Murphy, M. Molecular mechanisms of axon guidance in the developing corticospinal tract. *Progress in neurobiology* **85,** 214–235. (2008).

89. Li, Q. & Martin, J. H. Postnatal development of differential projections from the caudal and rostral motor cortex subregions. *Experimental brain research* **134,** 187–198. (2000).

90. Alisky, J. M., Swink, T. D. & Tolbert, D. L. The postnatal spatial and temporal development of corticospinal projections in cats. *Experimental brain research* **88,** 265–276. (1992).

91. Eyre, J. A., Taylor, J. P., Villagra, F., Smith, M. & Miller, S. Evidence of activity-dependent withdrawal of corticospinal projections during human development. *Neurology* **57,** 1543–1554. (2001).

92. Martin, J. H., Choy, M., Pullman, S. & Meng, Z. Corticospinal system development depends on motor experience. *The Journal of neuroscience* **24,** 2122–2132. (2004).

93. Martin, J. H. & Lee, S. J. Activity dependent competition between developing corticospinal terminations. *Neuroreport* **10,** 2277–2282. (1999).

94. Friel, K. M. & Martin, J. H. Role of sensory motor cortex activity in postnatal development of corticospinal axon terminals in the cat. *Journal of Comparative Neurology* **485,** 43–56. (2005).

95. Salimi, I. & Martin, J. H. Rescuing transient corticospinal terminations and promoting growth with corticospinal stimulation in kittens. *The Journal of neuroscience* **24,** 4952–4961. (2004).

96. Chakrabarty, S. & Martin, J. H. Postnatal development of the motor representation in primary motor cortex. *Journal of Neurophysiology* **84,** 2582–2594. (2000).

97. Meng, Z., Li, Q. & Martin, J. H. The transition from development to motor control function in the corticospinal system. *The Journal of neuroscience* **24,** 605–614. (2004).

98. Martin, J. H. The corticospinal system: from development to motor control. *The Neuroscientist* **11,** 161–173. (2005).

99. Rosamond, W. *et al.* Heart Disease and Stroke Statistics-2007 Update: A Report From the American Heart Association Statistics Committee and Stroke Statistics Subcommittee (vol 115, pg e69, 2007). *Circulation* **122,** E9–E9. (2010).

100. *Italian Ministry of Health.* <http://www.salute.gov.it/portale/salute/p1_5.jsp?id=28&area=Malattie_cardiovascolari> (2013).

101. Nelson, K. B. Perinatal ischemic stroke. *Stroke* **38,** 742–745. (2007).

102. Raju, T. N. K., Nelson, K. B., Ferriero, D. & Lynch, J. K. Ischemic perinatal stroke: summary of a workshop sponsored by the National Institute of Child Health and Human Development and the National Institute of Neurological Disorders and Stroke. *Pediatrics* **120,** 609–616. (2007).

103. Kirton, A. Modeling developmental plasticity after perinatal stroke: defining central therapeutic targets in cerebral palsy. *Pediatric neurology* **48,** 81–94. (2013).

104. Edvinson, L., MacKenzie, E. T. & McCulloch, J. Cerebral Blood Flow and Metabolism. *Alzheimer Disease & Associated Disorders* **7,** 129. (1993).

105. Bruno, V. *et al.* Metabotropic glutamate receptor subtypes as targets for neuroprotective drugs. *Journal of Cerebral Blood Flow & Metabolism* **21,** 1013–1033. (2001).

106. Pellegrini-Giampietro, D. E. The distinct role of mGlu 1 receptors in post-ischemic neuronal death. *Trends in pharmacological sciences* **24,** 461–470. (2003).

107. Gonzalez, R., Hirsch, J., Koroshetz, W., Lev, M. & Schaefer, P. Acute ischemic stroke: imaging and intervention. *American Journal of Neuroradiology* **28,** 1622. (2007).

108. Crack, P. J. & Taylor, J. M. Reactive oxygen species and the modulation of stroke. *Free Radical Biology and Medicine* **38,** 1433–1444. (2005).

109. Zador, Z., Stiver, S., Wang, V. & Manley, G. T. in *Aquaporins* 159–170 (Springer, 2009).

110. George, P. M. & Steinberg, G. K. Novel stroke therapeutics: unraveling stroke pathophysiology and its impact on clinical treatments. *Neuron* **87,** 297–309. (2015).

111. Dirnagl, U., Iadecola, C. & Moskowitz, M. A. Pathobiology of ischaemic stroke: an integrated view. *Trends in neurosciences* **22,** 391–397. (1999).

112. Huang, J., Upadhyay, U. M. & Tamargo, R. J. Inflammation in stroke and focal cerebral ischemia. *Surgical neurology* **66,** 232–245. (2006).

113. Doyle, K. P., Simon, R. P. & Stenzel-Poore, M. P. Mechanisms of ischemic brain damage. *Neuropharmacology* **55,** 310–318. (2008).

114. Johnston, M. V. Excitotoxicity in perinatal brain injury. *metabolism* **7,** 61 (2005).

115. Knox, R. *et al.* Enhanced NMDA receptor tyrosine phosphorylation and increased brain injury following neonatal hypoxia-ischemia in mice with neuronal Fyn overexpression. *Neurobiology of disease* **51,** 113–119. (2013).

116. Jiang, X., Mu, D., Sheldon, R. A., Glidden, D. V. & Ferriero, D. M. Neonatal Hypoxia-Ischemia Differentially Upregulates MAGUKs and Associated Proteins in PSD-93-Deficient Mouse Brain. *Stroke* **34,** 2958–2963. (2003).

117. Lafemina, M. J., Sheldon, R. A. & Ferriero, D. M. Acute hypoxia-ischemia results in hydrogen peroxide accumulation in neonatal but not adult mouse brain. *Pediatric research* **59,** 680–683. (2006).

118. Manabat, C. *et al.* Reperfusion differentially induces caspase-3 activation in ischemic core and penumbra after stroke in immature brain. *Stroke* **34,** 207–213. (2003).

119. West, T., Atzeva, M. & Holtzman, D. M. Caspase-3 deficiency during development increases vulnerability to hypoxic-ischemic injury through caspase-3-independent pathways. *Neurobiology of disease* **22,** 523–537. (2006).

120. Lassiter, H. A. *et al.* The Administration of Complement Component C9 Enhances the Survival of Neonatal Rats with Escherichia coli Sepsis1. *Pediatric research* **42,** 128–136. (1997).

121. Hedtjärn, M., Mallard, C., Iwakura, Y. & Hagberg, H. Combined deficiency of IL-1β18, but not IL-1$\alpha\beta$, reduces susceptibility to hypoxia-ischemia in the immature brain. *Developmental neuroscience* **27,** 143–148. (2005).

122. Saunders, N. R., Habgood, M. D. & Dziegielewska, K. M. Barrier mechanisms in the brain, II. Immature brain. *Clinical and Experimental Pharmacology and Physiology* **26,** 85–91. (1999).

123. Fernández-López, D. *et al.* Blood-brain barrier permeability is increased after acute adult stroke but not neonatal stroke in the rat. *The Journal of Neuroscience* **32,** 9588–9600. (2012).

124. Hudome, S. *et al.* The role of neutrophils in the production of hypoxic-ischemic brain injury in the neonatal rat. *Pediatric research* **41,** 607–616. (1997).

125. Kolb, B. & Muhammad, A. Harnessing the power of neuroplasticity for intervention. *Frontiers in Human Neuroscience* **8,** 42–54 (2013).

126. Carmichael, S. T. Rodent models of focal stroke: size, mechanism, and purpose. *NeuroRx* **2,** 396–409. (2005).

127. Gautier, J. C. & Mohr, J. P. Intracranial internal carotid artery disease. *Stroke. New York, Churchill-Livingstone* (1986).

128. Dittmar, M., Spruss, T., Schuierer, G. & Horn, M. External carotid artery territory ischemia impairs outcome in the endovascular filament model of middle cerebral artery occlusion in rats. *Stroke* **34,** 2252–2257. (2003).

129. Tamura, A., Graham, D. I., McCulloch, J. & Teasdale, G. M. Focal cerebral ischaemia in the rat: 1. Description of technique and early neuropathological consequences following middle cerebral artery occlusion. *Journal of Cerebral Blood Flow & Metabolism* **1,** 53–60. (1981).

130. Hainsworth, A. H. & Markus, H. S. Do in vivo experimental models reflect human cerebral small vessel disease? A systematic review. *Journal of Cerebral Blood Flow & Metabolism* **28,** 1877–1891. (2008).

131. Schmidt, A. *et al.* Photochemically induced ischemic stroke in rats. *Experimental & translational stroke medicine* **4,** 1. (2012).

132. Schneider, G. *et al.* Pathophysiological changes after traumatic brain injury: comparison of two experimental animal models by means of MRI. *Magnetic Resonance Materials in Physics, Biology and Medicine* **14,** 233–241. (2002).

133. Sharkey, J. Perivascular microapplication of endothelin-1: a new model of focal cerebral ischaemia in the rat. *Journal of Cerebral Blood Flow & Metabolism* **13,** 865–871. (1993).

134. Windle, V. *et al.* An analysis of four different methods of producing focal cerebral ischemia with endothelin-1 in the rat. *Experimental neurology* **201,** 324–334. (2006).

135. Nikolova, S. *et al.* Endothelin-1 induced MCAO: dose dependency of cerebral blood flow. *Journal of neuroscience methods* **179,** 22–28. (2009).

136. Macrae, I. M., Robinson, M. J., Graham, D. I., Reid, J. L. & McCulloch, J. Endothelin-1-induced reductions in cerebral blood flow: dose dependency, time course, and neuropathological consequences. *Journal of Cerebral Blood Flow & Metabolism* **13,** 276–284. (1993).

137. Horie, N. *et al.* Mouse model of focal cerebral ischemia using endothelin-1. *Journal of neuroscience methods* **173,** 286–290. (2008).

138. Roome, R. B. *et al.* A reproducible Endothelin-1 model of forelimb motor cortex stroke in the mouse. *Journal of neuroscience methods* **233,** 34–44. (2014).

139. Hagberg, H., Bona, E., Gilland, E. & Puka-Sundvall, M. Hypoxia-ischaemia model in the 7-day-old rat: possibilities and shortcomings. *Acta Paediatrica* **86,** 85–88. (1997).

140. Hagberg, H., Peebles, D. & Mallard, C. Models of white matter injury: Comparison of infectious, hypoxic-ischemic, and excitotoxic insults. *Mental retardation and developmental disabilities research reviews* **8,** 30–38. (2002).

141. Clowry, G. J. The dependence of spinal cord development on corticospinal input and its significance in understanding and treating spastic cerebral palsy. *Neuroscience & Biobehavioral Reviews* **31,** 1114–1124. (2007).

142. Umeda, T. & Isa, T. Differential contributions of rostral and caudal frontal forelimb areas to compensatory process after neonatal hemidecortication in rats. *European Journal of Neuroscience* **34,** 1453–1460. (2011).

143. Vannucci, R. C. & Vannucci, S. J. Perinatal hypoxic-ischemic brain damage: evolution of an animal model. *Developmental neuroscience* **27,** 81–86. (2005).

144. Clowry, G. J., Basuodan, R. & Chan, F. What are the Best Animal Models for Testing Early Intervention in Cerebral Palsy? *Frontiers in Neurology* **5,** 258. (2014).

145. Lee, J. *et al.* Predictors of outcome in perinatal arterial stroke: A population-based study. *Annals of neurology* **58,** 303–308. (2005).

146. Kirton, A. Life after perinatal stroke. *Stroke* **44,** 3265–3271. (2013).

147. Ashwal, S., Cole, D. J., Osborne, S., Osborne, T. N. & Pearce, W. J. A new model of neonatal stroke: reversible middle cerebral artery occlusion in the rat pup. *Pediatric neurology* **12,** 191–196. (1995).

148. Derugin, N., Ferriero, D. M. & Vexler, Z. S. Neonatal reversible focal cerebral ischemia: a new model. *Neuroscience research* **32,** 349–353. (1998).

149. Ashwal, S., Tone, B., Tian, H. R., Chong, S. & Obenaus, A. Comparison of two neonatal ischemic injury models using magnetic resonance imaging. *Pediatric research* **61,** 9–14. (2007).

150. Wen, T.-C., Rogido, M., Gressens, P. & Sola, A. A reproducible experimental model of focal cerebral ischemia in the neonatal rat. *Brain research protocols* **13,** 76–83. (2004).

151. Kuluz, J. W. *et al.* New Pediatric Model of Ischemic Stroke in Infant Piglets by Photothrombosis Acute Changes in Cerebral Blood Flow, Microvasculature, and Early Histopathology. *Stroke* **38,** 1932–1937. (2007).

152. Saggu, R. Characterisation of Endothelin-1-Induced intrastriatal lesions within the juvenile and adult rat brain using MRI and 31P MRS. *Translational stroke research* **4,** 351–367. (2013).

153. Macrae, I. M. Preclinical stroke research-advantages and disadvantages of the most common rodent models of focal ischaemia. *British journal of pharmacology* **164,** 1062–1078. (2011).

154. Sahota, P. & Savitz, S. I. Investigational therapies for ischemic stroke: neuroprotection and neurorecovery. *Neurotherapeutics* **8,** 434–451. (2011).

155. Korninger, C. & Collen, D. Studies on the specific fibrinolytic effect of human extrinsic (tissue-type) plasminogen activator in human blood and in various animal species in vitro. *Thrombosis and haemostasis* **46,** 561–565. (1981).

156. Cronin, C. A. Intravenous tissue plasminogen activator for stroke: a review of the ECASS III results in relation to prior clinical trials. *The Journal of emergency medicine* **38,** 99–105. (2010).

157. Goel, R., Vedantham, S. & Goldenberg, N. A. Antithrombotic therapies: anticoagulation and thrombolysis. *Pediatric clinics of North America* **60,** 1463–1474. (2013).

158. Erecinska, M., Thoresen, M. & Silver, I. A. Effects of hypothermia on energy metabolism in Mammalian central nervous system. *Journal of Cerebral Blood Flow & Metabolism* **23,** 513–530. (2003).

159. Liu, L. & Yenari, M. A. Therapeutic hypothermia: neuroprotective mechanisms. *Front Biosci* **12,** 25 (2007).

160. Polderman, K. H. Mechanisms of action, physiological effects, and complications of hypothermia. *Critical care medicine* **37,** S186–S202. (2009).

161. Harbert, M. J. *et al.* Hypothermia is correlated with seizure absence in perinatal stroke. *Journal of child neurology* **26,** 1126–1130. (2011).

162. Van der Worp, H. B., Sena, E. S., Donnan, G. A., Howells, D. W. & Macleod, M. R. Hypothermia in animal models of acute ischaemic stroke: a systematic review and meta-analysis. *Brain* **130,** 3063–3074. (2007).

163. Gonzalez, F. & Ferriero, D. Neuroprotection in the newborn infant. *Clinics in perinatology* **36,** 859–880. (2009).

164. Sola, A., Rogido, M., Lee, B. H., Genetta, T. & Wen, T.-C. Erythropoietin after focal cerebral ischemia activates the Janus Kinase-Signal transducer and activator of transcription signaling pathway and improves brain injury in postnatal day 7 Rats. *Pediatric research* **57,** 481–487. (2005).

165. Chang, Y. S. *et al.* Erythropoietin improves functional and histological outcome in neonatal stroke. *Pediatric research* **58,** 106–111. (2005).

166. Larpthaveesarp, A., Georgevits, M., Ferriero, D. M. & Gonzalez, F. F. Delayed erythropoietin therapy improves histological and behavioral outcomes after transient neonatal stroke. *Neurobiology of disease* **93,** 57–63. (2016).

167. Dzietko, M., Derugin, N., Wendland, M. F., Vexler, Z. S. & Ferriero, D. M. Delayed VEGF treatment enhances angiogenesis and recovery after neonatal focal rodent stroke. *Translational stroke research* **4,** 189–200. (2013).

168. Fox, C. *et al.* Minocycline Confers Early but Transient Protection in the Immature Brain following Focal Cerebral Ischemia–Reperfusion. *Journal of Cerebral Blood Flow & Metabolism* **25,** 1138–1149. (2005).

169. Tsuji, M., Wilson, M. A., Lange, M. S. & Johnston, M. V. Minocycline worsens hypoxic-ischemic brain injury in a neonatal mouse model. *Experimental neurology* **189,** 58–65. (2004).

170. Bednar, M. M. The role of sildenafil in the treatment of stroke. *Current Opinion in Investigational Drugs* **9,** 754–759. (2008).

171. Moretti, R. *et al.* Sildenafil, a cyclic GMP phosphodiesterase inhibitor, induces microglial modulation after focal ischemia in the neonatal mouse brain. *Journal of neuroinflammation* **13,** 1. (2016).

172. Arvidsson, A., Collin, T., Kirik, D., Kokaia, Z. & Lindvall, O. Neuronal replacement from endogenous precursors in the adult brain after stroke. *Nature medicine* **8,** 963–970 (2002).

173. Parent, J. M., Vexler, Z. S., Gong, C., Derugin, N. & Ferriero, D. M. Rat forebrain neurogenesis and striatal neuron replacement after focal stroke. *Annals of neurology* **52,** 802–813. (2002).

174. Kobayashi, T. *et al.* Intracerebral infusion of glial cell line-derived neurotrophic factor promotes striatal neurogenesis after stroke in adult rats. *Stroke* **37,** 2361–2367. (2006).

175. Dempsey, R. J., Sailor, K. A., Bowen, K. K., Türeyen, K. & Vemuganti, R. Stroke-induced progenitor cell proliferation in adult spontaneously hypertensive rat brain: effect of exogenous IGF-1 and GDNF. *Journal of neurochemistry* **87,** 586–597. (2003).

176. Wang, L., Zhang, Z., Wang, Y., Zhang, R. & Chopp, M. Treatment of stroke with erythropoietin enhances neurogenesis and angiogenesis and improves neurological function in rats. *Stroke* **35,** 1732–1737. (2004).

177. Bliss, T. M., Andres, R. H. & Steinberg, G. K. Optimizing the success of cell transplantation therapy for stroke. *Neurobiology of disease* **37,** 275–283. (2010).

178. Stroemer, P., Hope, A., Patel, S., Pollock, K. & Sinden, J. Development of a human neural stem cell line for use in recovery from disability after stroke. *Frontiers in bioscience: a journal and virtual library* **13,** 2290–2292. (2007).

179. Takahashi, T., Goto, T., Miyama, S., Nowakowski, R. S. & Caviness, V. S. Sequence of neuron origin and neocortical laminar fate: relation to cell cycle of origin in the developing murine cerebral wall. *The Journal of neuroscience* **19,** 10357–10371. (1999).

180. Oki, K. *et al.* Human-induced pluripotent stem cells form functional neurons and improve recovery after grafting in stroke-damaged brain. *Stem Cells* **30,** 1120–1133. (2012).

181. Bhasin, A. *et al.* Stem cell therapy: a clinical trial of stroke. *Clinical neurology and neurosurgery* **115,** 1003–1008. (2013).

182. Steinberg, G. K. *et al.* A novel phase 1/2A study of intraparenchymal transplantation of human modified bone marrow derived cells in patients with stable ischemic stroke. *Stroke* **45,** A149–A149. (2014).

183. Deluca, S. C., Echols, K., Law, C. R. & Ramey, S. L. Intensive pediatric constraint-induced therapy for children with cerebral palsy: randomized, controlled, crossover trial. *Journal of child neurology* **21,** 931–938. (2006).

184. Kwakkel, G., Veerbeek, J. M., van Wegen, E. E. H. & Wolf, S. L. Constraint-induced movement therapy after stroke. *The Lancet Neurology* **14,** 224–234. (2015).

185. Wolf, S. L. *et al.* Effect of constraint-induced movement therapy on upper extremity function 3 to 9 months after stroke: the EXCITE randomized clinical trial. *Jama* **296,** 2095–2104. (2006).

186. Liepert, J., Hamzei, F. & Weiller, C. Motor cortex disinhibition of the unaffected hemisphere after acute stroke. *Muscle & nerve* **23,** 1761–1763. (2000).

187. Pascual-Leone, A. *et al.* Study and modulation of human cortical excitability with transcranial magnetic stimulation. *Journal of Clinical Neurophysiology* **15,** 333–343. (1998).

188. Pascual-Leone, A., Amedi, A., Fregni, F. & Merabet, L. B. The plastic human brain cortex. *Annu. Rev. Neurosci.* **28,** 377–401. (2005).

189. Nitsche, M. A. & Paulus, W. Excitability changes induced in the human motor cortex by weak transcranial direct current stimulation. *The Journal of physiology* **527,** 633–639. (2000).

190. Dayan, E., Censor, N., Buch, E. R., Sandrini, M. & Cohen, L. G. Noninvasive brain stimulation: from physiology to network dynamics and back. *Nature neuroscience* **16,** 838–844. (2013).

191. Utz, K. S., Dimova, V., Oppenländer, K. & Kerkhoff, G. Electrified minds: transcranial direct current stimulation (tDCS) and galvanic vestibular stimulation (GVS) as methods of non-invasive brain stimulation in neuropsychology–a review of current data and future implications. *Neuropsychologia* **48,** 2789–2810. (2010).

192. Kirton, A. *Can noninvasive brain stimulation measure and modulate developmental plasticity to improve function in stroke-induced cerebral palsy?* in *Seminars in pediatric neurology* **20** (Elsevier, 2013), 116–126.

193. Kirton, A., Chen, R., Friefeld, S., Gunraj, C. & Pontigon, A.-M. Contralesional repetitive transcranial magnetic stimulation for chronic hemiparesis in subcortical paediatric stroke: a randomised trial. *The Lancet Neurology* **7,** 507–513. (2008).

194. Gillick, B. T. *et al.* Safety and feasibility of transcranial direct current stimulation in pediatric hemiparesis: randomized controlled preliminary study. *Physical therapy* **95,** 337–349. (2015).

195. Cramer, S. C. Repairing the human brain after stroke: I. Mechanisms of spontaneous recovery. *Annals of neurology* **63,** 272–287. (2008).

196. Zeiler, S. R. *et al.* Medial premotor cortex shows a reduction in inhibitory markers and mediates recovery in a mouse model of focal stroke. *Stroke* **44,** 483–489. (2013).

197. Whishaw, I. Q. Loss of the innate cortical engram for action patterns used in skilled reaching and the development of behavioral compensation following motor cortex lesions in the rat. *Neuropharmacology* **39,** 788–805. (2000).

198. Moon, S.-K., Alaverdashvili, M., Cross, A. R. & Whishaw, I. Q. Both compensation and recovery of skilled reaching following small photothrombotic stroke to motor cortex in the rat. *Experimental neurology* **218,** 145–153. (2009).

199. Murphy, T. H. & Corbett, D. Plasticity during stroke recovery: from synapse to behaviour. *Nature Reviews Neuroscience* **10,** 861–872. (2009).

200. Takeuchi, N. & Izumi, S.-I. Maladaptive plasticity for motor recovery after stroke: mechanisms and approaches. *Neural plasticity* **2012.** (2012).

201. Song, S., Miller, K. D. & Abbott, L. F. Competitive Hebbian learning through spike-timing dependent synaptic plasticity. *Nature neuroscience* **3,** 919–926 (2000).

202. Whitlock, J. R., Heynen, A. J., Shuler, M. G. & Bear, M. F. Learning induces long-term potentiation in the hippocampus. *science* **313,** 1093–1097. (2006).

203. Biernaskie, J. & Corbett, D. Enriched rehabilitative training promotes improved forelimb motor function and enhanced dendritic growth after focal ischemic injury. *The Journal of Neuroscience* **21,** 5272–5280. (2001).

204. Dromerick, A. W. *et al.* Very early constraint-induced movement during stroke rehabilitation (VECTORS) A single-center RCT. *Neurology* **73,** 195–201. (2009).

205. Krakauer, J. W., Carmichael, S. T., Corbett, D. & Wittenberg, G. F. Getting neurorehabilitation right what can be learned from animal models? *Neurorehabilitation and neural repair* **26,** 923–931. (2012).

206. Iadecola, C. & Anrather, J. The immunology of stroke: from mechanisms to translation. *Nature medicine* **17,** 796–808. (2011).

207. Benakis, C., Garcia-Bonilla, L., Iadecola, C. & Anrather, J. The role of microglia and myeloid immune cells in acute cerebral ischemia. *Frontiers in cellular neuroscience* **8,** 461. (2015).

208. Overman, J. J. *et al.* A role for ephrin-A5 in axonal sprouting, recovery, and activity-dependent plasticity after stroke. *Proceedings of the National Academy of Sciences* **109,** E2230–E2239. (2012).

209. Ren, J., Kaplan, P. L., Charette, M. F., Speller, H. & Finklestein, S. P. Time window of intracisternal osteogenic protein-1 in enhancing functional recovery after stroke. *Neuropharmacology* **39,** 860–865. (2000).

210. Li, S. *et al.* GDF10 is a signal for axonal sprouting and functional recovery after stroke. *Nature neuroscience.* (2015).

211. Omura, T. *et al.* Robust axonal regeneration occurs in the injured CAST/Ei mouse CNS. *Neuron* **86,** 1215–1227. (2015).

212. Liu, K. *et al.* PTEN deletion enhances the regenerative ability of adult corticospinal neurons. *Nature neuroscience* **13,** 1075–1081. (2010).

213. Sun, F. *et al.* Sustained axon regeneration induced by co-deletion of PTEN and SOCS3. *Nature* **480,** 372–375. (2011).

214. Lu, Y., Belin, S. & He, Z. Signaling regulations of neuronal regenerative ability. *Current opinion in neurobiology* **27,** 135–142. (2014).

215. Danilov, C. A. & Steward, O. Conditional genetic deletion of PTEN after a spinal cord injury enhances regenerative growth of CST axons and motor function recovery in mice. *Experimental neurology* **266,** 147–160. (2015).

216. Wiltrout, C., Lang, B., Yan, Y., Dempsey, R. J. & Vemuganti, R. Repairing brain after stroke: a review on post-ischemic neurogenesis. *Neurochemistry international* **50,** 1028–1041. (2007).

217. Li, S. *et al.* An age-related sprouting transcriptome provides molecular control of axonal sprouting after stroke. *Nature neuroscience* **13,** 1496–1504. (2010).

218. Giger, R. J., Hollis, E. R. & Tuszynski, M. H. Guidance molecules in axon regeneration. *Cold Spring Harbor perspectives in biology* **2,** a001867. (2010).

219. Brown, C. E., Aminoltejari, K., Erb, H., Winship, I. R. & Murphy, T. H. In vivo voltage-sensitive dye imaging in adult mice reveals that somatosensory maps lost to stroke are replaced over weeks by new structural and functional circuits with prolonged modes of activation within both the peri-infarct zone and distant sites. *The Journal of neuroscience* **29,** 1719–1734. (2009).

220. Frost, S. B., Barbay, S., Friel, K. M., Plautz, E. J. & Nudo, R. J. Reorganization of remote cortical regions after ischemic brain injury: a potential substrate for stroke recovery. *Journal of neurophysiology* **89,** 3205–3214. (2003).

221. Biernaskie, J., Szymanska, A., Windle, V. & Corbett, D. Bi-hemispheric contribution to functional motor recovery of the affected forelimb following focal ischemic brain injury in rats. *European Journal of Neuroscience* **21,** 989–999. (2005).

222. Benowitz, L. I. & Carmichael, S. T. Promoting axonal rewiring to improve outcome after stroke. *Neurobiology of disease* **37,** 259–266. (2010).

223. Lindau, N. T. *et al.* Rewiring of the corticospinal tract in the adult rat after unilateral stroke and anti-Nogo-A therapy. *Brain* **137,** 739–756. (2014).

224. Morecraft, R. J. *et al.* Frontal and frontoparietal injury differentially affect the ipsilateral corticospinal projection from the nonlesioned hemisphere in monkey (Macaca mulatta). *Journal of Comparative Neurology* **524,** 380–407. (2016).

225. Ayling, O. G. S., Harrison, T. C., Boyd, J. D., Goroshkov, A. & Murphy, T. H. Automated light-based mapping of motor cortex by photoactivation of channelrhodopsin-2 transgenic mice. *Nature methods* **6,** 219–224. (2009).

226. Harrison, T. C., Ayling, O. G. S. & Murphy, T. H. Distinct cortical circuit mechanisms for complex forelimb movement and motor map topography. *Neuron* **74,** 397–409. (2012).

227. Anenberg, E. *et al.* Ministrokes in channelrhodopsin-2 transgenic mice reveal widespread deficits in motor output despite maintenance of cortical neuronal excitability. *The Journal of Neuroscience* **34,** 1094–1104. (2014).

228. Fenno, L., Yizhar, O. & Deisseroth, K. The development and application of optogenetics. *Neuroscience* **34,** 389 (2011).

229. Deisseroth, K. Optogenetics: 10 years of microbial opsins in neuroscience. *Nature neuroscience* **18,** 1213–1225. (2015).

230. Silasi, G., Boyd, J. D., LeDue, J. & Murphy, T. Improved methods for chronic light-based motor mapping in mice: automated movement tracking with accelerometers, and chronic EEG recording in a bilateral thin-skull preparation. *Frontiers in neural circuits* **7,** 123. (2013).

231. Harrison, T. C., Silasi, G., Boyd, J. D. & Murphy, T. H. Displacement of sensory maps and disorganization of motor cortex after targeted stroke in mice. *Stroke* **44,** 2300–2306. (2013).

232. Lim, D. H., LeDue, J., Mohajerani, M. H., Vanni, M. P. & Murphy, T. H. Optogenetic approaches for functional mouse brain mapping. *Frontiers in neuroscience* **7,** 54. (2013).

233. Lim, D. H., LeDue, J. M., Mohajerani, M. H. & Murphy, T. H. Optogenetic mapping after stroke reveals network-wide scaling of functional connections and heterogeneous recovery of the peri-infarct. *The Journal of Neuroscience* **34,** 16455–16466. (2014).

234. Murphy, T. H., Li, P., Betts, K. & Liu, R. Two-photon imaging of stroke onset in vivo reveals that NMDA-receptor independent ischemic depolarization is the major cause of rapid reversible damage to dendrites and spines. *The Journal of Neuroscience* **28,** 1756–1772. (2008).

235. Risher, W. C., Ard, D., Yuan, J. & Kirov, S. A. Recurrent spontaneous spreading depolarizations facilitate acute dendritic injury in the ischemic penumbra. *The Journal of Neuroscience* **30,** 9859–9868. (2010).

236. Takano, T. *et al.* Cortical spreading depression causes and coincides with tissue hypoxia. *Nature neuroscience* **10,** 754–762. (2007).

237. Brown, C. E., Li, P., Boyd, J. D., Delaney, K. R. & Murphy, T. H. Extensive turnover of dendritic spines and vascular remodeling in cortical tissues recovering from stroke. *The Journal of neuroscience* **27,** 4101–4109. (2007).

238. Brown, C. E., Wong, C. & Murphy, T. H. Rapid morphologic plasticity of peri-infarct dendritic spines after focal ischemic stroke. *Stroke* **39,** 1286–1291. (2008).

239. Mostany, R. *et al.* Local hemodynamics dictate long-term dendritic plasticity in peri-infarct cortex. *The Journal of Neuroscience* **30,** 14116–14126. (2010).

240. Papadopoulos, C. M. *et al.* Functional recovery and neuroanatomical plasticity following middle cerebral artery occlusion and IN-1 antibody treatment in the adult rat. *Annals of neurology* **51,** 433–441. (2002).

241. Lee, J.-K., Kim, J.-E., Sivula, M. & Strittmatter, S. M. Nogo receptor antagonism promotes stroke recovery by enhancing axonal plasticity. *The Journal of neuroscience* **24,** 6209–6217. (2004).

242. Tsai, S.-Y., Papadopoulos, C. M., Schwab, M. E. & Kartje, G. L. Delayed anti-nogo-a therapy improves function after chronic stroke in adult rats. *Stroke* **42,** 186–190. (2011).

243. Chen, P., Goldberg, D. E., Kolb, B., Lanser, M. & Benowitz, L. I. Inosine induces axonal rewiring and improves behavioral outcome after stroke. *Proceedings of the National Academy of Sciences* **99,** 9031–9036. (2002).

244. Smith, J. M. *et al.* Inosine promotes recovery of skilled motor function in a model of focal brain injury. *Brain* **130,** 915–925. (2007).

245. Zai, L. *et al.* Inosine augments the effects of a Nogo receptor blocker and of environmental enrichment to restore skilled forelimb use after stroke. *The Journal of Neuroscience* **31,** 5977–5988. (2011).

246. Wahl, A. S. *et al.* Asynchronous therapy restores motor control by rewiring of the rat corticospinal tract after stroke. *Science* **344,** 1250–1255. (2014).

247. Fang, P.-c. *et al.* Combination of NEP 1-40 treatment and motor training enhances behavioral recovery after a focal cortical infarct in rats. *Stroke* **41,** 544–549. (2010).

248. Soleman, S., Yip, P. K., Duricki, D. A. & Moon, L. D. F. Delayed treatment with chondroitinase ABC promotes sensorimotor recovery and plasticity after stroke in aged rats. *Brain* **135,** 1210–1223. (2012).

249. Gherardini, L., Gennaro, M. & Pizzorusso, T. Perilesional treatment with chondroitinase ABC and motor training promote functional recovery after stroke in rats. *Cerebral cortex* **25,** 202–212. (2015).

250. Taub, E., Uswatte, G., Mark, V. W. & Morris, D. M. The learned nonuse phenomenon: implications for rehabilitation. *Eura Medicophys* **42,** 241–55 (2006).

251. Rutten, G.-J. M., Ramsey, N. F., Van Rijen, P. C., Franssen, H. & Van Veelen, C. W. M. Interhemispheric reorganization of motor hand function to the primary motor cortex predicted with functional magnetic resonance imaging and transcranial magnetic stimulation. *Journal of child neurology* **17,** 292–297. (2002).

252. Staudt, M. *et al.* Two types of ipsilateral reorganization in congenital hemiparesis. *Brain* **125,** 2222–2237. (2002).

253. Kennard, M. A. Age and other factors in motor recovery from precentral lesions in monkeys. *American Journal of Physiology–Legacy Content* **115,** 138–146. (1936).

254. Eyre, J. A. *et al.* Is hemiplegic cerebral palsy equivalent to amblyopia of the corticospinal system? *Annals of neurology* **62,** 493–503. (2007).

255. Martin, J. H. Systems neurobiology of restorative neurology and future directions for repair of the damaged motor systems. *Clinical neurology and neurosurgery* **114,** 515–523. (2012).

256. Whishaw, I. Q. & Pellis, S. M. The structure of skilled forelimb reaching in the rat: a proximally driven movement with a single distal rotatory component. *Behavioural brain research* **41,** 49–59. (1990).

257. Hutson, T. H., Verhaagen, J., Yáñez-Muñoz, R. J. & Moon, L. D. F. Corticospinal tract transduction: a comparison of seven adeno-associated viral vector serotypes and a non-integrating lentiviral vector. *Gene therapy* **19,** 49–60. (2012).

258. Paxinos, G. & Watson, C. The rat brain atlas in stereotaxic coordinates. *San Diego: Academic* (1998).

259. Metz, G. A. & Whishaw, I. Q. The ladder rung walking task: a scoring system and its practical application. *JoVE (Journal of Visualized Experiments),* e1204–e1204. (2009).

260. De Medinaceli, L., Freed, W. J. & Wyatt, R. J. An index of the functional condition of rat sciatic nerve based on measurements made from walking tracks. *Experimental neurology* **77,** 634–643. (1982).

261. Metz, G. A. & Schwab, M. E. Behavioral characterization in a comprehensive mouse test battery reveals motor and sensory impairments in growth-associated protein-43 null mutant mice. *Neuroscience* **129,** 563–574. (2004).

262. Montoya, C. P., Campbell-Hope, L. J., Pemberton, K. D. & Dunnett, S. B. The "staircase test": a measure of independent forelimb reaching and grasping abilities in rats. *Journal of neuroscience methods* **36,** 219–228. (1991).

263. Weigel, A., Schild, D. & Zeug, A. Resolution in the ApoTome and the confocal laser scanning microscope: comparison. *Journal of biomedical optics* **14,** 014022–014022. (2009).

264. Asante, C. O. & Martin, J. H. Differential joint-specific corticospinal tract projections within the cervical enlargement. *PloS one* **8,** e74454. (2013).

265. Herson, P. S. *et al.* Experimental pediatric arterial ischemic stroke model reveals sex-specific estrogen signaling. *Stroke* **44,** 759–763. (2013).

266. Kadam, S. D., Mulholland, J. D., Smith, D. R., Johnston, M. V. & Comi, A. M. Chronic brain injury and behavioral impairments in a mouse model of term neonatal strokes. *Behavioural brain research* **197,** 77–83. (2009).

267. Goulding, M. Circuits controlling vertebrate locomotion: moving in a new direction. *Nature Reviews Neuroscience* **10,** 507–518. (2009).

268. Cao, Y. *et al.* Nogo-66 receptor antagonist peptide (NEP1-40) administration promotes functional recovery and axonal growth after lateral funiculus injury in the adult rat. *Neurorehabilitation and neural repair* **22,** 262–278. (2008).

269. García-Alías, G. *et al.* Chondroitinase ABC combined with neurotrophin NT-3 secretion and NR2D expression promotes axonal plasticity and functional recovery in rats with lateral hemisection of the spinal cord. *The Journal of Neuroscience* **31,** 17788–17799. (2011).

270. Siegel, C. S., Fink, K. L., Strittmatter, S. M. & Cafferty, W. B. J. Plasticity of intact rubral projections mediates spontaneous recovery of function after corticospinal tract injury. *The Journal of Neuroscience* **35,** 1443–1457. (2015).

271. Lassek, A. M. & Rasmussen, G. L. A comparative fiber and numerical analysis of the pyramidal tract. *Journal of Comparative Neurology* **72,** 417–428. (1940).

272. Nielson, J. L. *et al.* Unexpected survival of neurons of origin of the pyramidal tract after spinal cord injury. *The Journal of Neuroscience* **30,** 11516–11528. (2010).

273. Gorgels, T. G. M. F. A quantitative analysis of axon outgrowth, axon loss, and myelination in the rat pyramidal tract. *Developmental Brain Research* **54,** 51–61. (1990).

274. Yip, P. K., Wong, L.-F., Sears, T. A., Yáñez-Muñoz, R. J. & McMahon, S. B. Cortical overexpression of neuronal calcium sensor-1 induces functional plasticity in spinal cord following unilateral pyramidal tract injury in rat. *PLoS Biol* **8,** e1000399. (2010).

275. Blackmore, M. G. *et al.* Krüppel-like Factor 7 engineered for transcriptional activation promotes axon regeneration in the adult corticospinal tract. *Proceedings of the National Academy of Sciences* **109,** 7517–7522. (2012).

276. Lee, D.-H. *et al.* Mammalian target of rapamycin's distinct roles and effectiveness in promoting compensatory axonal sprouting in the injured CNS. *The Journal of Neuroscience* **34,** 15347–15355. (2014).

277. Brosamle, C. & Schwab, M. E. Cells of origin, course, and termination patterns of the ventral, uncrossed component of the mature rat corticospinal tract. *J Comp Neurol* **386,** 293303 (1997).

278. Rumajogee, P., Bregman, T., Miller, S. P., Yager, J. Y. & Fehlings, M. G. Rodent Hypoxia-Ischemia Models for Cerebral Palsy Research: A Systematic Review. *Frontiers in neurology* **7** (2016).

279. Carmichael, S. T., Wei, L., Rovainen, C. M. & Woolsey, T. A. New patterns of intracortical projections after focal cortical stroke. *Neurobiology of disease* **8,** 910–922. (2001).

280. Friel, K., Chakrabarty, S., Kuo, H.-C. & Martin, J. Using motor behavior during an early critical period to restore skilled limb movement after damage to the corticospinal system during development. *The Journal of Neuroscience* **32,** 9265–9276. (2012).

281. Li, Q. & Martin, J. H. Postnatal development of connectional specificity of corticospinal terminals in the cat. *Journal of Comparative Neurology* **447,** 57–71. (2002).

282. Jin, D. *et al.* Restoration of skilled locomotion by sprouting corticospinal axons induced by co-deletion of PTEN and SOCS3. *Nature communications* **6** (2015).

283. Wang, Z., Reynolds, A., Kirry, A., Nienhaus, C. & Blackmore, M. G. Overexpression of Sox11 promotes corticospinal tract regeneration after spinal injury while interfering with functional recovery. *The Journal of Neuroscience* **35,** 3139–3145. (2015).

284. Jayaprakash, N. *et al.* Optogenetic Interrogation of Functional Synapse Formation by Corticospinal Tract Axons in the Injured Spinal Cord. *The Journal of Neuroscience* **36,** 5877–5890. (2016).

285. Azim, E., Jiang, J., Alstermark, B. & Jessell, T. M. Skilled reaching relies on a V2a propriospinal internal copy circuit. *Nature* **508,** 357–363. (2014).

286. Bourane, S. *et al.* Identification of a spinal circuit for light touch and fine motor control. *Cell* **160,** 503–515. (2015).

287. García-Alías, G., Barkhuysen, S., Buckle, M. & Fawcett, J. W. Chondroitinase ABC treatment opens a window of opportunity for task-specific rehabilitation. *Nature neuroscience* **12,** 1145–1151. (2009).

288. Nakagawa, H., Ueno, M., Itokazu, T. & Yamashita, T. Bilateral movement training promotes axonal remodeling of the corticospinal tract and recovery of motor function following traumatic brain injury in mice. *Cell death & disease* **4,** e534 (2013).

289. Zeiler, S. R. & Krakauer, J. W. The interaction between training and plasticity in the post-stroke brain. *Current opinion in neurology* **26,** 609 (2013).

290. Wahl, A.-S. & Schwab, M. E. Finding an optimal rehabilitation paradigm after stroke: enhancing fiber growth and training of the brain at the right moment. *Frontiers in human neuroscience* **8** (2014).

291. Zhang, J. & Chopp, M. Cell-based therapy for ischemic stroke. *Expert opinion on biological therapy* **13,** 1229–1240. (2013).